universität wien

MASTERARBEIT | MASTER'S THESIS

Titel | Title

Assessment of the role of neutrophils in mediating left ventricular dysfunction

verfasst von | submitted by

Bahareh Soltani

angestrebter akademischer Grad | in partial fulfilment of the requirements for the degree of

Master of Science (MSc)

Wien | Vienna, 2024

Studienkennzahl lt. Studienblatt | Degree programme code as it appears on the student record sheet:	UA 066 830
Studienrichtung lt. Studienblatt | Degree programme as it appears on the student record sheet:	Masterstudium Molecular Microbiology, Microbial Ecology and Immunobiology
Betreut von | Supervisor:	Univ.-Prof. Mag. Dr. Pavel Kovarik

I. Content

II. List of illustrations

III. List of tables

IV. List of abbreviations

1.	**AMI**	**Acute myocardial infraction**
2.	**ATP**	**Adenosine triphosphate**
3.	**BSA**	**Bovine serum albumin**
4.	**CAD**	**Coronary artery disease**
5.	**CM**	**Cardiomyocyte**
6.	**CO**	**Cardiac output**
7.	**DAMP**	**Damage-associated molecular patterns**
8.	**DAPI**	**4´,6-diamidino-2-phenylindol**
9.	**DC**	**Dendritic cell**
10.	**DM**	**Diabetes mellitus**
11.	**ECG**	**Electrocardiogram**
12.	**ECH**	**Echocardiography**
13.	**EDV**	**End-diastolic volume**
14.	**EF**	**Ejection fraction**
15.	**EPO**	**Erythropoietin**
16.	**ESAS**	**Erythropoiesis-stimulating agents**
17.	**eNOS**	**Endothelial nitric oxide synthase**
18.	**ESV**	**End-systolic volume**

19.	FACS	Fluorescence-Activated cell sorting
20.	FMO	Fluorescence minus one
21.	FSC	Forward scatter
22.	G6PD	Glucose-6-phosphate Dehydrogenase
23.	Hb	Hemoglobin
24.	HR	Heart rate
25.	IHC	Immunohistochemistry
26.	IL-10	Interleukin-6
27.	IR	Ischemia-reperfusion
28.	LDL	Low-density lipoprotein
29.	LV	Left ventricular
30.	MHC	Major Histocompatibility Complex
31.	MI	Myocardial Infarction
32.	MPO	Myeloperoxidase
33.	NAC	N-acetylcysteine
34.	NADP	Nicotinamide Adenine Dinucleotide
35.	NADPH	Nicotinamide Adenine Dinucleotide Phosphate
36.	NET	Neutrophil extracellular trap
37.	NK	Natural killer cell
38.	NO	Nitric oxide
39.	PAD	Peripheral artery disease
40.	PBS	Phosphate buffered saline
41.	PFA	Paraformaldehyde
42.	RBC	Red blood cell
43.	RT	Room temperature
44.	ROS	Reactive oxygen species
45.	SSC	Side scatter
46.	SV	Stroke volume
47.	TCR	T-cell receptor
48.	TFCR	Transferring receptor
49.	Treg	Regulatory T-cell
50.	4-HNE	4- hydroxynonenal

1 Abstract

Acute myocardial infarction (AMI) is characterized by cardiac cell death resulting from prolonged ischemia and reduced blood flow. Acute and chronic anemia are associated with worse outcomes in AMI. However, the underlying mechanism for poor prognosis after AMI remains largely unknown. Previously, we showed that acute anemia leads to a compensatory increased in heart function, evidenced by increased stroke volume (SV) and cardiac output (CO). Additionally, we demonstrated that endothelial function is critically affected in both chronic and acute anemia after AMI in mice. The effect of acute and chronic anemia on heart function, particularly in relation to immune cell infiltration, remains poorly investigated after AMI. This thesis aims to examine the impact of both acute and chronic anemia on heart function, with a specific focus on immune cell infiltration. We hypothesize that both acute and chronic anemia are associated with worsening heart function after AMI, which is further linked to oxidative stress promoting neutrophil infiltration. To test this hypothesis, established mouse models of acute and chronic blood loss anemia were used. Cardiac function was assessed using echocardiography (ECH) at baseline, 24 hours, and 7 days post-ischemia/reperfusion (IR) injury, with and without antioxidant N-Acetyl-Cysteine (NAC) treatment. Additionally, immune cell infiltration was analyzed using flow cytometry before and after AMI in both acute and chronic anemic mice, with a focus on neutrophil infiltration. Immunofluorescence staining was also performed to assess neutrophil distribution within the infarcted myocardium. ECH data demonstrated that acute anemia resulted in a significant reduction in CO at 24 hours post-AMI, without affecting other cardiac parameters. At 7 days post-AMI, SV was significantly increased in acute anemic mice, while other parameters remained unchanged. In chronic anemic mice, cardiac function data revealed a reduced heart rate (HR) and compensatory increased end-diastolic volume (EDV) 24 hours post-AMI, with no other parameters affected. Notably, NAC treatment did not lead to significant improvements in cardiac function in acute and chronic anemic mice 24 hours of 7 days post-AMI. To further evaluate the impact of anemia on immune cell infiltration, flow cytometry and immunohistochemistry were performed. Flow cytometry analysis revealed a significant increase in neutrophil abundance in acute anemic mice. In contrast, chronic anemic mice without IR, as well as acute and chronic anemic mice with IR, showed no significant changes in myocardial immune cell populations, including leucocytes, monocytes, neutrophils, T cells, B cells, and NK cells. In conclusion, $Ly6G^{+}$ neutrophils were increased in acute anemic mice, highlighting a potential link between acute anemia, neutrophil mediated oxidative stress. Altogether, this data concludes that acute anemia is associated with worsening cardiac function after the acute phase of AMI, whereas chronic anemia is associated with compensatory changes in heart function. Oxidative stress-promoting neutrophils are specifically infiltrated in the myocardium of acute anemic mice.

2 Zusammenfassung

Akuter Myokardinfarkt (AMI) ist durch den Tod von Herzmuskelzellen infolge einer verlängerten Ischämie und einer reduzierten Blutversorgung gekennzeichnet. Akute und chronische Anämie sind mit einer Verschlechterung der Prognose bei AMI assoziiert. Der zugrunde liegende Mechanismus dieser schlechten Prognose nach AMI ist jedoch weitgehend unbekannt. In früheren Studien haben wir gezeigt, dass akute Anämie zu einer kompensatorischen Steigerung der Herzfunktion führt, was sich in einer erhöhten Schlagvolumenzahl (SV) und einem gesteigerten Herzzeitvolumen (CO) widerspiegelt. Darüber hinaus konnten wir nachweisen, dass die Endothelfunktion sowohl bei chronischer als auch bei akuter Anämie nach AMI bei Mäusen erheblich beeinträchtigt ist. Der Einfluss von akuter und chronischer Anämie auf die Herzfunktion, insbesondere im Zusammenhang mit der Infiltration von Immunzellen, ist nach AMI bisher wenig untersucht. Ziel dieser Dissertation ist es, die Auswirkungen von akuter und chronischer Anämie auf die Herzfunktion mit einem besonderen Fokus auf die Infiltration von Immunzellen zu untersuchen. Wir postulieren, dass sowohl akute als auch chronische Anämie mit einer Verschlechterung der Herzfunktion nach AMI assoziiert sind, was mit oxidativem Stress einhergeht, der eine verstärkte Neutrophileninfiltration fördert. Um diese Hypothese zu überprüfen, wurden etablierte Mausmodelle für akute und chronische Blutverlustanämie verwendet. Die Herzfunktion wurde mittels Echokardiographie (ECH) in der Ausgangssituation sowie 24 Stunden und 7 Tage nach Ischämie/Reperfusions-(IR)-Verletzung mit und ohne Behandlung mit dem Antioxidans N-Acetyl-Cystein (NAC) untersucht. Zusätzlich wurde die Infiltration von Immunzellen vor und nach AMI bei Mäusen mit akuter und chronischer Anämie mittels Durchflusszytometrie analysiert, wobei ein besonderer Schwerpunkt auf der Neutrophileninfiltration lag. Immunfluoreszenzfärbungen wurden ebenfalls durchgeführt, um die Verteilung von Neutrophilen im infarktierten Myokard zu bewerten. Die ECH-Daten zeigten, dass akute Anämie 24 Stunden nach AMI zu einer signifikanten Reduktion des CO führte, ohne andere kardiale Parameter zu beeinflussen. Nach 7 Tagen war das SV bei Mäusen mit akuter Anämie signifikant erhöht, während andere Parameter unverändert blieben. Bei Mäusen mit chronischer Anämie zeigten die kardiologischen Daten 24 Stunden nach AMI eine reduzierte Herzfrequenz (HR) und ein kompensatorisch erhöhtes enddiastolisches Volumen (EDV), während andere Parameter unverändert blieben. NAC-Behandlung führte weder nach 24 Stunden noch nach 7 Tagen zu signifikanten Verbesserungen der Herzfunktion bei Mäusen mit akuter oder chronischer Anämie nach AMI. Um den Einfluss der Anämie auf die Immunzellinfiltration weiter zu bewerten, wurden Durchflusszytometrie und Immunhistochemie durchgeführt. Die Analyse der Durchflusszytometrie zeigte eine signifikante Zunahme der Neutrophilen bei Mäusen mit akuter Anämie. Im Gegensatz dazu zeigten Mäuse mit chronischer Anämie ohne IR sowie Mäuse mit akuter und chronischer Anämie mit IR keine signifikanten Veränderungen der myokardialen Immunzellpopulationen, einschließlich Leukozyten, Monozyten, Neutrophilen, T-Zellen, B-Zellen und NK-Zellen.

Zusammenfassend waren $Ly6G^+$-Neutrophile bei Mäusen mit akuter Anämie vermehrt, was auf einen möglichen Zusammenhang zwischen akuter Anämie und durch Neutrophile vermitteltem oxidativem Stress hinweist. Insgesamt zeigen diese Daten, dass akute Anämie mit einer Verschlechterung der Herzfunktion nach der akuten Phase des AMI verbunden ist, während chronische Anämie mit kompensatorischen Veränderungen der Herzfunktion einhergeht. Oxidativen Stress fördernde Neutrophile infiltrieren spezifisch das Myokard bei Mäusen mit akuter Anämie.

3 Introduction

3.1 Structure and function of the heart

The heart muscle or myocardium consists of four chambers and three layers (Fig.1): the inner layer (endocardium), the middle layer (myocardium, responsible for pumping blood), and the outer layer (epicardium) (Saxton, Tariq, & Bordoni, 2024; Tran, Weber, & Lopez, 2024). The heart´s chambers are arranged into two pumps, the right and left sides, which circulate blood throughout the body. The right side includes the right atrium and right ventricle. The right atrium receives deoxygenated blood from the body (excluding the lungs) and transfers it to the right ventricle. The right ventricle then pumps this blood to the lungs for oxygenation. Once oxygenated, the blood returns to the left atrium and is passed to the left ventricle. Finally, the left ventricle pumps the oxygenated blood throughout the body (Rehman & Rehman, 2024). The myocardium is comprised of specialized cells called cardiomyocytes (CMs) (Brakenhielm & Alitalo, 2019; Saxton et al., 2024). These cells consists of many mitochondria, enabling them to produce the Adenosine triphosphate (ATP) required to ensure the heart´s continues contraction and relaxation cycles (Saxton et al., 2024) . This activity is essential for maintaining blood circulation throughout the body. The contraction and relaxation of CMs depends on a consistent supply of oxygen and nutrients, which are delivered by left and right coronary arteries. Blood flow reduction to myocardium, results in damage or death of the affected cardiac tissue (Brakenhielm & Alitalo, 2019; Saxton et al., 2024), leading to malfunction of heart.

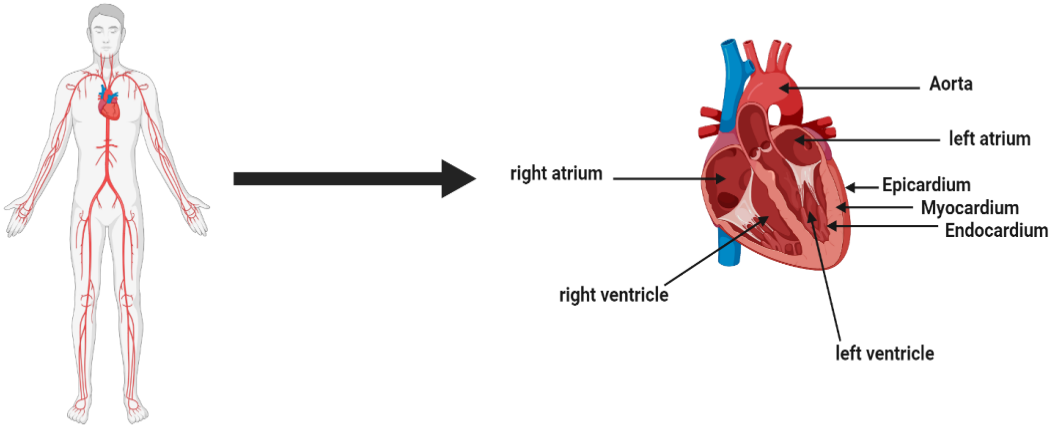

Figure 1. The figure depicts the human circulatory system. Highlighting key structure of the heart, including the four chambers: the right and left ventricles, the right and left atria, as well as the aorta and three layers of heart wall. Illustration created with Biorender.com.

3.2 Acute myocardial Infarction (AMI)

AMI is a critical cardiovascular condition caused by blood flow to a part of the cardiac tissue is restricted or blocked, resulting in ischemia and myocardial necrosis due to prolonged oxygen deficiency (Fig.2) (Ojha & Dhamoon, 2024; Thygesen, Alpert, White, & Joint, 2007). This blockage is often caused by a blood clot in the coronary arteries, which provide oxygenated blood to the myocardium (Ojha & Dhamoon, 2024; Reimer, Jennings, & Tatum, 1983). Despite advancement in medical care reducing AMI-related mortality rates, it remains one of the leading causes of death worldwide (Ojha & Dhamoon, 2024; Saleh & Ambrose, 2018), AMI is clinically classified into two main categories: ST-segment elevation myocardial infarction (STEMI) and non-ST-segment elevation myocardial infarction (NSTEMI). The distinction is based on the presence or absence of persistent ST-segment elevation on an ECG (Mitsis & Gragnano, 2021). Myocardial ischemia can be triggered by various pathological conditions, but the most common cause is the rupture of an atherosclerotic plaque. This rupture is typically associated with significant lipid accumulation within the coronary artery, leading to thrombus formation that obstructs blood flow. A complete occlusion of the artery generally results in STEMI, while partial occlusion may lead to NSTEMI or angina pectoris (Anderson & Morrow, 2017; Surendran, Atefi, Zhang, Aliani, & Ravandi, 2021). ECGs, electrography, coronary angiograph, and circulating sensitive biomarkers, such as troponin, myoglobin, and creatine kinase, play a crucial role in diagnosing AMI by detecting cardiac muscle cell death (Frangogiannis, 2015; Y. Wu et al., 2020). Altered or elevated levels of these markers are considered a hallmark of the condition (Y. Wu et al., 2020). Signals from damaged CM cells stimulate an inflammatory response, initiating the repair mechanism through the activity of immune cells. The repair mechanism involves adaptive structural changes in the myocardium, such as enlargement of the heart chambers and thickening of remaining muscle tissue. These changes lead to the reduction of overall heart function (Frangogiannis, 2015; Y. Wu et al., 2020).

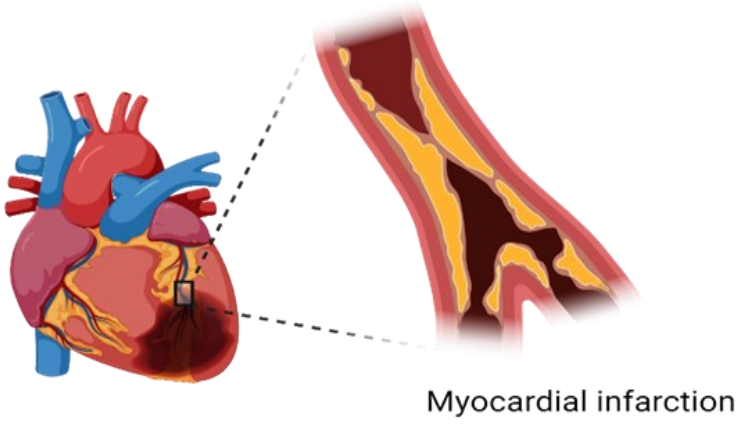

Figure 2. AMI and blocked coronary arteries leading to hypoxia. The figure illustrates the blockage in coronary arteries that restricts blood flow, causing hypoxia in the cardiac tissue. Illustration created with Biorender.com.

3.3 Plaque development and associated risk factors

Atherosclerosis itself is driven by internal inflammation, fibrosis, and necrosis in the formation of arterial plaques in the arteries. The process begins with the accumulation of low-density lipoproteins (LDLs) in the arterial endothelium, often accompanied by adaptive thickening of the vessel wall (Awad Hegazy, 2022; Bentzon, Otsuka, Virmani, & Falk, 2014). These LDLs undergo oxidative modifications, which active immune responses. This immune activation promotes the differentiation of monocytes into macrophages that engulf the modified lipids, formation foam cell, a hallmark of atherosclerosis plaques (Awad Hegazy, 2022; Libby, Ridker, & Hansson, 2011). Over time, these changes progressively impair endothelial integrity, increasing its permeability (Awad Hegazy, 2022; Bentzon et al., 2014). Blood lipids, particularly LDL cholesterol lipids are critical contributors to the development of atherosclerosis, endothelial dysfunction, and arterial plaques, all of which are key factors in the progression of coronary artery disease (CAD) (Awad Hegazy, 2022; Linton et al., 2000). Oxidized LDL plays a significant role by inducing endothelial injury and dysfunction (Aoyama, Chen, Fujiwara, Masaki, & Sawamura, 2000; Awad Hegazy, 2022; Yoshida, Kondratenko, Green, Steinberg, & Quehenberger, 1998). Coronary endothelial dysfunction is an early progressive event in CAD development, arising from endothelial injury caused by factors such as oxidized LDL, elevated blood glucose, hypertension, and increased oxidative stress from free radicals. This dysfunction is typically characterized by reduced production of endothelial nitric oxide (NO), impairing endothelium dependent vasodilation. As a result, there is increased platelet and monocyte adhesion, as well as enhanced smooth muscle cell proliferation eventually leading to plaque development, progression and rupture (Awad Hegazy, 2022; Luscher et al., 2009). AMI is associated with numerous risk factors, and identifying these risk factors is crucial for preventing premature AMI (Awad Hegazy, 2022; Yusuf et al., 2004). One significant risk factor is hypertension, which is directly linked to an increased mortality rate from CAD (Awad Hegazy, 2022; Kaplan, Psaty, Heckbert, Smith, & Lemaitre, 1999). Studies have shown that hypertensive patients twice as likely to develop AMI compared to those with normal blood pressure (Awad Hegazy, 2022; Piegas et al., 2003). Additionally, anemia has been shown to elevate the risk of AMI (Kanic, Kompara, Vollrath, Suran, & Kanic, 2019; Moghaddam et al., 2018), as it impairs oxygen delivery to the myocardium, leading to ischemia damage (G.A. Fishbein, M.C. Fishbein, L.M. Buja, Myocardial Ischemia and Its Complications, Editor(s): L. Maximilian Buja, Jagdish Butany, Cardiovascular Pathology, Academic Press, 2016). Diabetes mellitus (DM) is another major risk factor for CAD and AMI, which is

associated with increased mortality following AMI (Awad Hegazy, 2022; Stevens et al., 2004). The underlying pathophysiology involves chronic hyperglycaemia, leading to systemic oxidative stress and inflammation, which accelerate coronary atherosclerosis and contribute to microvascular dysfunction (Awad Hegazy, 2022; Severino et al., 2019). Smoking is another major independent risk factor for AMI and contributes significantly to both its morbidity and mortality. The risk of CAD is directly correlated with the duration and amount of tobacco use (Awad Hegazy, 2022; Prescott, Hippe, Schnohr, Hein, & Vestbo, 1998). Smoking increases blood pressure and HR, which elevate myocardial oxygen demand, while vasoconstriction reduces coronary artery diameter and blood flow. This imbalance between oxygen supply and demand can be further exacerbated by concurrent cocaine use (Awad Hegazy, 2022; Moliterno et al., 1994).

3.4 Red blood cells (RBCs)

Erythrocytes, commonly known as RBCs, are main components of blood, specialized cells critical for the transport of gases such as oxygen, carbon dioxide, and essential nutrients throughout the body. Their unique shape and morphology enhance flexibility, allowing them to pass through small capillaries, and increases their surface area to volume ratio to optimize gas exchange efficiency. Enclosed within a selectivity permeable phospholipid bilayer, the cells are structurally supported by a complex protein-based cytoskeleton. This architecture not only facilitates their cellular structure integrity but also serves as a key focus for understanding pathophysiological processes in various hematological diseases (Kuhn et al., 2017; Smith, 1987). RBCs have an average lifespan of approximately 120 days, during which they play a vital role in respiratory gas exchange. They transport oxygen from the lungs to peripheral tissues and facilitate the return of carbon dioxide to the lungs for exhalation. This process is mediated by hemoglobin (Hb), the oxygen-binding protein within RBCs (Fig.3). In the oxygen-rich environment of the lungs, Hb binds oxygen due to its high oxygen affinity. In peripheral tissues, lower oxygen partial pressure and the acidic environment reduce affinity of Hb for oxygen, promoting oxygen release. Simultaneously, carbon dioxide produced by cellular metabolism diffuses into RBCs, where it is enzymatically converted by carbonic anhydrase into bicarbonate (HCO_3^-) and hydrogen ions. The majority of carbon dioxide is transported back to the lungs as bicarbonate in the plasma. In the lungs, the reaction is reversed, releasing carbon dioxide for exhalation. This tightly regulated process ensures efficient gas transport and homeostasis (Barbalato & Pillarisetty, 2024; Kuhn et al., 2017). The ability of Hb to bind oxygen and facilitate carbon dioxide (CO_2) transport is tightly regulated by several factors, including oxygen partial pressure, pH, and various modulators. These factors influence affinity of Hb for oxygen and its capacity to release it in tissues. The conversion of CO_2 to bicarbonate in RBCs facilitates CO_2 removal from tissues (Johnson, Goyette, Ravindranath, & Ho, 2005; Kuhn et al., 2017). Hb in RBCs must remain in a reduced state to function properly, but several challenges complicate this process.

First, RBCs are exposed to high levels of oxygen bound to Hb, as well as various oxidants, which increases risk of oxidative damage. Second, the iron in Hb's heme group can catalyse the production of reactive oxygen species (ROS) through the Fenton reaction when free in solution, further exacerbating oxidative stress. Finally, RBCs have a limited ability to repair damaged components because they are anucleated, preventing them from synthesizing new proteins or effectively addressing cellular damage. These factors together make it difficult for RBCs to maintain the reduced state of Hb, which is crucial for efficient oxygen transport (Johnson et al., 2005; Kuhn et al., 2017). RBCs are involved in transporting NO, synthesizing NO via nitrite reduction under hypoxic conditions, and producing NO through endothelial nitric oxide synthase (eNOS) during normoxia, contributing to the circulating NO pool (Chen & Mehta, 1998; Kleinbongard et al., 2006; Rassaf et al., 2002; Wischmann et al., 2020; Wood et al., 2013). A depletion of circulating NO is associated with increased blood pressure, greater severity of AMI, and left ventricular (LV) remodelling after AMI. In anemia, RBC dysfunction may independently impair cardiac and vascular function, in addition to reduced oxygen delivery (Wischmann et al., 2020).

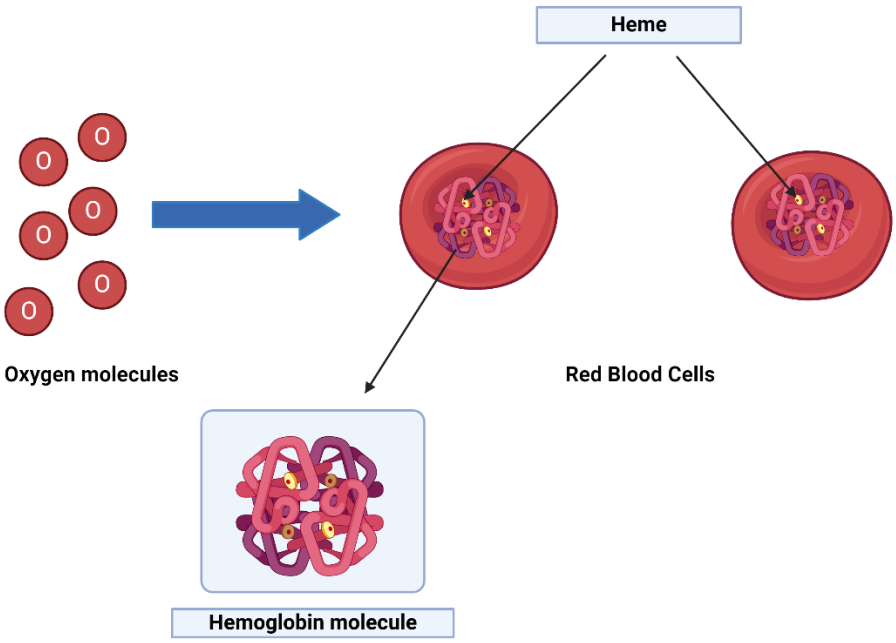

Figure 3. Oxygen molecules binding to Hb via heme group in red blood cells. The figure depicts oxygen molecules moving toward an RBC and binding to an iron atom in the heme group of Hb, enabling efficient oxygen transport throughout the body. Illustration created with Biorender.com.

3.5 RBC dysfunction

RBC dysfunction refers to impaired oxygen transport caused by various factors such as genetic variations, biochemical or physical abnormalities (Loyola-Leyva, Loyola-Rodriguez, Atzori, &

Gonzalez, 2018; Mohandas & Gallagher, 2008; Singh, Winocour, & Farrington, 2009; Williams et al., 2023). This dysfunction disrupts cellular processes, leading to membrane abnormalities, oxidative damage, enzyme deficiencies, and structural changes in RBCs. A common example is Glucose-6-phosphate Dehydrogenase (G6PD) deficiency, that impairs RBC function (Orrico et al., 2023). G6PD is essential for the protection of RBCs from oxidative damage caused by ROS. Because RBCs lack organelles, they rely on G6PD activity to maintain cell membrane integrity (Orrico et al., 2023). G6PD catalyzes the first step in the pentose phosphate pathway, converting Nicotinamide Adenine Dinucleotide (NADH) to Nicotinamide Adenine Dinucleotide Phosphate (NADPH) (Luzzatto, Ally, & Notaro, 2020). NADPH is critical for reducing glutathione, which detoxifies hydrogen peroxide into water, preventing oxidative damage. G6PD deficiency is associated with increased ROS production, leading to acute hemolytic anemia during infections (Beutler, 1994; Luzzatto et al., 2020). Recent evidence confirmed the crucial role of RBCs in cardiovascular hemeostasis. RBCs regulate cardiovascular function by exporting ATP and NO bioactivity, while also maintaining redox balance through an antioxidant system (Kuhn et al., 2017; Pernow, Mahdi, Yang, & Zhou, 2019; Salgado, Cao, Nagababu, Mohanty, & Rifkind, 2015). Altered RBC function, or erythropathy, worsens cardiovascular disease (CVD) by increasing ROS production (Farah, Michel, & Balligand, 2018; Kuhn et al., 2017; Mohanty, Nagababu, & Rifkind, 2014; Pernow et al., 2019; Schade, Kotthaus, & Clement, 2010; Vanhoutte, Shimokawa, Tang, & Feletou, 2009). RBCs are equipped with antioxidant systems vital for maintaining their function and integrity. Hemolysis, or the breakdown of RBCs, can lead to severe health issues, including endothelial dysfunction (Fig.4) which is characterized by reduced NO bioavailability, is an early signal of CVD (Farah et al., 2018; Kuhn et al., 2017; Pernow et al., 2019; Schade et al., 2010; Vanhoutte et al., 2009) and contributes to vessel constriction, inflammation, thrombosis, and proliferation. Several hypotheses have been suggested about the non-canonical roles of RBCs, with increasing evidence supporting their involvement in cardiovascular protection (Kuhn et al., 2017) Clinical studies associate anemia with severe cardiovascular issues, including a higher risk of thromboembolic events. Treatments increase RBC counts, such as blood transfusions and erythropoiesis-stimulating agents (ESAs), are commonly used (Ducrocq et al., 2015; Jolicoeur et al., 2009; Kuhn et al., 2017; Maldonado Rolon, 1975; Rousseau et al., 2010). In patients with AMI and anemia, treatments, such as blood transfusions have not improved outcomes and may even worsen the condition (Anker et al., 2009; Aronson et al., 2008; Wischmann et al., 2020). Apart from changes in oxygen-carrying Hb levels, alterations in other RBC functions interact with the cardiac and circulatory compensatory mechanisms of anemia, worsening the outcomes of AMI (Chen & Mehta, 1998; Kleinbongard et al., 2006; Rassaf et al., 2002; Wischmann et al., 2020; Wood et al., 2013).

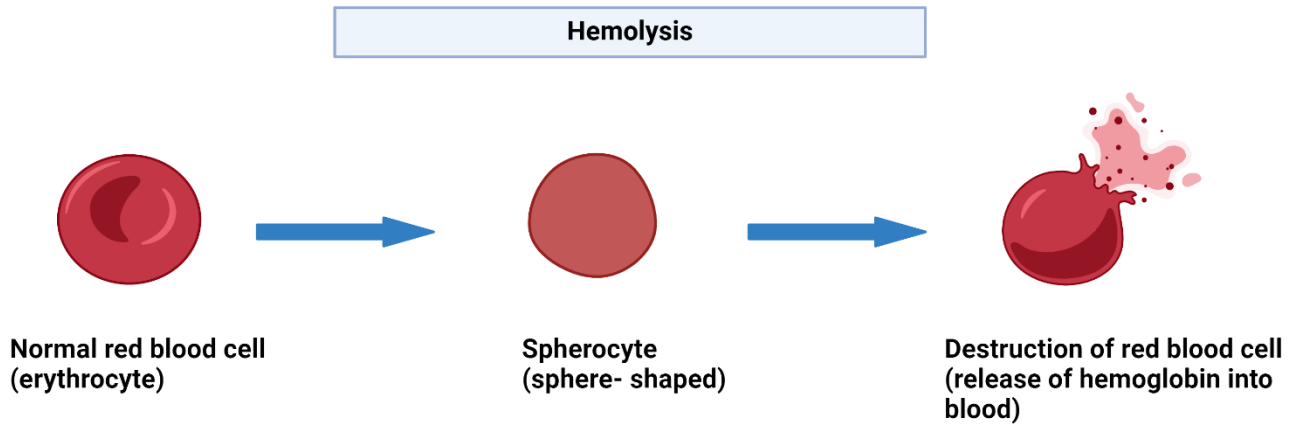

Figure 4. Transformation of normal erythrocytes to spherocytes and hemolysis. This figure depicts the transition from erythrocytes to spherocytes, resulting in hemolysis, where the cells break apart, releasing Hb into the bloodstream. Illustration created with Biorender.com

3.6 Anemia

Anemia is associated with RBC dysfunction which is a prevalent hematological condition defined by a decreased oxygen-carrying capacity of the blood due to a reduction in Hb levels or RBC count, leading to tissue hypoxia. This condition can arise from diverse etiologies, including nutritional deficiencies such as iron, vitamin B12, and folate, acute or chronic blood loss, and underlying pathological disorders, including chronic kidney disease, and inflammatory conditions (Badireddy, Baradhi, & Wilhite, 2024). Anemia is clinically defined as a reduction In Hb levels, hematocrit, and RBC count below defined reference ranges (Badireddy et al., 2024). Anemia results from an imbalance between the production of RBCs in the bone marrow and their destruction, with approximately 1% of RBCs being naturally removed daily under normal conditions. The primary mechanism contributing to anemia include increased destruction of erythrocytes and deficient or defective erythropoiesis. Increased RBC destruction may result from blood loss, which can be acute or chronic. Iron deficiency anemia is the most prevalent form of anemia, affecting approximately 8% to 9% of the global population. Anemia can be broadly categorized into acute and chronic types. Acute anemia typically results from sudden blood loss or hemolysis, whereas chronic anemia arises from various underlying causes. The symptoms of chronic anemia are primarily attributable to reduced oxygen carrying capacity of the blood and the resulting tissue hypoxia. The severity of these symptoms is influenced by factors such as the rate of decline in Hb or hematocrit levels (Badireddy et al., 2024; Turner, Parsi, & Badireddy, 2024).

3.7 The effect of anemia on infarcted cardiac tissue

Acute anemia has been shown to restrict blood flow, leading to hypoxia in the heart. In patients with AMI, anemia worsens coronary blood flow, resulting in an imbalance in oxygen transport levels. Studies have confirmed a strong association between anemia and higher mortality in patients with AMI. Additionally, myocardial ischemia induced inflammation, can result in a decrease in Hb levels, contributing to anemia in AMI patients (Padda et al., 2021; Riley et al., 2013; Shacham, Leshem-Rubinow, Ben-Assa, Roth, & Steinvil, 2014). Both acute and chronic anemia have significant effects on the cardiovascular system. Chronic anemia leads to more critical and long-term issues, while acute anemia alters the short time effect on the blood circulation, however, these changes can be restored after anemia treatment. Chronic anemia leads to thickening and enlargement of the heart´s left ventricle over time, resulting in volume overload (Metivier, Marchais, Guerin, Pannier, & London, 2000). This condition forces the heart to pump harder to compensate for the insufficient oxygen level, activating compensatory mechanisms such as an increase in heart rate (HR) and cardiac output (CO) as well as enhanced blood pumping activity (Martin et al., 1998). AMI reduces the body´s ability to deliver oxygen, which decreases myocardial blood flow during the relaxation phase and increasing the risk of bleeding during surgical procedure (Danesh, Collins, Peto, & Lowe, 2000; Madjid & Fatemi, 2013; Mozos, 2015; Steinvil et al., 2012).

3.8 Overview of immune system

The immune system defends the body against infections and disease by recognizing harmful signals and attempting to neutralize them. However, if the immune system fails in its defence, it can lead to further issues like allergies or autoimmune disease. All immune cells originate from precursors in the bone marrow, where they differentiate before maturing into fully functional cells (Fig.5). Stem cells in bone marrow develop into a variety of cell types. Innate immune cells, including neutrophils, eosinophils, basophils, mast cells, monocytes, dendritic cells, and macrophages are primary responders to infection. These cells are produced from a common myeloid progenitor stem cell found in bone marrow. Adaptive immune cells, such as B-cells and T-cells, are produced from the common lymphoid progenitor and are responsible for building an adaptive defence based on immunological memory from previous exposures. Natural killer (NK) cells, which are originated from the lymphoid progenitor, share characteristics of both innate and adaptive immune cells. These cells possess the ability to remember memories like adaptive cells, while also providing a rapid defence like innate cells**.** NK, T, and B cells are known as lymphocytes**.** Immune cells are constantly moving through the bloodstream to monitor for potential threats. The lymphatic system, consisting of vessels and tissues like lymph nodes, plays a crucial role in facilitating communication between bloodstream and tissues (Fang et al., 2018; Mozos, 2015).

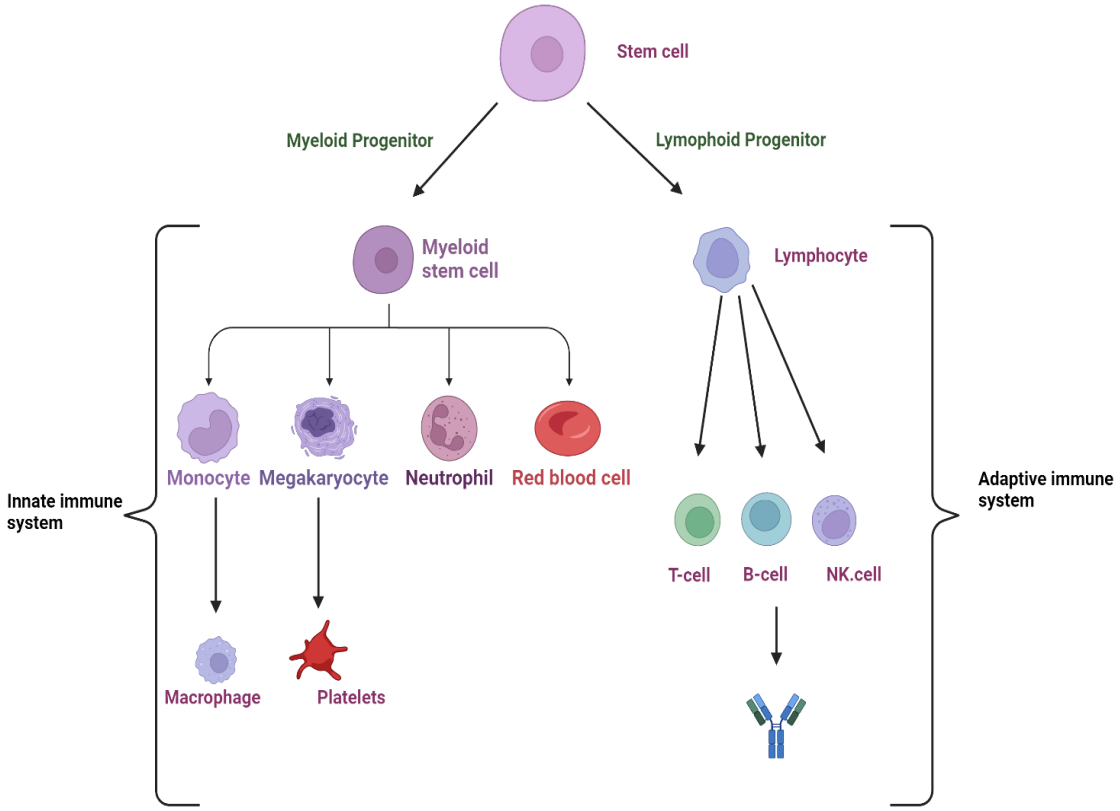

Figure 5. Hematopoiesis and differentiation of stem cells into immune cell lineage. The figure presents a flowchart of hematopoiesis, illustrating the differentiation of hematopoietic stem cells into myeloid and lymphoid progenitors, which then give rise to various immune cell lineage. Illustration created with Biorender.com.

3.9 Neutrophils and their role in myocardial infarction

Neutrophils are the first immune responders, which are immediately attracted to sites of infection where they play a critical role in innate immune response (Kolaczkowska & Kubes, 2013). Neutrophils produce ROS to eliminate pathogens. They also contribute to both acute and chronic inflammation, playing a crucial role in autoimmune diseases (Kolaczkowska & Kubes, 2013). Neutrophils are produced in the bone marrow, where they have a lifespan of approximately 10 days. After releasing in bloodstream, they circulate for around 24 hours before migrating into the tissues, where they remain active for 2 to 3 days (Tak, Tesselaar, Pillay, Borghans, & Koenderman, 2013). The production and release of neutrophils are tightly controlled by cytokines, transcription factors, and growth factors (Kaushansky, 2006; Lichtman, Chamberlain, Weed, Pincus, & Santillo, 1977; Tahir & Zahra, 2024; Tenen, Hromas, Licht, & Zhang, 1997). Neutrophils utilize three primary mechanisms against pathogens: neutrophil extracellular trap (NET) formation, degranulation, and

phagocytosis (Fig.6). These processes employ both oxidative and non-oxidative pathways to improve antimicrobial activity and reduce tissue damage (Segal, 2005; Winterbourn, Kettle, & Hampton, 2016). During phagocytosis, neutrophils capture microorganisms into a phagosome, a specific cell organelle (Nordenfelt & Tapper, 2011). This compartment limits damage to surrounding cells, allowing neutrophils to accumulate antimicrobials directly on the pathogen. Within the phagosome, granules release antimicrobial proteins, and the NADPH oxidase complex produces superoxide. This supports the enzyme myeloperoxidase (MPO) production in neutrophils, which effectively neutralizes pathogens (Klebanoff, Kettle, Rosen, Winterbourn, & Nauseef, 2013; Ulfig & Leichert, 2021; Valenta, Erard, Dupre-Crochet, & Nubetae, 2020). In addition to phagocytosis, neutrophils release ROS and antimicrobial enzymes to target pathogens. The formation of NETs is another essential mechanism. This process involves the decondensation of chromatin, which interacts with antimicrobial proteins from granules to form protein-DNA traps and neutralize pathogens. (Burgener & Schroder, 2020; Burn, Foti, Marsman, Patel, & Zychlinsky, 2021; Papayannopoulos, 2018). It is well known that neutrophils are rapidly recruited to the ischemia myocardium following AMI, where they play a critical role in initiating the inflammatory response (Epelman, Liu, & Mann, 2015; Puhl & Steffens, 2019). Tissue repair is another critical function of neutrophils, that they can also cause myocardial damage through the release of granular enzymes, pro-inflammatory mediators, and ROS (Carbone, Nencioni, Mach, Vuilleumier, & Montecucco, 2013; Ma, Yabluchanskiy, & Lindsey, 2013). During infections, the body employs emergency granulopoiesis to increase neutrophil production in bone marrow. In extreme cases, the spleen contributes to neutrophil production through extramedullary hematopoiesis (Kim, 2010). Some studies confirm that neutrophils are present in most tissue, including the heart, under normal conditions (Casanova-Acebes et al., 2018). After MI, neutrophils infiltrate the damaged myocardium within hours (Epelman et al., 2015; Puhl & Steffens, 2019). They are attracted by inflammatory signals and release of damage-associated molecular patterns (DAMPs) from the damaged heart tissue (Peiseler & Kubes, 2019). DAMPs activate immune cells to recruit additional neutrophils via chemokines receptors and adhesion molecules on endothelial cells (Futosi, Fodor, & Mocsai, 2013; Peiseler & Kubes, 2019). Infiltration of neutrophils in ischemic myocardium leads to production of ROS in a process known as respiratory burst, which can modify proteins, lipids, and amino acids, resulting in tissue damage (Amulic, Cazalet, Hayes, Metzler, & Zychlinsky, 2012; Ma et al., 2013).

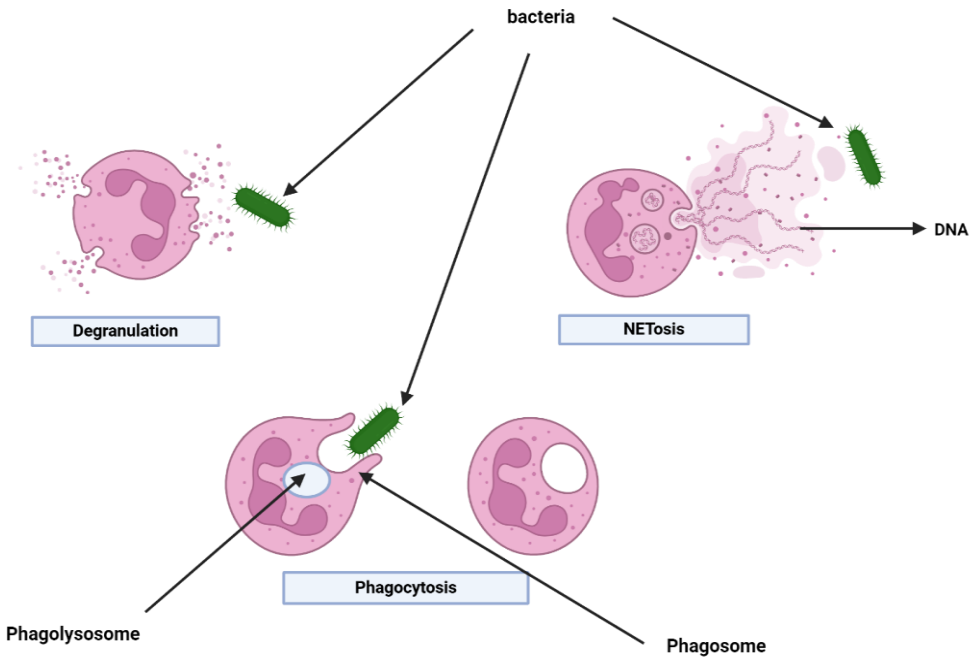

Figure 6. Overview of antimicrobial mechanisms in neutrophils. The figure illustrates the key antimicrobial mechanisms of neutrophils, including degranulation, NETosis, and phagocytosis, which are essential for immune defence against pathogens. Illustration created with Biorender.com.

3.10 Monocytes and macrophages role in infarcted cardiac tissue

Monocytes and macrophages are essential components of the innate immune system, playing critical roles in pathogen clearance and the removal of dead cells through phagocytosis. Phagocytes contribute to both the initiation and resolution of inflammation by releasing inflammatory cytokines, producing ROS, and activating the adaptive immune system (Auffray, Sieweke, & Geissmann, 2009). Both cell types are produced from a common myeloid progenitor in bone marrow. Monocytes, which are short-lived cells, enter the bloodstream before the initiation of programmed apoptosis. (Fahy, Doseff, & Wewers, 1999). However, under specific differentiation signals, monocytes can avoid apoptosis by transforming into macrophages, which are long-live cells found in all organs (Wiktor-Jedrzejczak & Gordon, 1996). These macrophages contribute to immune defence and tissue repair. The balance between survival and cell death in monocytes and macrophages is regulated by apoptosis and survival proteins (Voss et al., 2007). In response to damaged signals, monocytes can block apoptotic pathways, ensuring their survival and enabling them to support long-term inflammatory response (Goyal et al., 2002). Through this regulatory mechanism, monocytes and macrophages maintain the inflammatory process during immune system stress (Parihar, Eubank, & Doseff, 2010; Savill & Fadok, 2000). Macrophage number is increased following AMI or cardiac injury

(White, Mallory, & Salcedo-Salgar, 1936). Macrophages have dual functions in both tissue damage and repair mechanisms. Macrophages help regulate the heart´s inflammatory response post-AMI. In the early phase of heart repairing, phagocytosis is their primary function as they eliminate dead cells, coupled with efferocytosis, which removes apoptotic cells (Wan et al., 2013). These mechanisms drive macrophages toward an anti-inflammatory phenotype, which is essential for shifting from inflammation to tissue repair (Frangogiannis et al., 2003; Hilgendorf et al., 2014; Mouton et al., 2018). AMI induces cytokines signalling and alteration in the extracellular matrix within the infarcted heart. In response, macrophages secrete molecules that induce fibrosis and blood vessel formation, facilitating the repair of damaged tissue (Kubota & Frangogiannis, 2022; Sager et al., 2016). During the early phase of inflammation, macrophages are activated to initiate the inflammatory response. This activation leads to the production of pro-inflammatory cytokines and chemokines, which recruit additional myocyte-derived macrophages to the infarcted region. These infiltrating macrophages act as professional phagocytes, clearing dead cells from the infarcted site (Kubota & Frangogiannis, 2022).

3.11 B-cells and T-cells role in infarcted cardiac tissue

The adaptive immune system consists of B cells and T cells, also known as B and T lymphocytes, and is defined by its capacity to recognize specific antigens and generate targeted effector responses, establishing long-term immunological memory. B cells and T cells produce from common lymphoid progenitor in the bone marrow, however, T cell development requires additional differentiation in the thymus, whereas B cells mature in the bone marrow and are released into peripheral tissues. Thymic development involves the recombination of gene segments to produce antigen-specific T cell receptor (TCR) and the maturation of T cells within the thymus. This process facilitates that T cells detects antigens presented by the self-Major Histocompatibility complex (self-MHC) molecules while clearing cells that could attack the body´s own tissues to inhibit activation of autoimmune responses. After their development, naiive T cells leave the thymus and circulate through secondary lymph organs, such as lymph nodes and spleen. Naiive T cells are activated in these regions in the presence of antigen-persisting dendritic cells (DCs), which stimulate their proliferation and differentiation into effector T cells. These effector T cells migrate to sites of infection, where they enhance inflammation against infected cells and help B cells in producing antibodies and switching classes including various immune functions (Kaveri, Silverman, & Bayry, 2012; Thapa & Farber, 2019). B cells and T cells also play critical roles in tissue remodelling and repairing following MI. After MI, effector T cells are activated in lymph nodes and quickly infiltrate the damaged cardiac tissue (Hofmann & Frantz, 2015). Initially, B cells respond to ischemia by producing pro-inflammatory cytokines, which reduce cardiac contraction and contribute to cardiomyocyte apoptosis (Nian, Lee,

Khaper, & Liu, 2004). Subsequently, B cells infiltrate the infarcted cardiac tissue and, in response to specific signals, produce anti-inflammatory cytokines like interleukin-10 (IL-10) to migrate myocardial injury and maintain myocardial function (L. Wu et al., 2019). Research suggests that monocytes and macrophages also play a defending role in adaptive immunity by regulating T cells recruitment. CD4+ cells, which act as co-receptors, can differentiate into various subtypes, including regulatory T (Treg) cells and helper T cells, each with distinct roles in the injury and repair processes of infarcted cardiac tissue (Blanton, Carrillo-Salinas, & Alcaide, 2019; Sun, Li, & Jin, 2021).

3.12 NK cells role in infarcted cardiac tissue

NK cells are a type of cytotoxic lymphocyte that act as early responders in the innate immune system. They constitute around 15% of circulating lymphocytes in peripheral blood (Bjorkstrom et al., 2010). These immune cells were initially discovered for their natural ability to kill target cells without prior activation (Robertson & Ritz, 1990). NK cells play a critical role in the defence against infections by secreting different cytokines in both innate and adaptive immunity (Morice, 2007; Trinchieri, 1989). In AMI, NK cells contribute to the development and progression of AMI by releasing pro-inflammatory cytokines (Biron, Nguyen, Pien, Cousens, & Salazar-Mather, 1999). Studies have shown a reduction in NK cell numbers in certain cardiovascular conditions, due to an increased rate of spontaneous apoptosis. This may reduce their regulatory functions in cardiac health (Backteman, Ernerudh, & Jonasson, 2014; Ortega-Rodriguez et al., 2020).

3.13 Objectives

Anemia is highly associated in patients with AMI (Shu et al., 2006). This thesis aims to investigate the effect of both acute and chronic anemia on heart function in relation to immune cell infiltration. We hypothesize that both acute and chronic anemia are associated with the worsening of heart function after AMI, which is further linked to increased oxidative stress, promoting neutrophil infiltration. To investigate this, established mouse models of acute and chronic blood loss anemia will be used. Cardiac function will be evaluated using echocardiography to measure CO, HR, Stroke volume (SV), Ejection fraction (EF), End-diastolic volume (EDV), and End-systolic volume (ESV) in both acute and chronic anemic mouse models at baseline, 24 h and 7 days post-IR injury, with and without N-Acetyl-Cysteine (NAC) treatment. Next, using flow cytometry, we will analyze immune cell infiltration before and after AMI in acute and chronic anemic mice, with a particular focus on neutrophil infiltration in cardiac tissue under both conditions with and without AMI.

Immunofluorescence staining will be performed to assess neutrophil distribution and oxidative stress in the infarcted myocardium.

4 Materials

4.1 Equipment

Table 1: List of equipment used

Name	Company
Centrifuge	Hettich
Centrifuge	Eppendorf AG
Centrifuge	Thermo Fischer Scientific
Shaker	Ditabis AG
Pipettes	Eppendorf
Microscope	Leica Microsystems
Flow cytometer (CytoFLEX LX)	Beckman Coulter
Syringe	Braun
Falcon 50 ml	Greiner bio-one
Falcon 15 ml	Greiner bio-one
Filter 100 µm	Miltenyi Biotech
Filter 40 µm	PluriSelect Life Sciences
Scale	Sartorius AG
Petridish	Greiner bio-one
Microscope	Leica
VisualSonics Sonography system	VisualSonics Inc.
Thermosonic gel	Parker Laboratories Inc.
Computer	VisualSonics Inc.
Vortex	VWR

4.2 Chemicals

Table 2: List of chemicals used

Name	Company
Enzyme D	Milteny Biotec
Enzyme R	Milteny Biotec
Enzyme A	Milteny Biotec
RPMI-Medium	Sigma-Aldrich
PBS (Phosphate buffered saline)	Sigma-Aldrich
Lysis buffer pH 7,4 (isotonic ammonium chloride solution)	UKD-Pharmacy
Debris removal solution	Milteny Biotec
Counting beads (CountBright™ Absolute Counting Beads)	Invitrogen
Zombie Aqua mix	BioLegend
Facs buffer (BSA + PBS)	Prepared in lab
Digestion solution	Prepared in lab
Mili -Q water	MiliporeSigma
Flow clean cleaning Agent	Beckman Coulter
Face beads QC Droplets	Beckman Coulter
Facs beads IR Droplets	Beckman Coulter
FC block (TruStain FcX™)	BioLegend
VersaComp Antibody Capture Bead Kit	Beckman Coulter
Saponin Quilaja sp.	Sigma-Aldrich
Fish Gelatine	Sigma-Aldrich
PBS (Phosphate buffered saline)	Sigma-Aldrich
Bovine Serum Albumin (BSA) Fraction V	Carl Roth
Quenching Kit (Vector TrueView Reagent A, B, C)	Vector laboratories
ProLong™Diamond Antifade Mountant with DAPI	Invitrogen

4.3 Antibodies

4.3.1 Flow cytometry Antibodies

Table 3: List of antibodies used for flow cytometry

Antibody	Conjugated fluorophore	Host species	Target	Clone	Catalog number	Company
Anti-CD19	FITC	Mouse	CD19	MB19-1	101506	BioLegend
Anti-CD3 (epsilon)	APC	Armenian Hamster	CD3	145-2C11	100312	BioLegend
Anti-CD11b	APC	Rat	CD11b	M1/70	101226	BioLegend
Anti-Nk1.1	PE-Cy7	Mouse	Nk1.1	PK136	108714	BioLegend
Anti-Ly6C	PE	Rat	Ly6C	HK1.4	128008	BioLegend
Anti-Ly6G	PreCP/Cyanine 5.5	Rat	Ly6G	1A8	127616	BioLegend
Anti-CD45	Brilliant Violet 421™	Rat	CD45	30-F11	103134	BioLegend

Table 4: List of fluorescent-labelled antibodies

Antibody	Information	Stock concentration
CD45	Leucocytes	0.2 mg/ml
CD11b/LY6C	Monocytes	0.2 mg/ml
LY6G	Neutrophils	0.2 mg/ml
CD3	T cells	0.2 mg/ml
CD19	B cells	0.5 mg/ml
NK1.1	NK cells	0.2 mg/ml

4.3.2 Immunohistochemistry antibodies

Table 5: Primary antibodies for histological staining

Primary Antibody	Host species	Target	Dilution	Catalog number	Company
4-Hydroxynoned (4-HNE)	Rabbit	CMs	1:200	Ab46545	Abcam
Ly6G	Mouse	Neutrophils	1:50	551459	BD-pharmingen

Table 6: Secondary antibodies for histological staining

Secondary Antibody	Related primary antibody	Conjugated fluorophore	Host species	Catalog number	Company	Dilution
Goat anti-Rabbit	4-hne	Alexa TM Fluor plus 555	Goat	A32732	Invitrogen	1.1000
Goat anti-Mouse	Ly6G	Alexa TM Fluor 594	Goat	A21422	Invitrogen	1.1000

Table 7: List of primary antibody dilutions for histological staining

Primary antibody	Stock concentration	Used concentration
4-HNE	1 mg/ml	0.003 mg/ml
Ly6G	0.5 mg/ml	0.006 mg/ml

Table 8: List of secondary antibody dilutions for histological staining

Secondary antibody	Stock concentration	Used concentration
Goat anti-Rabbit Alexa Fluor 555 (for 4-HNE)	2 mg/ml	0.002 mg/ml
Goat anti-Mouse Alexa Fluor 680 (for Ly6G)	2 mg/ml	0.002 mg/ml

Table 9: Overview of the software used

Name	Company
GraphPad Prism (v8.0.2 (263))	GraphPad Software
BioRender	BioRender software
Office (Word,Excel,Powerpoint)	Microsoft
VevoLab	Fujofilm VisualSonics
CytoExpert	Beckman Coulter
Leica Application Suite X Life Science	Leica Microsystems

5 Methods

5.1 Mouse models

All animal experiments were approved by the State Office for Nature, Environment, and Consumer Protection of North Rhein- Westfalen (LANUV), in accordance with the European Convention for the Protection of Vertebrate Animals. The approved protocols were assigned the following numbers: 84-02.04. 2018.A234 and 84-02.04. 2020.A073. The mouse models used in these experiments were well established previously by our research group and others.

5.2 Induction of anemia in mice

C57BL/6J mice (10–12 weeks old) were used to induce anemia and were divided into three groups: a control group without anemia (n=8), referred to as the “sham group”, and groups with acute (n=8) or chronic anemia (n=8). To induce mild acute anemia, repeated blood withdrawals were performed through blood withdrawal sampling from the facial vein, for three consecutive days. At the end of the third day, mice with Hb levels below 10 g/dl were selected for further experiments (Fig.7). To induce chronic anemia, initially blood was withdrawn for the first three consecutive days, followed by every three days over a time of six weeks. After six weeks, mice with Hb levels <10 g/dl were selected for further experiments (Fig.8).

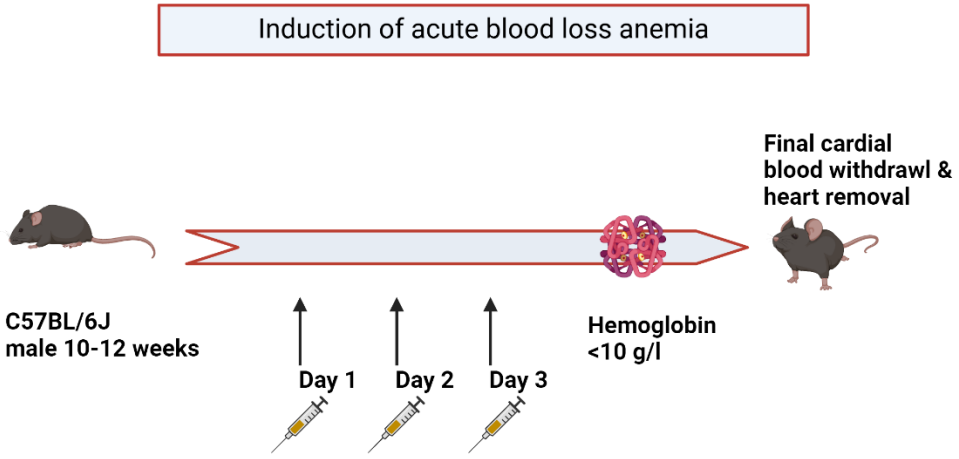

Figure 7. Induction of acute anemia in male C57BL/6J mice. Male C57BL/6J mice (10-12 weeks old) were used to induce acute anemia through daily blood withdrawals over a three-day period to reduce Hb levels. Illustration created with BioRender.com.

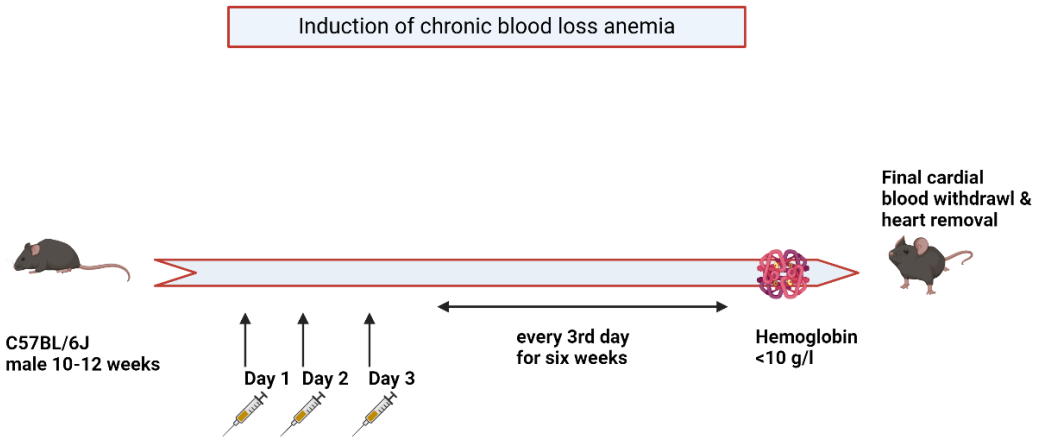

Figure 8. Induction of chronic anemia in male C57BL/6J mice. Male C57BL/6J mice (10-12 weeks old) were selected to induce chronic anemia through daily blood withdrawals for three days, followed by withdrawals every third day for six weeks. Illustration created with BioRender.com.

5.3 Induction of AMI by IR surgery in mice

To mimic AMI, ischemia/reperfusion (I/R) surgeries were performed in acute and chronic anemic mice. Before the surgery the mice were injected with analgesic Temgesic (0.05 - 0.1 mg/kg) 30 minutes before surgery to reduce pain. Next, mice were anesthetized with 3% isoflurane inhalation in a chamber, and a tube was inserted into the trachea for mechanical ventilation. A rodent ventilator provided 2% isoflurane in oxygen- enriched air (40% oxygen) at a rate of 140 breaths per minute. Body temperature was continuously measured and maintained at 37°C using a heating lamp and a heated operating table. During this procedure, an ECG was continuously recorded to monitor cardiac activity. The skin was disinfected with Octenisept, and a 1.5 cm incision was made on the chest region. The muscle layer was opened, and the chest wall was kept intact. A lateral thoracotomy was performed with a 1 cm incision to open the chest under. Two ends of the Prolene suture were placed around the left anterior descending coronary artery using a polyethylene cannula. The suture was tightened to block the artery, causing ischemia, as evidenced by the graying of the heart tissue. The suture was then fixed, and ST-segment elevation on the ECG was used to confirm proper occlusion and documented via printout. The chest was kept moist during the ischemic period by using warm sodium chloride (0.9%). The heart was kept in an ischemic state for 45 minutes. After 45 minutes, the suture was released to restore blood flow (reperfusion). The chest was closed in layers using 4/0 silk for the ribs and muscle layer and 5-0 Prolene for the skin. The isoflurane was discontinued, by which the animal was slowly awakened. The animal was placed in a mask with oxygen-enriched air until it began breathing normally. To relieve pain after surgery, Temgesic (0.1 mg/kg) was

administered every 6-8 hours. Mice were sacrificed 24 hours after surgery for further experiments. This protocol was performed with the support of Stefanie Becher.

5.4 NAC treatment in the anemic mice

To evaluate the effect of oxidative stress in anemia on AMI, additional group of acute and chronic anemic mice were treated (1%, drinking water) with NAC, which is a precursor to cysteine (Fig.9,10).

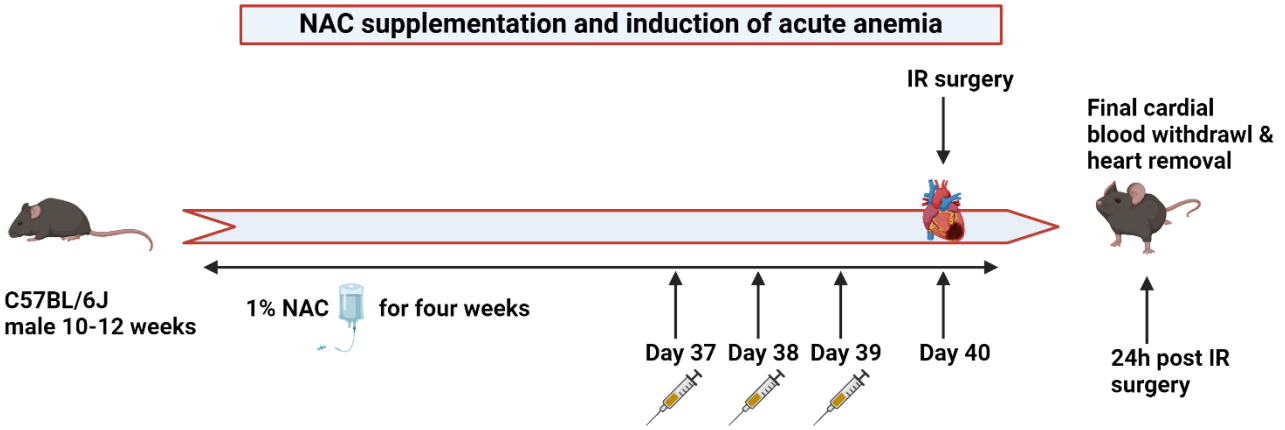

Figure 9. Induction of acute anemia in male C57BL/6J mice following NAC treatment. Male C57BL/6J mice (10-12 weeks old) were given 1% NAC in their drinking water for four weeks. Acute anemia was induced starting on day 36 of NAC supplementation. Illustration created with BioRender.com.

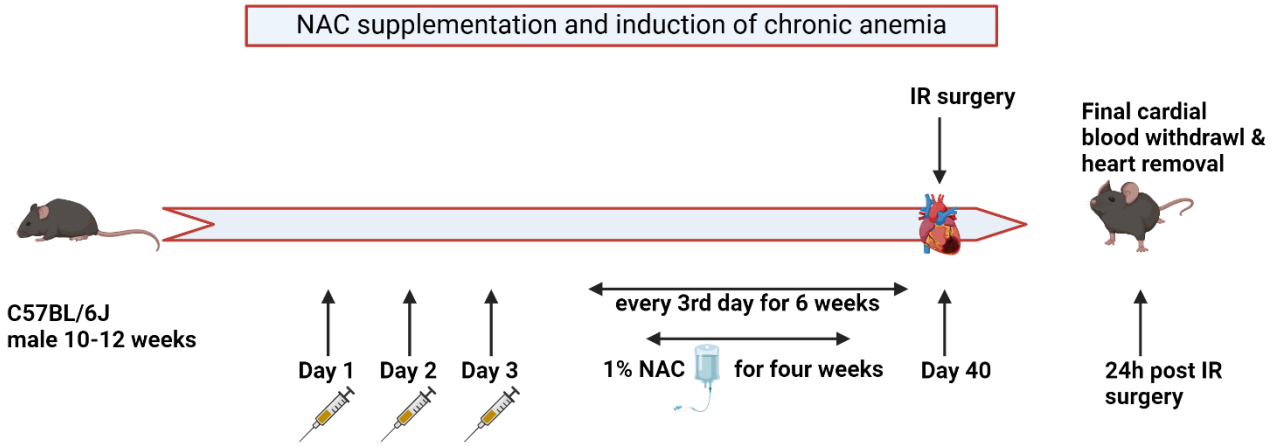

Figure 10. Induction of chronic anemia in male C57BL/6J mice following NAC treatment. Male C57BL/6J mice (10-12 weeks old) were given 1% NAC in their drinking water for four weeks. Chronic anemia was induced starting on day 15 of NAC supplementation. Illustration created with BioRender.com.

5.5 Echocardiography

A Fujifilm VisualSonics Vevo 3100 (Toronto, Canada) high-frequency imaging platform equipped with an 18-38 MHz linear microscan transducer, was used to analyze cardiac function. Echocardiography was performed on both anemic and non-anemic mouse groups 24 hours and 7 days post- AMI. Mice were first anesthetized by placing them in an induction chamber with 2.5-3% isoflurane and oxygen-enriched room air. After anesthesia induction, the mice were positioned on a heated examination table, where their electrocardiogram, respiratory rate, heart rate, and body temperature were monitored regularly. A breathing mask was used to maintain anesthesia throughout the procedure. To improve the quality of cardiac imaging, chest hair was removed using a chemical depilatory (Veet, Heidelberg, Germany). The chest area was covered with pre-warmed Aquasonic 100 gel (Parker Laboratories, Fairfield, USA) to facilitate sound transmission. Imaging was performed using the parasternal long-axis view, and the Vevo LV tracking function was utilized to measure various cardiac parameters including left ventricular volumes, EDV, ESV, CO, SV, HR, and EF in both diastolic (Fig.12) and systolic (Fig.13) states of the heart. This allowed for the identification of maximum and minimum cross-sectional areas. Data analysis was performed using Vevo Lab software developed by Fujifilm VisualSonics (Japan), which quantifies cardiac parameters. The ultrasound imaging was performed by Isabella Solga.

5.5.1 The Procedure for using the L-Trace function to measure cardiac parameters in mice

5.5.1.1 Measurement of heart function

The measurements were performed using the LV-Trace program within the VevoLab software, allowing for the precise identification of cardiac parameters by analyzing the heat structure and function in real time.

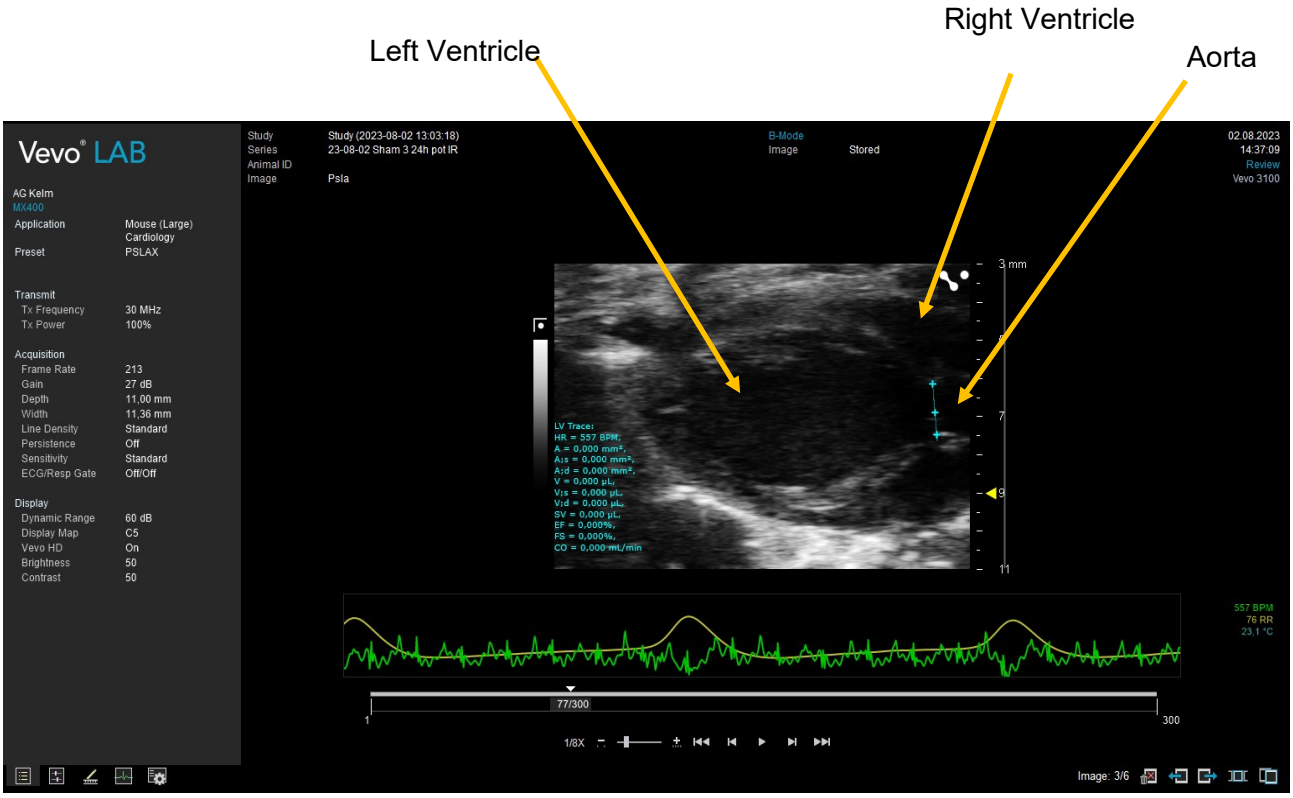

Figure 11. L-Trace function. Demonstrating anatomical structures of the heart, including left and right ventricles and the aorta. Image generated using VevoLAB software.

Figure 12. L-Trace in diastolic state of the heart. It depicts the diastolic phase of the heart, highlighting the relaxation and filling of the ventricles. Image generated using VevoLAB software.

Figure 13. L-Trace in systolic state of the heart. Illustration systolic phase of the heart, highlighting the contraction and ejection of blood from the ventricle. Image generated using VevoLAB software.

5.5.1.2 Measurement of heart wall thickness

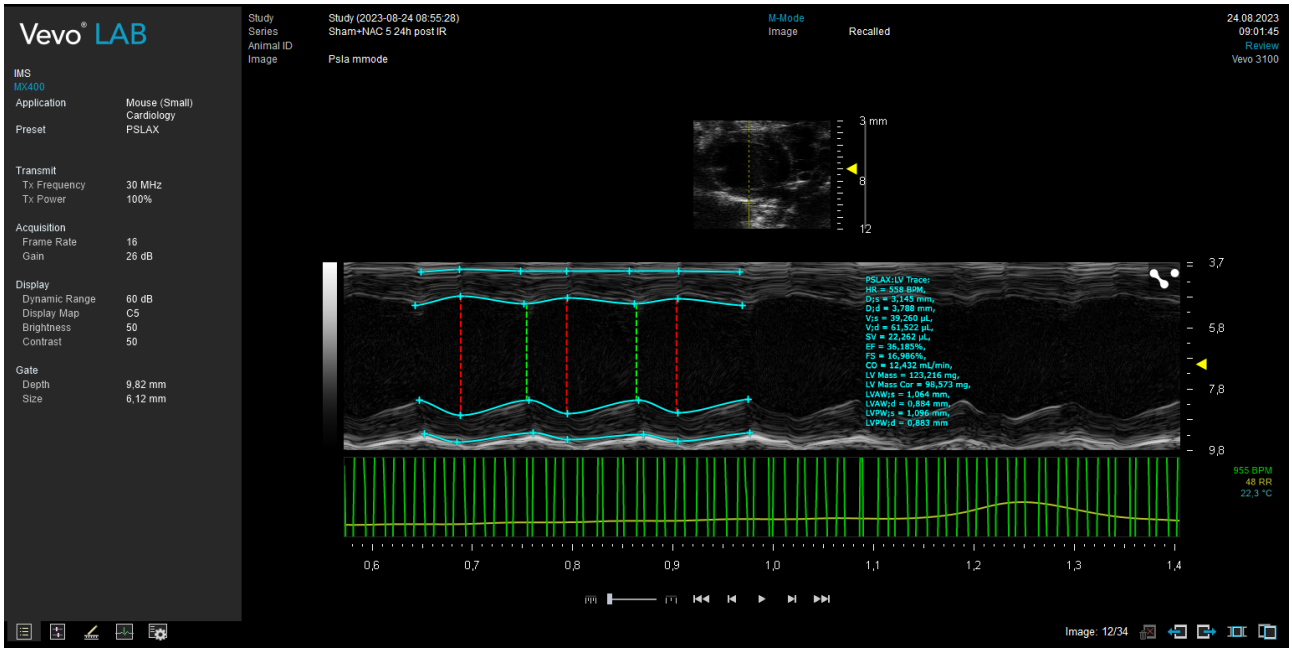

Figure 14. Heart thickness measurement by L-Trace. Using the L-Trace function to measure heart wall thickness during cardiac cycle. Image generated using VevoLAB software.

5.6 Flow cytometry

Flow cytometry enables analysis of single cells and fluorescent parameters simultaneously. Each particle is measured for visible light scatter and fluorescence parameters. Light scatter is analyzed in two different directions: forward scatter (FSC), which demonstrates the proportional size of the cell, and side scatter (SSC), which reflects the internal complexity or granularity of the cells (McKinnon, 2018). Staining with targeted antibodies, specific immune cell populations within cardiac tissue were assessed using the CytoFLEX LX flow cytometer (Beckman Coulter). Immune cell infiltration was quantified in both acute and chronic anemic mice groups, with and without AMI.

5.6.1 Heart preparation for flow cytometric analysis

5.6.1.1 Heart digestion

Male C57BL/6J mice (10-12 weeks old) were anesthetized via injection with ketamine (100 mg/kg body weight) and xylazine (10 mg/kg body weight). The anesthesia of the mice was confirmed by lack of the reflexes. Mice were sacrificed, blood was collected by heart puncture and perfused with cold Phosphate-buffered saline (PBS) to remove all blood cells. The hearts were then isolated from the body and placed in cold PBS. Next, hearts were dried with paper towels and weighed. Under a microscope, the right ventricles were carefully removed and discarded. The left ventricles were isolated and cut into approximately 1 mm pieces using a scalpel. The samples were transferred into a prepared digestion solution consisting of an enzyme cocktail (Miltenyi Biotech's Multi-Tissue Dissociation Kit 1) consisting of 60 µl of enzyme D (neutral protease), 30 µl of enzyme R (DNase) and 7.5 µl of enzyme A (collagenase) and 1.4 ml of RPMI medium. The samples were placed on a shaker and incubated for 20 minutes at 8000 x g and 37°C. Next, the tissues were filtered through a 50 ml falcon tube using a 100 µm strainer. Any remaining tissue on the strainer was pushed through with a syringe plunger. Once all tissues had passed through, the strainer was washed with 5 ml of cold PBS. The samples were then filtered again through a 40 µm strainer into a new 50 ml Falcon tube and washed with PBS to a final volume of 10 ml. The samples were centrifuged at 500 x g at 4°C for 5 minutes. The supernatant was discarded, and the pellet was resuspended in 5 ml of isotonic ammonium chloride (lysis buffer) and placed on ice for 5 minutes. Cold PBS was added to a final volume of 10 ml, followed by centrifugation at 500 x g at 4°C for 5 minutes. The supernatant was discarded, and the pellet was resuspended in 5 ml of PBS. The sample solution was transferred to a 15 ml falcon tube and kept on ice. One ml of debris removal solution (Milteny Biotec) was carefully added to create two distinct layers. After centrifugation at 500 x g at 4°C for 5 minutes, the upper clear layer and middle debris layer were carefully collected and discarded. The lower phase, above the pellet, was mixed with 5 ml of cold PBS and centrifuged at 500 x g at 4°C for 10 minutes. The supernatant was discarded, and the pellet was resuspended in 500 µl of cold PBS and kept on ice. For antibody staining, each sample was divided into two separate Fluorescence-Activated Cell Sorting (FACS) tubes: one for staining and one as an unstained negative control. A 100 µl aliquot of the sample was added to each tube (stained and unstained).

5.6.1.2 Staining of cells for flow cytometry

To facilitate accurate cell counting in each sample, 15 µl of counting beads (CountBright™ Absolute Counting Beads, invitrogen) were added to the sample. The samples were then centrifuged at 500 x g at 4°C for 5 min. After discarding the supernatant, the pellet in the unstained tube was resuspended in 50 µl of cold PBS. The pellet in the stained tube was resuspended in 50 µl of zombie mix (prepared by mixing 490 µl of PBS, 10 µl of Fc block, and 2 µl of Zombie Aqua). The sample was incubated in the dark at RT for 10 minutes. After incubation, the sample was centrifuged at 500 x g at 4°C for 5 minutes. The supernatant was discarded, and the pellets in both FACS tubes (stained and unstained) were resuspended in 100 µl of FACS buffer (0.5% bovine serum albumin (BSA) in 50 ml of PBS). Following this, different antibodies (see table 3) were added in specific amounts (according to the protocol) to the stained sample tube.and the sample was incubated in the dark for 20 minutes. After incubation, the sample was centrifuged at 500 x g at 4°C for 5 minutes. The supernatant was carefully discarded, and the pellet was resuspended in 200 µl of FACS buffer for flow cytometric analysis. Flow cytometric data were collected using the CytoFLEX LX and analyzed with the cytoExpert software.

5.6.2 Determination of absolute cell counts using counting beads

Counting beads (CountBright™ Absolute Counting Beads) were utilized to quantify immune cells. A fixed volume of 15 µl, containing a known concentration of 1000 beads/µl (provided by the manufacture), was added to each sample. After staining and acquisition using the CytoFlex LX flow cytometer, the counting beads enabled the calculation of the absolute cell count in each sample. The following formula was applied:

$$\text{Absolute cell counts} = \frac{\text{Cell count} \times \text{Bead volume}}{\text{Sample volume} + \text{Bead count}} \times \textit{Counting bead concentration}$$

5.6.3 Flow cytometry compensation

Compensation is a critical process in flow cytometry to reduce spectral overlap between different fluorescent dyes (fluorochromes). Flow cytometry detects spectral ranges of the emitted photons. Therefore, the signal of a fluorescent dye may penetrate a channel used for the detection of another

dye and spillover occurs, leading to inaccurate measurements. Proper compensation is essential to address this issue ensure accurate quantification of each fluorochrome (Szaloki & Goda, 2015). Compensation was performed according to company instructions. Additionally, antibody compensation was performed using the VersaComp Antibody Capture Bead Kit (Beckman Coulter). This kit consists of positive and negative beads. The positive beads are coated with specific antigens, enabling them to bind to antibodies of interest and thus detect the positive signal. In contrast, the negative beads are uncoated, serving as control cells that do not bind to antibodies. Since Zombie markers are not antibodies, they cannot bind to compensation beads, which are specifically designed for antibody trapping. Therefore, to facilitate proper compensation for zombie markers, we used dead and viable splenic cells. This ensures that the compensation procedure accurately accounts for any spectral overlap from the zombie marker. The spleen was placed onto a 100 µm cell strainer falcon tube. The spleen was then mashed with a 1 ml syringe plunger to break it down. The cell strainer was rinsed multiple times with cold PBS until the total volume reached 15 ml. The sample was centrifuged at 500 x g at 4 °C for 5 minutes, and the supernatant was discarded. The pellet was resuspended in 5 ml of PBS and transferred onto a 40 µm cell strainer, rinsed cell strainer several times (in total 10 ml PBS). Next, the samples were centrifuged at 500 x g at 4 °C for 5 minutes, and the pellet was resuspended in 5 ml RBC lysis buffer and incubated for 5 minutes at RT. After incubation, the sample was brought to a total volume of 15 ml with PBS and mixed carefully. The sample was centrifuged again at 500 x g at 4°C for 5 minutes. Subsequently, the supernatant was removed, and the pellet was resuspended in 6 ml of PBS and stored on ice for further experiments

Zombie dyes were used in this experiment to identify and analyze dead cells within a sample. The dyes cannot enter living cells due to the integrity of their cell membrane. As a result, the dye binds only to dead cells which have impaired membranes, allowing the dye to penetrate and stain them (Peña, Ball, & Squires, 2018). To compensate for the zombie dye, spleen tissue was used in the procedure. First, 500 µl of digested spleen cells were treated with 500 µl of 70% ethanol to induce cell death, which served as a negative control. After ethanol treatment, the sample was centrifuged at 500 x g at 4°C for 5 minutes. The supernatant was then discarded, and the pellet was resuspended in 500 µl of FACS buffer. This centrifugation step was repeated, and after discarding the supernatant, the pellet was resuspended in an additional 500 µl of FACS buffer. The cells were centrifuged again at 500xg, 4°C for 5 minutes. After removing the supernatant, 500 µl of viable cells (intact cells) were added to the pellet containing dead cells. Finally, 2 µl of the zombie dye were added to the sample for compensation analysis by flow cytometry.

To perform compensation for the antibody of interest, one drop of negative beads and one drop of positive beads were added to each antibody tube. The appropriate number of antibodies were then added to their respective tubes, and the tubes were vortexed immediately to ensure proper mixing.

The samples were incubated in the dark for 20 minutes. Following the incubation, 1 ml of FACS buffer was added to each test tube, and the samples were centrifuged at 300 x g at 4°C for 6 minutes. The compensation matrix for each antibody was subsequently generated using the flow cytometer (Beckman Coulter), utilizing the channel-specific compensation settings (Table 10).

Table 10: Flow cytometry channels of interest and corresponding labelled antibodies

Channel	Labelled
B525	CD19
B690	Ly6G
Y585	Ly6C
Y763	NK1.1
R660	CD3
R763	CD11b
V450	CD45
V525	Zombie

A. Zombie **B. CD19**

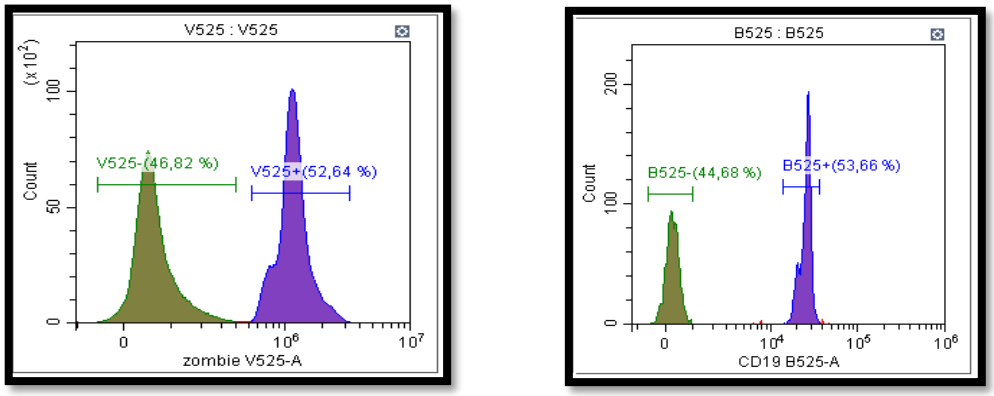

Figure 15. Representative compensation plots for zombie V525 dye staining of spleen cells and CD19 staining of positive and negative beads in the B525 channel. A: The histogram illustrates the fluorescence intensity of the Zombie V525 viability dye in splenic single cells. Two distinct populations are identified: dye-negative (viable cells, shown in green), and dye-positive (dead cells, shown in blue). B: CD19 compensation plot generated using positive and negative beads in

the B525 channel. This histogram displays the fluorescence intensity in the B525 channel with compensation beads bound to the CD19 antibody. Two peaks are observed: the CD19-positive population (blue, 53.66%) and CD19-negative population (green, 44.68%). This plot allows for accurate adjustment of compensation settings, ensuring proper separation of positive and negative populations for subsequent antibody analysis. Data was obtained through flow cytometry analysis.

Autofl.	Channel	-B525%	-B690%	-Y585%	-Y763%	-R660%	-R763%	-V450%	-V525%
2,29	B525		0,16	0,58	1,38	0,22	0,03	0,10	0,70
0,53	B690	1,34		4,08	3,67	1,90	0,28	0,03	0,14
1,92	Y585	0,01	0,06		9,88	0,05	0,00	0,01	0,09
0,06	Y763	0,00	10,45	0,56		3,84	18,72	0,00	0,00
0,07	R660	0,00	2,34	0,00	0,16		12,26	0,00	0,01
1,04	R763	0,00	17,41	0,00	10,52	17,15		0,00	0,01
7,19	V450	0,06	0,12	0,00	0,20	0,21	0,10		11,74
4,61	V525	1,69	0,15	0,02	0,29	0,27	0,10	9,29	

Figure 16. Compensation matrix for each channel. Illustrating the correction of spectral overlap in the flow cytometry analysis. Data obtained through CytoFlex LX.

5.6.4 Fluorescence Minus One Control (FMO-Control)

Fluorescence signals can interfere with signals from other channels, complicating the accurate identification of cell populations. To address this issue, the FMO control was used to establish precise gating in flow cytometry. In the presence of multiple fluorophores in the experiment, the FMO control helps distinguish positive and negative cell populations by considering the background fluorescent intensity of each antibody. To identify emission signal overlap, the FMO control procedure was performed by adding all the required antibody fluorophores to samples except for the antibody under investigation.

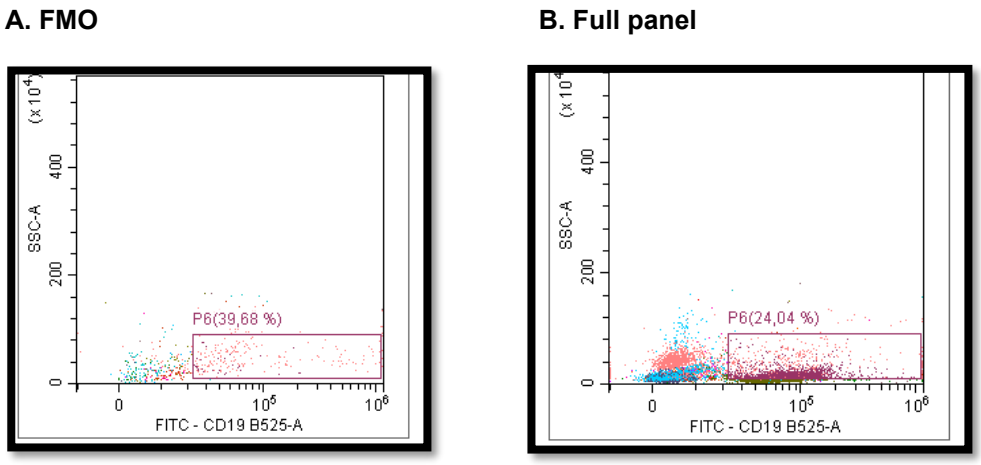

Figure 17. FMO control plot compared to full panel for identification of the CD19 population. Panel A: shows the FMO control, indicating the absence of CD19 expression in heart tissue. Panel B: displays the $CD19^{+}$ population, enabling accurate gating and determination of background fluorescence for $CD19^{+}$ population. Data was obtained through flow cytometry analysis.

5.6.5 Gating strategy

A gating strategy was employed to distinguish cell populations based on size using FSC and cellular granularity via SSC from the debris. Based on the size and therefore lower FSC the debris is in the lower left corner of the plot. By setting a gate surrounding the distinct population of cells not including the debris, the later could be excluded. In the next step, doublet discrimination using FSC-area and FSC-higher was performed to isolate single cells from potential false positive doublets (Fig. 18A). Afterwards, a viability dye (Zombie), that stains cells with compromised membranes was used to exclude dead cells within the single cell population by plotting zombie against CD45, which marks viable immune cells (Fig.18B). Subsequently, NK 1.1 and CD11b was used to identify NK cells and myeloid cells such as macrophages, dendritic cells and granulocytes (Fig.18C). Following this, Ly6G against Ly6C gating strategy was performed, as these markers help differentiation neutrophils within the immune cell population (Fig.18D). Finally, CD3 against CD19 gating strategy was applied, where CD3 identifies T cells and CD19 identifies B cells, enabling the differentiation of these adaptive immune cells within the immune population (Fig.18 E).

A

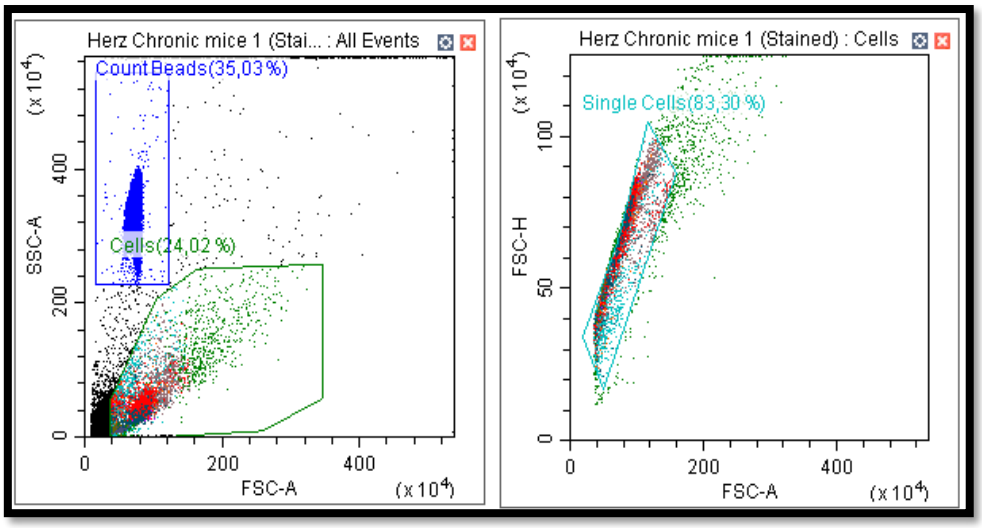
Herz Chronic mice 1 (Stai... : All Events
CountBeads(35,03 %)
Cells(24,02 %)
SSC-A
FSC-A
Herz Chronic mice 1 (Stained) : Cells
Single Cells(83,30 %)
FSC-H
FSC-A

B

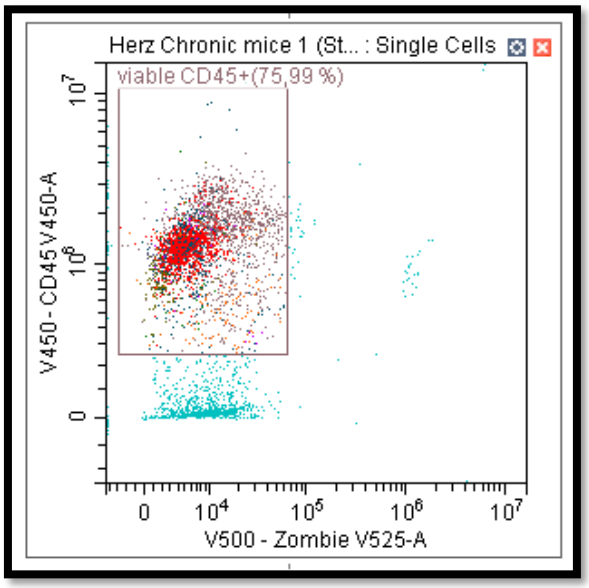
Herz Chronic mice 1 (St... : Single Cells
viable CD45+(75,99 %)
V450 - CD45 V450-A
V500 - Zombie V525-A

C

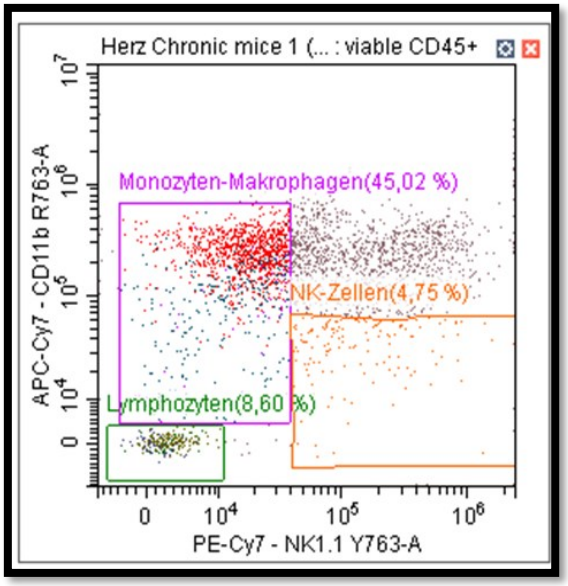
Herz Chronic mice 1 (... : viable CD45+
Monozyten-Makrophagen(45,02 %)
NK-Zellen(4,75 %)
Lymphozyten(8,60 %)
APC-Cy7 - CD11b R763-A
PE-Cy7 - NK1.1 Y763-A

D

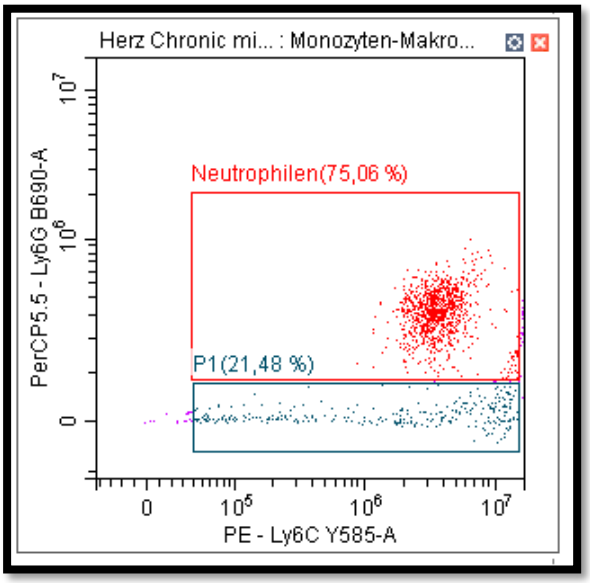
Herz Chronic mi... : Monozyten-Makro...
Neutrophilen(75,06 %)
P1(21,48 %)
PerCP5.5 - Ly6G B690-A
PE - Ly6C Y585-A

E

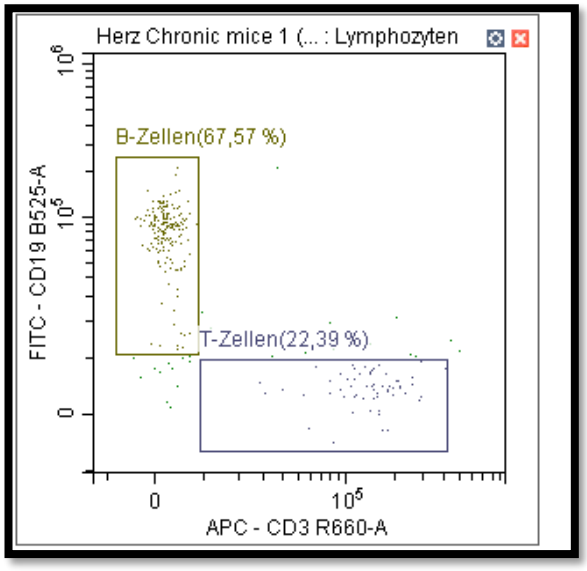
Herz Chronic mice 1 (... : Lymphozyten
B-Zellen(67,57 %)
T-Zellen(22,39 %)
FITC - CD19 B525-A
APC - CD3 R660-A

Figure 18. Gating strategy for immune cell identification in cardiac cells by flow cytometry (CytoFlex LX). Panel A: FSC against SSC plot showing the distribution of the total cell population. The x-axis represents FSC, which correlates with cell size, and the y-axis represents SSC, which indicates cell granularity. The plot includes beads for quantifying cell numbers and display the percentage of total cell counts, with a clear population boundary for debris. **Panel B:** Zombie viability dye against CD45 expression plot. The zombie dye labels dead cells, while CD45 marks immune cells. **Panel C:** This plot identifies viable $CD45^+$ immune cells, including lymphocytes, monocytes/macrophages, and NK cells, allowing for accurate identification of viable immune cell populations. **Panel D:** This panel depicts Ly6G against Ly6C expression within $CD45^+$ population, allowing for the identification of neutrophils ($Ly6G^+$) and monocytes ($Ly6C^+$). **Panel E:** CD3 against CD19 expression within the $CD45^+$ population. This panel shows the differentiation of T cell ($CD3^+$) and B cells ($CD19^+$) within the immune compartment, enabling the identification and characterization of adaptive immune cells. Data was obtained through flow cytometry analysis.

5.6.6 Normalization of immune cell counts

After performing flow cytometric analysis, immune cell counts were normalized using two parameters: total sample volume and heart weight. First, to account for variations in sample volume, immune cell counts were adjusted by multiplying the counts by the total volume of the sample used in the flow cytometry experiment. Next, to address differences in heart size between mice, the volume-normalized immune cell counts were further adjusted to a standard unit of 10 mg of heart tissue. This was achieved by multiplying the immune cell count (after volume normalization) by 10 and dividing the result by the heart weight (in mg). This normalization steps ensured that immune cell infiltration was expressed as counts 10 mg of heart tissue, enabling accurate comparisons across samples with varying heart sizes.

5.7 Immunohistochemistry

Immunohistochemistry (IHC) is a reliable method that enables the detection and localization of specific antigens within cells and tissue samples through antibody-antigen interactions. The primary antibody, which can be either monoclonal or polyclonal, plays a critical role in this process. Monoclonal antibodies target a single epitope, providing accurate targeting, while polyclonal antibodies bind to multiple epitopes. Secondary antibodies are designed to specifically bind to their corresponding primary antibodies, facilitating signals amplification and visualization (Magaki, Hojat, Wei, So, & Yong, 2019). Neutrophils, the most abundant circulating immune cells, play a critical role

in response to cardiac injury (Carai et al., 2023; Colotta, Re, Polentarutti, Sozzani, & Mantovani, 1992). Following cardiac damage, injured CMs activated resident macrophages, while endothelial cells release chemokines and DAMPs. These signals work together to facilitate neutrophil the recruitment of neutrophils to the damaged cardiac tissue (Carai et al., 2023; Denning, Aziz, Gurien, & Wang, 2019; Frantz et al., 2018; Tschope et al., 2021). Activated neutrophils enhance the inflammatory response by releasing MPO, anti-microbial proteins, ROS, and pro-inflammatory cytokines (Carai et al., 2023; Mantovani, Cassatella, Costantini, & Jaillon, 2011). In the current research work, IHC was employed to investigate ROS production and neutrophil infiltration in infarcted cardiac tissue. ROS production serves as a marker of cellular damage, while neutrophil infiltration indicates inflammation and immune response. Cardiac tissues were stained with primary antibodies targeting specific antigens, including Ly6G (a neutrophil surface marker), MPO, an indicator of neutrophil activity, and 4-hydroxynoneal (4-HNE, a marker of lipid peroxidation). Fluorescently labelled secondary antibodies were subsequently applied, enabling visualization under a Leica fluorescence microscope. This approach allowed for the identification of ROS production in CMs and neutrophils, providing insights into the extent of tissue damage and the associated inflammatory response. The following animal groups were selected for immunofluorescence staining: the sham-operated mice group (without anemia), with and without MI (n=6), serving as the control group, and the acute anemic mice group, with and without MI (n=6), 24 hours post-AMI.

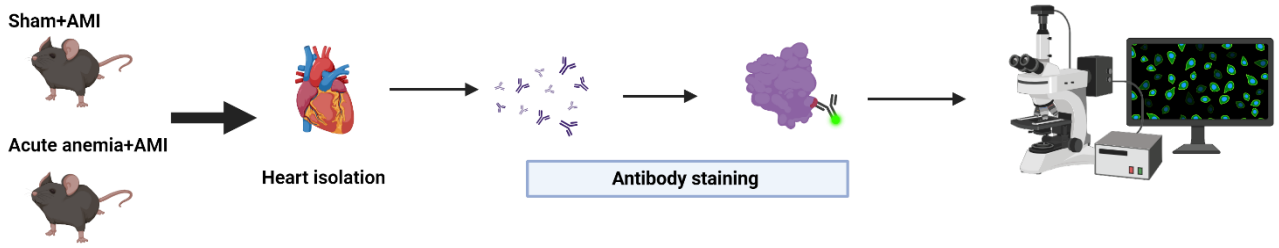

Figure 19. Overview of animal groups used for immunofluorescence staining. Immunofluorescence stainings were performed in heart sections of sham and acute mice post-MI. Illustration created with BioRender.com.

5.7.1 Sectioning the cardiac tissue

The isolated heart from mouse was fixed in a 4°C paraformaldehyde (PFA) solution (Thermo Fischer Scientific) for 30 minutes and then rehydrated overnight in a 30% sucrose solution at 4°C. The following day, the heart tissue was embedded in Tissue-Tek® (Sakura Finetek Umkirch, Germany) and stored at -80°C for subsequent staining. A cryotome (Leica CM3050 S, Wetzlar, Germany) was used for sectioning the heart. The heart was divided into three areas, A, B, and C, with a total 10 layers cut from each region, spaced by 250 µm in depth (Fig.20). For each layer, 20 sections were cut, starting from the apex. Afterwards, the heart sections were either stored at -20°C for further use or directly processed for staining.

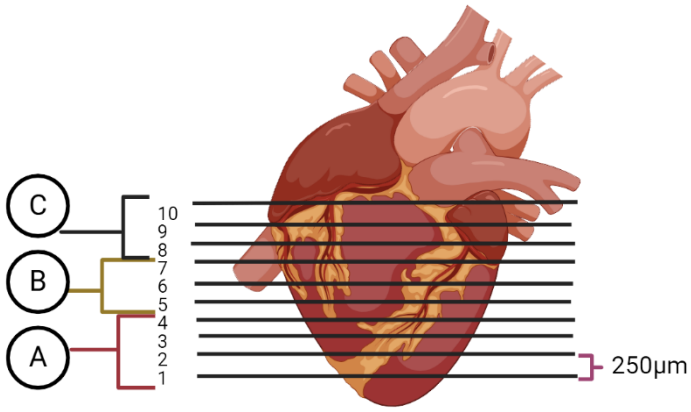

Figure 20. Illustration of heart sectioning with cryostat. The heart was divided into three regions (A, B, and C), each region contains different sections, with a 250 µm distance between adjacent sections, representing different areas of infarcted and non-infarcted tissue. Illustration created with BioRender.com.

5.7.2 Immunostaining procedure

The tissue sections were defrosted for 20-30 minutes at RT. Subsequently, the slides were rehydrated in 1x PBS three times, each for three times. To prevent nonspecific binding, the slides were incubated in a blocking solution consisting of 0.5% BSA (Karl Roth), 0.2% fish gelatine (Sigma-Aldrich), and 0.1% saponin (Quilaja sp, Sigma Aldrich) in 300 ml of 1xPBS for 1 hour at RT. After removing the blocking solution, the slides were washed three times with 1x PBS for 3 minutes each. The slides were then incubated overnight with primary antibodies (see Table 5) in a humid chamber at 4°C with antibody dilutions prepared using the blocking solution buffer. The following day, the slides were washed three times with 1x PBS and incubated with appreciate secondary antibodies diluted 1:1000 in 1x PBS for 1 hour at RT in the dark (see Table 6). After incubation, the slides were

washed three times with 1x PBS. To reduce tissue autofluorescence, the slides were treated with the Vector TrueVIEW Autofluorescence Quenching Kit (Vector Laboratories, Newark, California, United States) for 5 min in the dark (25 µl per section), followed by an additional 5-minute incubation. The slides were then washed three times in 1x PBS, and subsequently three times with distilled water. Finally, the slides were mounted with Prolong Diamond Antifade Mounting containing 4´,6-diamidino-2-phenylindol (DAPI) for 5 min to stain the nuclei. Coverslips (Engelbrecht Medizin- und Labortechnik Edeemünde, Germany), were applied, and the slides were stored in the dark at 4°C until microscopic examination. The Leica DM6 B microscope and DFC9000 camera were used to capture the images at a 20x magnification using the LAS X software. The ImageJ software was used to perform the analysis.

6 Results

6.1 Echocardiography

6.1.1.1 The effect of acute blood loss anemia on heart function 24 hours post-AMI

To investigate the effect of acute blood loss anemia on heart function 24 hours post-AMI, heart function was assessed in both anemic and sham mice using ECH. The HR was not significantly changed in anemic mice (378 ± 31 bpm) compared to the sham (458 ± 20 bpm) group of mice (Figure 21A, Table 11). The EDV was comparable between anemic mice (64 ± 60 µl) and the control (68 ± 4 µl) group of mice (Figure 21B, Table 11). Similarly, the ESV was not different between the acute anemic mice (36 ± 6 µl) and the sham (35 ± 4 µl) group of mice (Figure 21C, Table 11). The SV was similar between the acute anemic mice (31 ± 5 µl) and the sham (43 ± 4 µl) group of mice (Figure 21D, Table 11). The EF was unchanged in acute anemic mice (33 ± 5 %) compared to the control (39 ± 3 %) group of mice (Figure 21E, Table 11). The CO was significantly reduced in acute anemic mice (12 ± 2 ml/min, P=0.0133) compared to the sham (19 ± 2 ml/min) group of mice (Figure 21F, Table 11). These results conclude that cardiac output is reduced in anemic mice 24 hours after AMI.

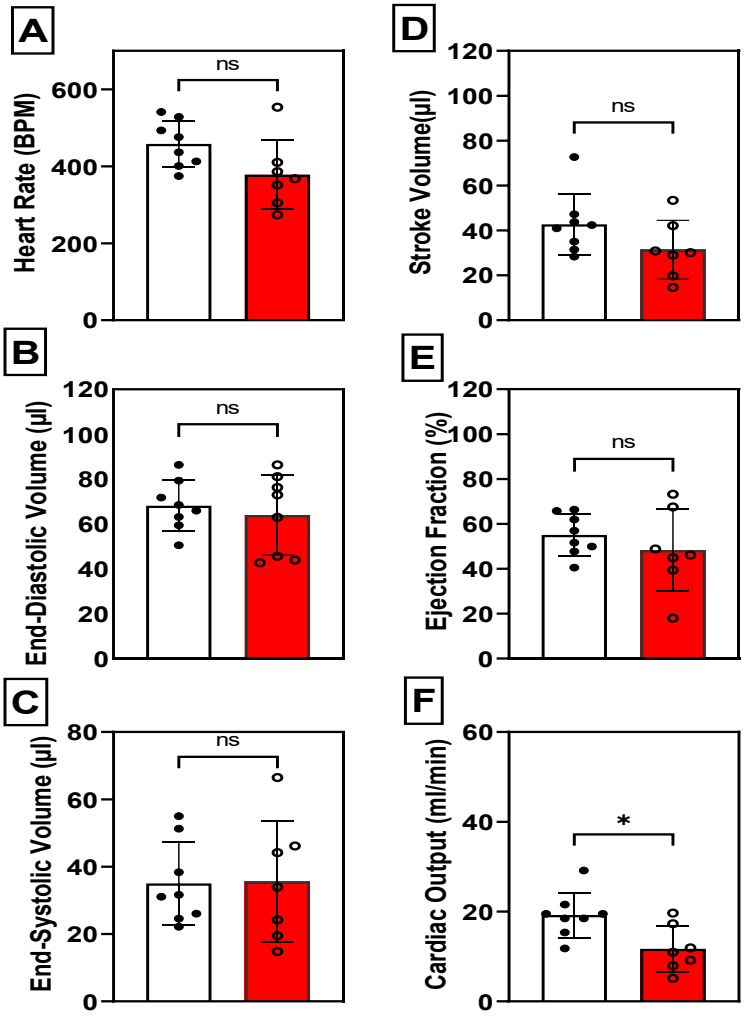

Figure 21. The effect of acute blood loss anemia on heart function 24 hours post-AMI. Echo evaluation of control (white bar) and acute blood loss anemic (red bar) mice 24 hours post-AMI. Left ventricular parameters, including HR, EDV, SV, ESV, CO, and EF, were evaluated. All values are presented as mean ± SEM. Two groups were compared using an unpaired Student ‘s t-test. *p ≤ 0.05; n.s., not significant.

Table 11: Summary of cardiac functional parameters 24 hours post-AMI in acute anemic mice

N	Acute	Sham	P-Value
Cardiac Output (CO, ml/min)	12 ± 2	19 ± 2	0.0133
Heart Rate (HR, bpm)	378 ± 31	458 ± 20	0.0638
Stroke Volume (SV, µl)	31 ± 5	43 ± 4	0.1270
Ejection Fraction (EF, %)	33 ± 5	39 ± 3	0.3700

End-Diastolic Volume (EDV, µl)	64 ± 60	68 ± 4	0.5882
End-Systolic Volume (ESV, µl)	36 ± 6	35 ± 4	0.9413

6.1.1.2 The effect of acute blood loss anemia on heart function 7 days post-AMI

To investigate the effect of acute blood loss anemia on heart function 7 days post-AMI, heart function was assessed in both anemic and sham mice using ECH. The HR was comparable between the anemic mice (456 ± 23 bpm) and the sham (651 ± 101 bpm) group of mice (Figure 22A, Table 12). The EDV was similar in anemic mice (79 ± 8 µl) and control (67 ± 11 µl) group of mice (Figure 22B, Table 12). Similarly, the ESV was not different between the acute anemic mice (25 ± 6 µl) and the sham (44 ± 10 µl) group of mice (Figure 22C, Table 12). The SV was significantly increased in the acute anemic mice (53 ± 6 µl, P=0.0124) compared to the sham (27 ± 5 µl) group of mice (Figure 22D, Table 12). The EF was similar in acute anemic mice (45 ± 5 %) and control (48 ± 5 %) group of mice (Figure 22E, Table 12). The CO was comparable between the acute anemic mice (24 ± 3 ml/min) and the sham (19 ± 6 ml/min) group of mice (Figure 22F, Table 12). These results conclude that stroke volume is significantly increased in anemic mice 7 days after AMI, while other parameters remain largely unaffected.

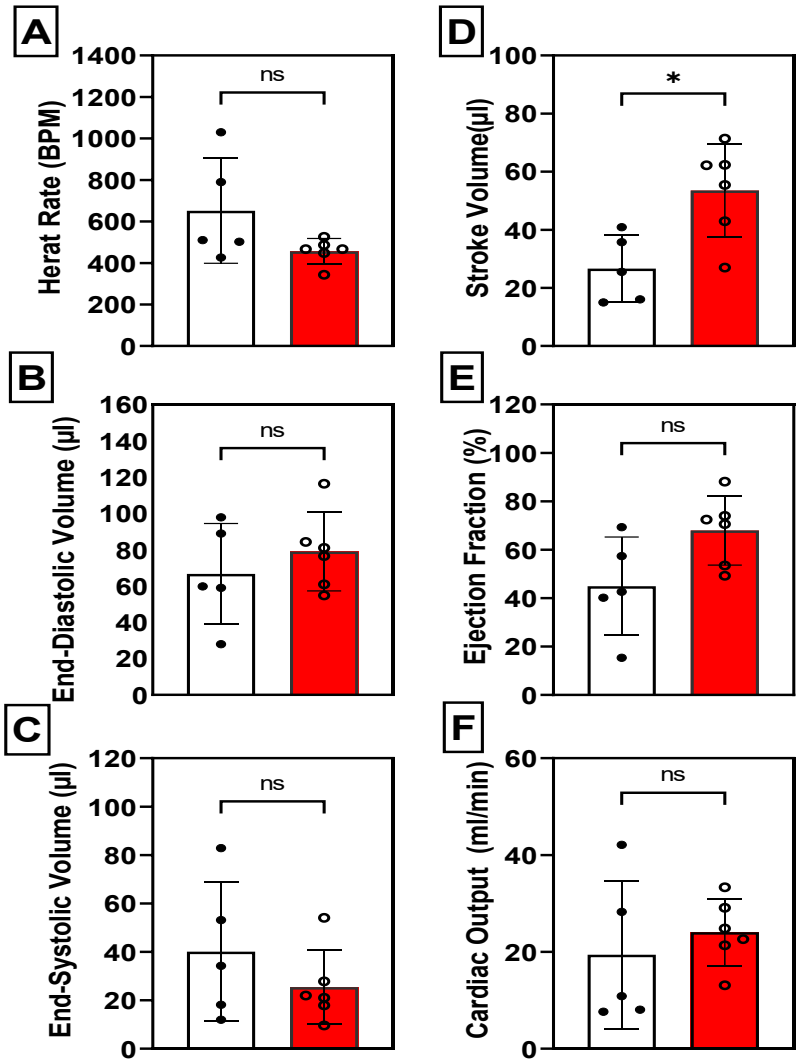

Figure 22. The effect of acute blood loss anemia on heart function 7 days post-AMI. Echo evaluation of control (white bar) and acute anemic (red bar) mice 7 days post-AMI. Left ventricular parameters, including HR, EDV, CO, and EF, SV, ESV, were evaluated. All values are presented as mean ± SEM. Two groups were compared using an unpaired Student ‘s t-test. *p ≤ 0.05; n s., not significant.

Table 12: Summary of cardiac functional parameters 7 days post-AMI in acute anemic mice

N	Acute	Sham	P-Value
Cardiac Output (CO, ml/min)	24 ± 2.6	19.4 ± 6.1	0.5172
Heart Rate (HR, bpm)	456 ± 23	651 ± 101	0.0977
Stroke Volume (SV, µl)	53 ± 6	27 ± 5	0.0124
Ejection Fraction (EF, %)	45 ± 5	48 ± 5	0.0552
End-Diastolic Volume (EDV, µl)	79 ± 8	67 ± 11	0.4315
End-Systolic Volume (ESV, µl)	25 ± 6	44 ± 10	0.3055

6.1.1.3 The effect of acute blood loss anemia on heart function 24 hours post-AMI in NAC-treated mice

To investigate the effect of acute blood loss anemia on heart function after AMI in NAC-treated mice (ROS scavenger), heart function was assessed in both anemic and sham mice 24 hours post-AMI using ECH. The HR was comparable between the anemic mice (470 ± 30 bpm) and the sham (614 ± 113 bpm) group of mice (Figure 23A, Table 13). The ESV was significantly reduced in acute anemic mice (78 ± 6 µl, P=0.0254) compared to the control (102 ± 5 µl) group of mice (Figure 23B, Table 13). Similarly, the EDV was significantly decreased in acute anemic mice (23 ± 3 µl, P=0.0333) compared to the sham (36 ± 4 µl) group of mice (Figure 23C, Table 13). The SV was similar in anemic mice (54 ± 6 µl) and sham (66 ± 9 µl) group of mice (Figure 23D, Table 13). The EF was no difference between the acute anemic mice (42 ± 5 %) and the control (26 ± 6 %) group of mice (Figure 23E, Table 13). The CO was similar between the acute anemic mice (25 ± 3 ml/min) and the sham (25 ± 3 ml/min) group of mice (Figure 23F, Table 13). These results conclude that ROS scavenger NAC treatment does not change heart function in acute anemic mice 24 hours post AMI.

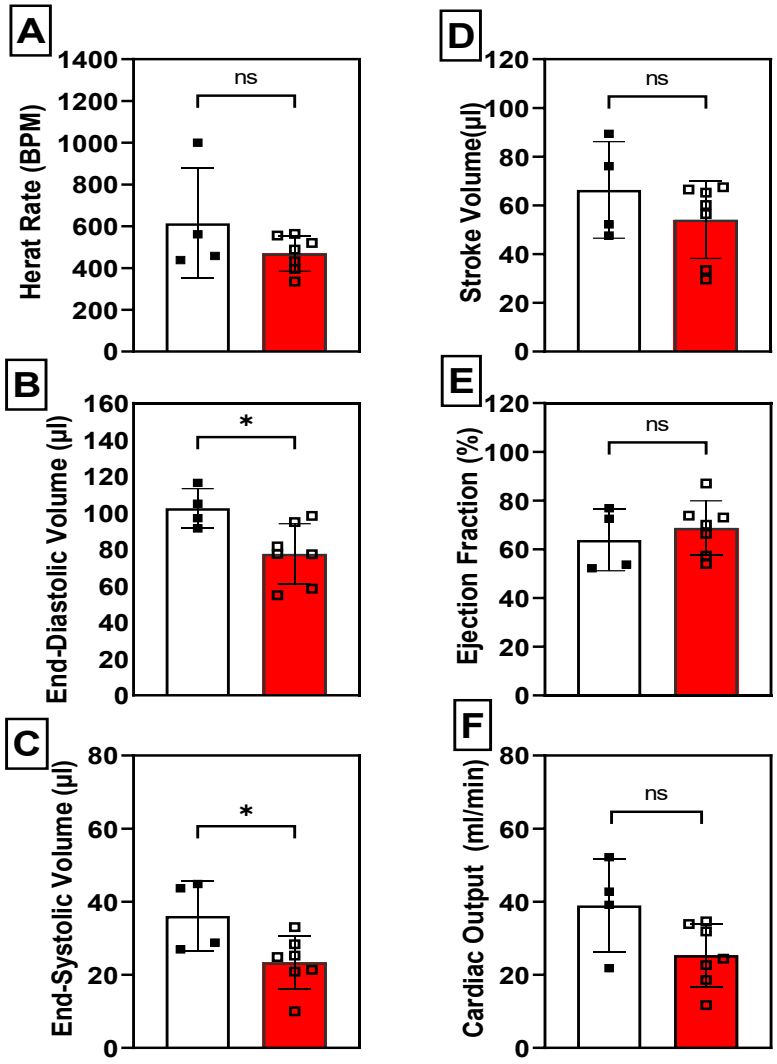

Figure 23. The effect of acute blood loss anemia on heart function 24 hours post-AMI in NAC-treated mice. Echo evaluation of control (white bar) and acute blood loss anemic (red bar) mice 24 hours post-AMI. Left ventricular parameters, including HR, EDV, ESV, CO, and EF, SV, were evaluated. All values are presented as mean ± SEM. Two groups were compared using an unpaired Student ‘s t-test. *p ≤ 0.05; n.s., not significant.

Table 13: Summary of cardiac functional parameters 24 hours post-AMI in acute anemic NAC-treated mice

N	Acute	Sham	P-Value
Cardiac Output (CO, ml/min)	25 ± 3	25 ± 3	0.0612
Heart Rate (HR, bpm)	470 ± 30	614 ± 113	0.2018
Stroke Volume (SV, µl)	54 ± 6	66 ± 9	0.2899

Ejection Fraction (EF, %)	42 ± 5	26 ± 6	0.5112
End-Diastolic Volume (EDV, µl)	78 ± 6	102 ± 5	0.0254
End-Systolic Volume (ESV, µl)	23 ± 3	36 ± 4	0.0333

6.1.1.4 The effect of acute blood loss anemia on heart function 7 days post-AMI in NAC-treated mice

To investigate the effects of acute blood loss anemia on heart function 7 days post-AMI in ROS scavenger NAC-treated mice, heart function was assessed in both anemic and sham mice using ECH. The HR was comparable between the acute anemic mice (458 ± 31 bpm) and the sham (469 ± 24 bpm) group of mice (Figure 24A, Table 14). The EDV was significantly reduced in acute anemic mice (65 ± 3 µl, P=< 0.0001) compared to the control (104 ± 5 µl) group of mice (Figure 24B, Table 14). The ESV was similar in anemic mice (22 ± 3 µl) compared to the sham (27 ± 4 µl) group of mice (Figure 24C, Table 14). The SV was significantly decreased in anemic mice (43 ± 3 µl, P=0.0008) compared to sham (77 ± 6 µl) group of mice (Figure 24D, Table 14). The EF did not differ between the acute anemic mice (65 ± 5 %) and the control (64 ± 5 %) group of mice (Figure 24E, Table 14). The CO was significantly reduced in anemic mice (23 ± 4 ml/min, P=0.05) compared to sham (39 ± 5 ml/min) group of mice (Figure 24F, Table 14). These results conclude that NAC-treatment does not change heart function in acute anemic mice 7 days post AMI.

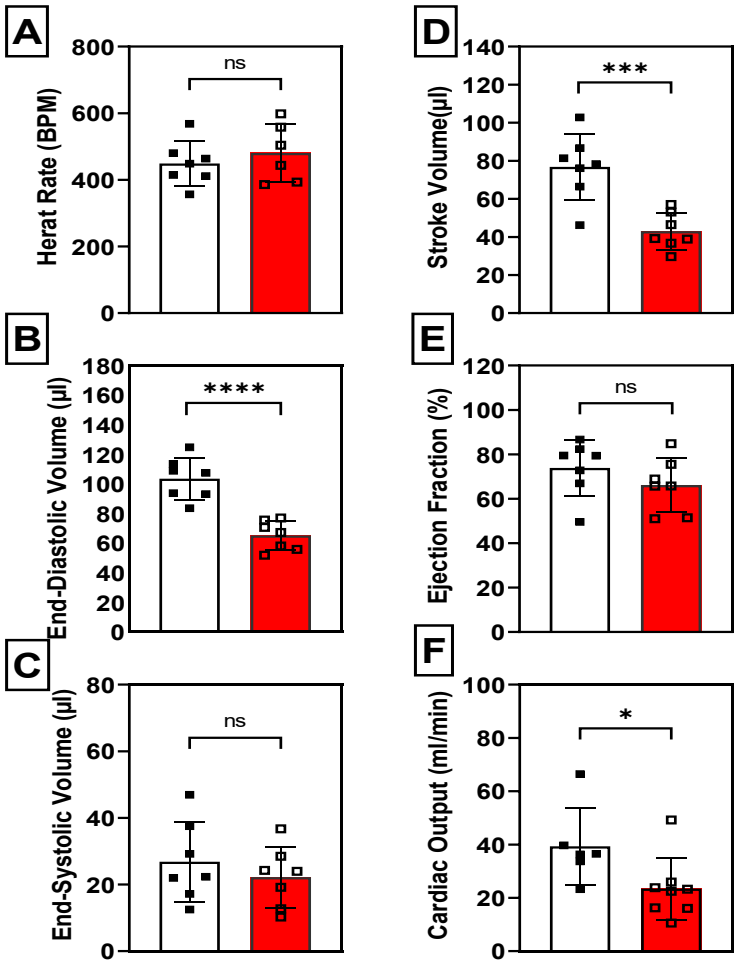

Figure 24. The effect of acute blood loss anemia on heart function 7 days post-AMI in NAC-treated mice. Echo evaluation of control (white bar) and acute blood loss anemic (red bar) mice 7 days post-AMI. Left ventricular parameters, including HR, EDV, ESV, CO, EF, SV, were evaluated. All values are presented as mean ± SEM. Two groups were compared using an unpaired Student ‘s t-test. *p ≤ 0.05; ***p ≤ 0.001; ****p ≤0.0001; n.s., not significant.

Table 14: Summary of cardiac functional parameters 7 days post-AMI in acute NAC-treated mice

N	Acute	Sham	P-Value
Cardiac Output (CO, ml/min)	23 ± 4	39 ± 5	0.05
Heart Rate (HR, bpm)	458 ± 31	469 ± 24	0.4764
Stroke Volume (SV, µl)	43 ± 3	77 ± 6	0.0008
Ejection Fraction (EF, %)	65 ± 5	64 ± 5	0.2620
End-Diastolic Volume (EDV, µl)	65 ± 3	104 ± 5	< 0.0001
End-Systolic Volume (ESV, µl)	22 ± 3	27 ± 4	0.4353

6.1.1.5 The effect of the chronic blood loss anemia on heart function 24 hours post-AMI

To investigate the effects of chronic blood loss anemia on heart function 24 hours post-AMI, heart function was assessed in both anemic and sham mice using ECH. The HR was significantly reduced in chronic anemic mice (440 ± 14 bpm, P=0.0151) compared to sham (581 ± 61 bpm) group of mice (Figure 25A, Table 15). Similarly, the EDV was significantly increased in chronic mice (77 ± 7 µl, P=0.0259) compared to sham (53 ± 6 µl) group of mice (Figure 25B, Table 15). The ESV was comparable between the chronic anemic mice (55 ± 7 µl) and the sham (37 ± 6 µl) group of mice (Figure 25C, Table 15). The SV was comparable between the anemic mice (22 ± 5 µl) and the control (16 ± 2 µl) group of mice (Figure 25D, Table 15). The EF was similar in chronic mice (24 ± 7 %) and sham (25 ± 6 %) group of mice (Figure 25E, Table 15). The CO did not differ between the anemic mice (10 ± 2 ml/min) and the sham (9 ± 1 ml/min) group of mice (Figure 25F, Table 15). These results conclude that end-diastolic volume is increased to compensate the reduced heart rate in chronic anemic mice 24 hours post-AMI.

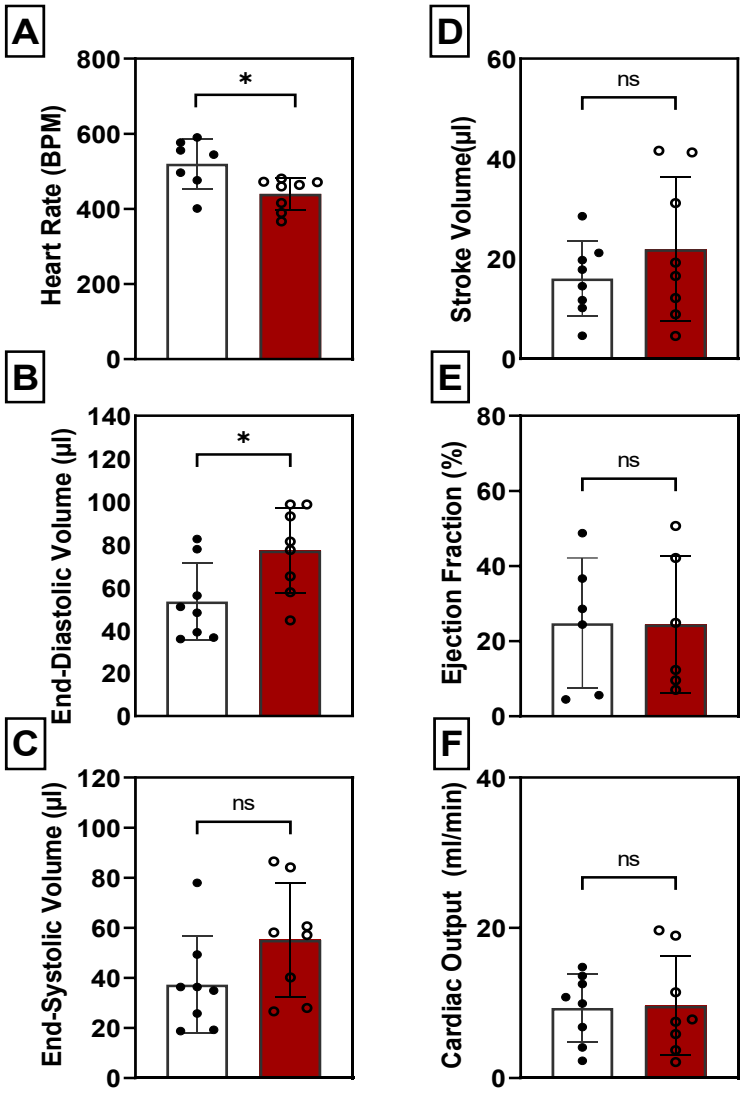

Figure 25. The effect of chronic blood loss anemia on heart function 24 hours post-AMI. Echo evaluation of control (white bar) and chronic anemic (dark red bar) mice 24 hours post-AMI. Left ventricular parameters, including heart rate HR, EDV, ESV, CO, EF, SV, were evaluated. All values are presented as mean ± SEM. Two groups were compared using an unpaired Student ‘s t-test. *p ≤ 0.05; n.s., not significant.

Table 15: Summary of cardiac functional parameters 24 hours post-AMI in chronic anmeic mice

N	Chronic	Sham	P-Value
Cardiac Output (CO, ml/min)	10 ± 2	9 ± 1	0.9216
Heart Rate (HR, bpm)	440 ± 14	581 ± 61	0.0151

Stroke Volume (SV, µl)	22 ± 5	16 ± 2	0.3224
Ejection Fraction (EF, %)	24 ± 7	25 ± 6	0.9754
End-Diastolic Volume (EDV, µl)	77 ± 7	53 ± 6	0.0259
End-Systolic Volume (ESV, µl)	55 ± 7	37 ± 6	0.1136

6.1.1.6 The effect of chronic blood loss anemia on heart function 7 days post AMI

To investigate the effects of chronic blood loss anemia on heart function 7 days post-AMI, heart function was assessed in both anemic and sham mice using ECH. The HR was similar in anemic mice (434 ± 33 bpm) and sham (484 ± 27 bpm) group of mice (Figure 26A, Table 16). Similarly, the EDV did not differ between the chronic mice (63 ± 6 µl) and sham (74 ± 8 µl) group of mice (Figure 26B, Table 16). The ESV was comparable between the anemic mice (37 ± 5 µl) and the control (38 ± 6 µl) group of mice (Figure 26C, Table 16). The SV was similar in chronic anemic mice (26 ± 2 µl) and sham (37 ± 7 µl) group of mice (Figure 26D, Table 16). The EF was comparable between the chronic mice (40 ± 4 %) and the control (54 ± 9 %) group of mice (Figure 26E, Table 16). The CO did not differ between the anemic mice group (11 ± 1 ml/min) and the sham (18 ± 4 ml/min) group of mice (Figure 26F, Table 16). These results conclude that heart function remains unaffected in chronic anemic mice group 7 days post-AMI.

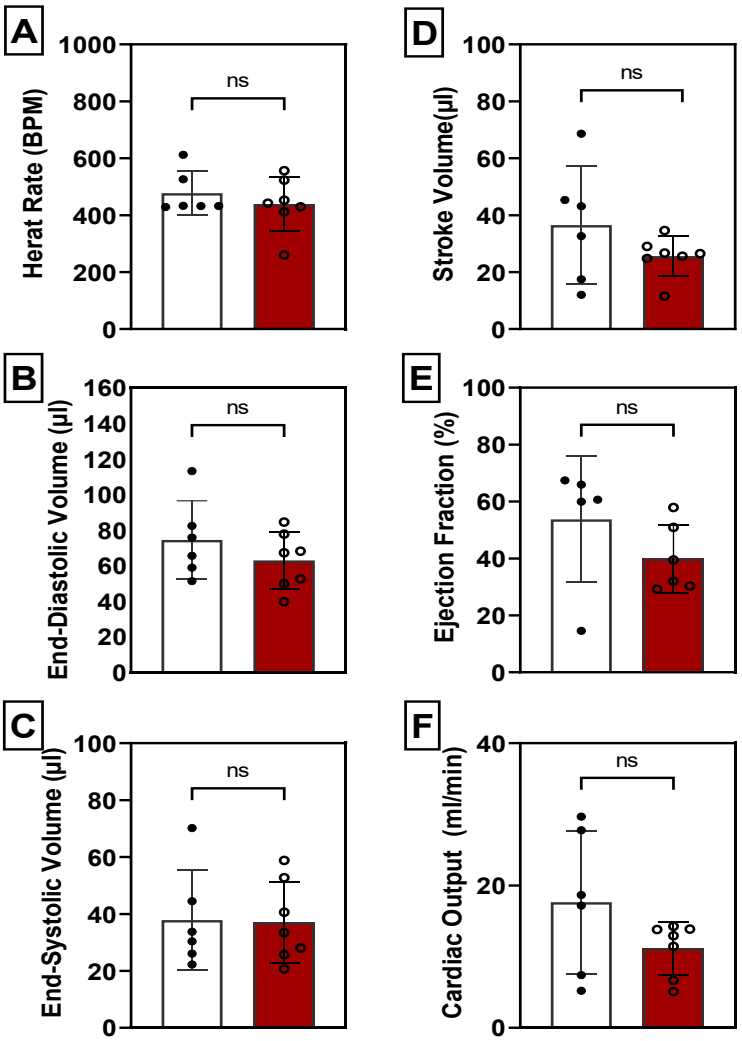

Figure 26. The effect of chronic blood loss anemia on heart function 7 days post-AMI. Echo evaluation of control (white bar) and chronic anemic (dark red bar) mice 7 days after acute myocardial infarction (AMI). Left ventricular parameters, including HR, EDV, ESV, CO, EF, SV were evaluated. All values are presented as mean ± SEM. Two groups were compared using an unpaired Student ‘s t-test. n.s., not significant

Table 16: Summary of cardiac functional parameters 7 days post-AMI in chronic anemic mice

N	Chronic	Sham	P-Value
Cardiac Output (CO, ml/min)	11 ± 1	18 ± 4	0.1401
Heart Rate (HR, bpm)	434 ± 33	484 ± 27	0.4464
Stroke Volume (SV, µl)	26 ± 2	37 ± 7	0.2101
Ejection Fraction (EF, %)	40 ± 4	54 ± 9	0.2197

End-Diastolic Volume (EDV, µl)	63 ± 6	74 ± 8	0.2928
End-Systolic Volume (ESV, µl)	37 ± 5	38 ± 6	0.9393

6.1.1.7 The effect of chronic blood loss anemia on heart function 24 hours post-AMI in NAC-treated mice

To investigate the effects of chronic blood loss anemia on heart function 24 hours post-AMI in ROS scavenger NAC-treated mice, heart function was assessed in both anemic and sham mice using ECH. The HR was similar in chronic mice (532 ± 63 bpm) and sham (521 ± 56 bpm) group of mice (Figure 27A, Table 17). The EDV did not differ between the anemic mice (70 ± 6 µl) and the control (70 ± 3 µl) group of mice (Figure 27B, Table 17). Similarly, the ESV was comparable between the chronic group (46 ± 5 µl) and the sham (44 ± 4 µl) group of mice (Figure 27C, Table 17). The SV was similar in chronic mice (24 ± 2 µl) compared to sham (31 ± 3 µl) group of mice (Figure 27D, Table 17). The EF was comparable between the anemic group (36 ± 3 %) and the control (40 ± 3 %) group of mice (Figure 27E, Table 17). The CO did not differ between the chronic mice (13 ± 2 ml/min) and sham (16 ± 1 ml/min) group of mice (Figure 27F, Table 17). These results conclude that NAC treatment does not change heart function in chronic anemic mice 24 hours post AMI.

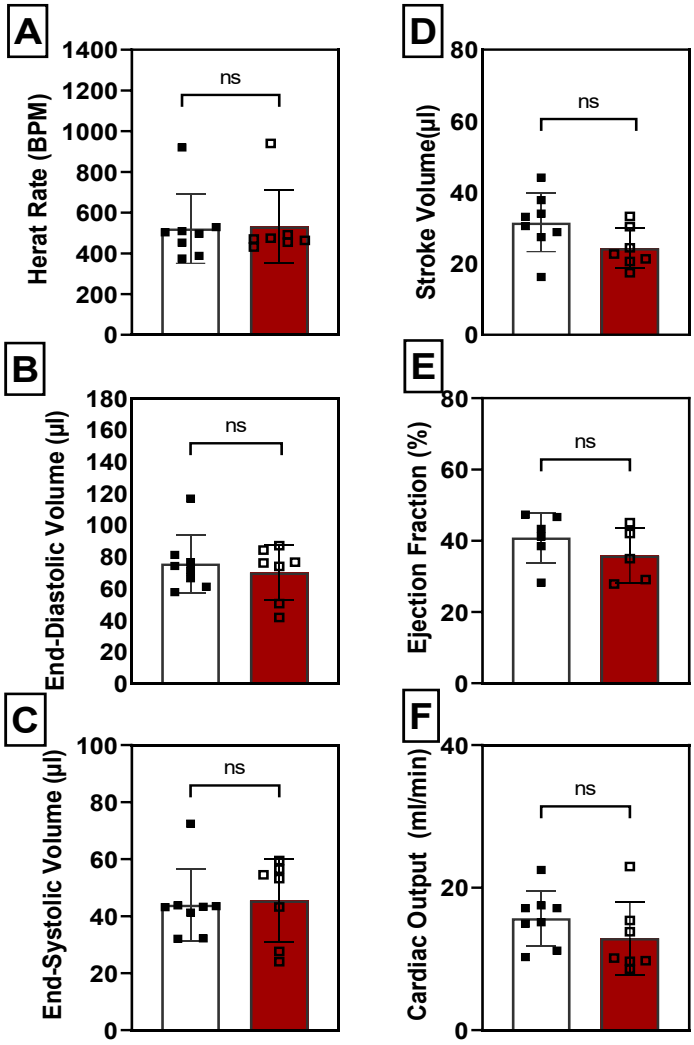

Figure 27. The effect of chronic blood loss anemia on heart function 24 hours post-AMI in NAC-treated mice. Echo evaluation of control (white bar) and chronic anemic (dark red bar) mice 24 hours after acute myocardial infarction (AMI). Left ventricular parameters, including HR, EDV, ESV, CO, EF, SV, were evaluated. All values are presented as mean ± SEM. Two groups were compared using an unpaired Student ‘s t-test. n.s., not significant.

Table 17: Summary of cardiac functional parameters 24 hours post-AMI in chronic anemic NAC-treated mice

N	Chronic	Sham	P-Value
Cardiac Output (CO, ml/min)	13 ± 2	16 ± 1	0.2449
Heart Rate (HR, bpm)	532 ± 63	521 ± 56	0.9086

Stroke Volume (SV, µl)	24 ± 2	31 ± 3	0.0714
Ejection Fraction (EF, %)	36 ± 3	40 ± 3	0.2814
End-Diastolic Volume (EDV, µl)	70 ± 6	70 ± 3	0.5495
End-Systolic Volume (ESV, µl)	46 ± 5	44 ± 4	0.8280

6.1.1.8 The effect of chronic blood loss anemia on heart function 7 days post-AMI in NAC-treated mice

To investigate the effects of chronic blood loss anemia on heart function 7 days post-AMI in ROS scavenger NAC-treated mice, heart function was assessed in both anemic and sham mice using ECH. The HR was comparable between the chronic anemic mice (459 ± 40 bpm) and the sham (473 ± 18 bpm) group of mice (Figure 28A, Table 18). The EDV was similar in anemic group (62 ± 11 µl) and control (89 ± 10 µl) group of mice (Figure 28B, Table 18). Similarly, the ESV did not differ between the chronic mice (45 ± 10 µl) and the sham (57 ± 7 µl) group of mice (Figure 28C, Table 18). The SV was comparable between the anemic mice group (17 ± 4 µl) and the sham (31 ± 7 µl) group of mice (Figure 28D, Table 18). The EF was similar in chronic group (30 ± 7 %) and sham (35 ± 5 %) group of mice (Figure 28E, Table 18). The CO did not differ between the chronic anemic mice (6 ± 1 ml/min) and the sham (16 ± 4 ml/min) group of mice (Figure 28F, Table 18). These results conclude that NAC treatment does not change heart function in chronic anemic mice 7 days post AMI.

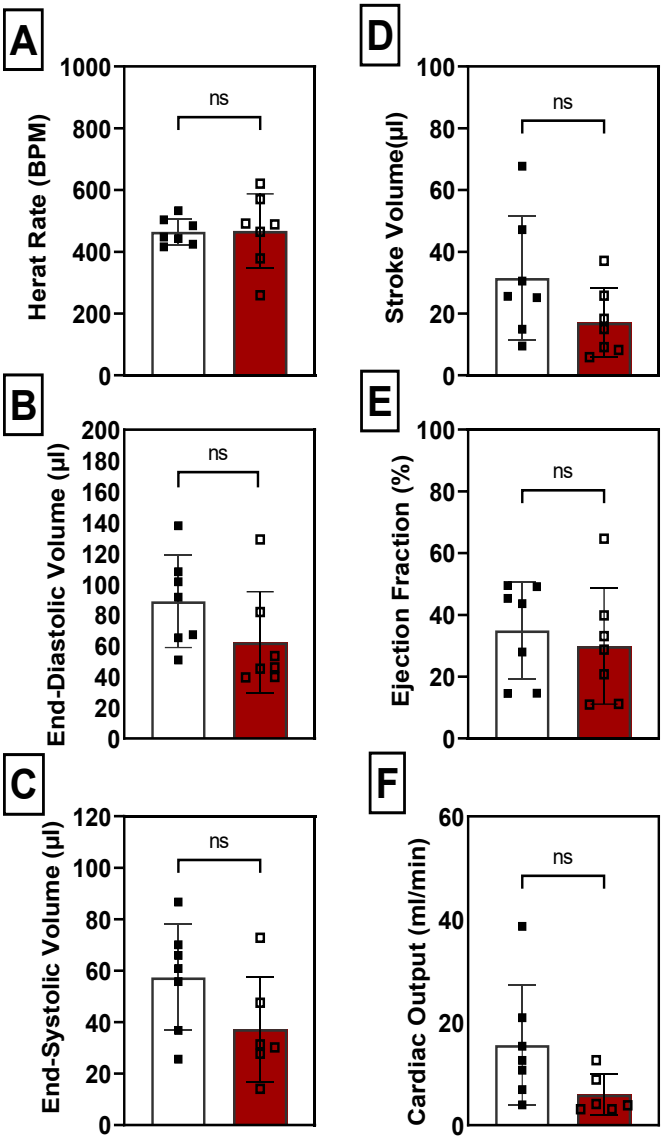

Figure 28. The effect of chronic blood loss anemia on heart function 7 days post-AMI in NAC-treated mice. Echo evaluation of control (white bar) and chronic anemic (dark red bar) mice 7 days after acute myocardial infarction (AMI). Left ventricular parameters, including HR, EDV, ESV, CO, EF, SV, were evaluated. All values are presented as mean ± SEM. Two groups were compared using an unpaired Student ‘s t-test. n.s., not significant.

Table 18: Summary of cardiac functional parameters 7 days post-AMI in chronic anemic NAC-treated mice

N	Chronic	Sham	P-Value
Cardiac Output (CO, ml/min)	6 ± 1	16 ± 4	0.0793
Heart Rate (HR, bpm)	459 ± 40	473 ± 18	0.9476
Stroke Volume (SV, µl)	17 ± 4	31 ± 7	0.1208
Ejection Fraction (EF, %)	30 ± 7	35 ± 5	0.5924
End-Diastolic Volume (EDV, µl)	62 ± 11	89 ± 10	0.1377
End-Systolic Volume (ESV, µl)	45 ± 10	57 ± 7	0.1056

6.2 Flow cytometry

6.2.1 The effect of the acute blood loss anemia on immune cell infiltration in cardiac tissue

To investigate the effects of acute blood loss anemia on immune cell infiltration in cardiac tissue, main immune cell types were analyzed in both acute anemic and sham mice using flow cytometry. The analysis was focused on immune cell types, such as CD45 cells, lymphocytes, monocytes/macrophages, NK cell, B-cell, T-cell, and neutrophils. Total-CD45 cell infiltration was not different between the acute anemic (1926 ± 349) and sham (1259 ± 115) group of mice (Figure 29A, Table 19). Similarly, lymphocyte infiltration did not differ between the anemic mice (589 ± 145) and the sham (534 ± 70) group (Figure 29B, Table 19). Monocyte/macrophage infiltration was comparable between the acute anemic (640 ± 138) and the sham (356 ± 57) group of mice (Figure 29C, Table 19). NK cell infiltration remained unaffected between the acute mice (254 ± 53) and the control (141 ± 38) group (Figure 29D, Table 19). B-cell infiltration was similar between the anemic mice (132 ± 23) and the sham (211 ± 46) group (Figure 29E, Table 19). Similarly, T-cell infiltration also remained unchanged between the acute mice (11 ± 6) and the sham (8 ± 4) group (Figure 29F, Table 19). However, neutrophils infiltration was significantly increased in the acute anemic (153 ± 39, P=0.0433) compared to the control (57 ± 10) group of mice (Figure 29G, Table 19). These results conclude that neutrophils promote the oxidative stress are significantly increased in acute anemic mice cardiac tissue, while other immune cells remain mostly unaffected.

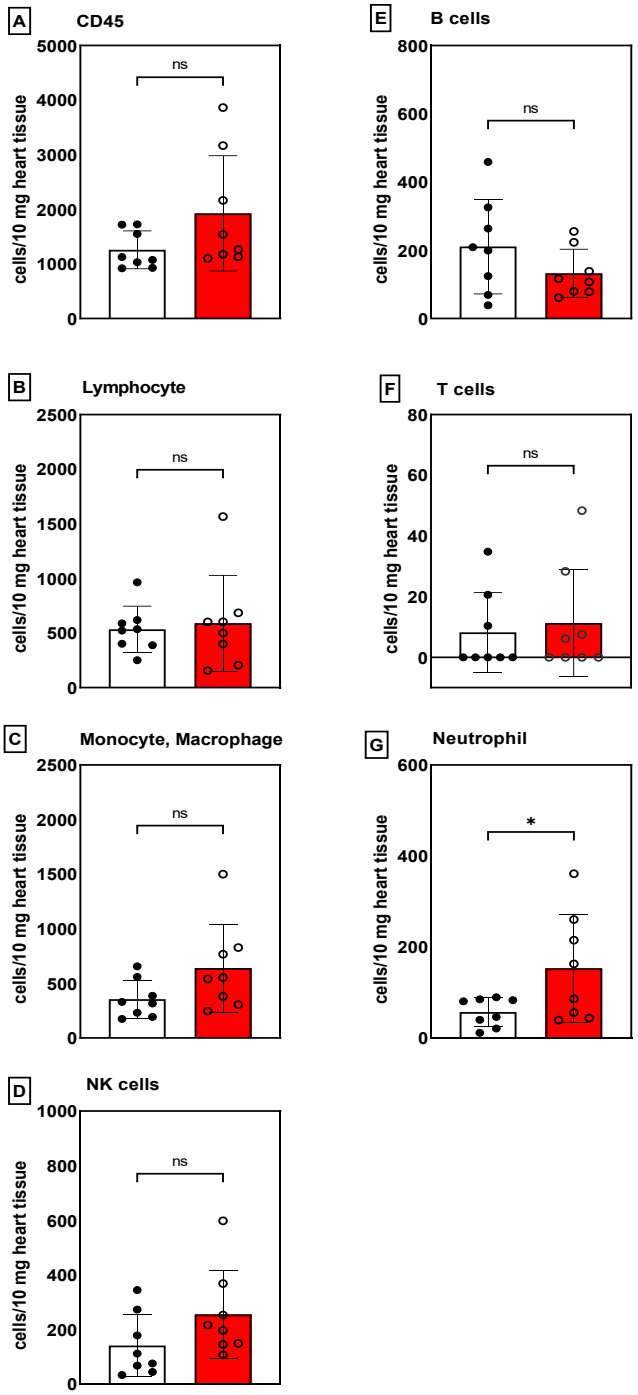

Figure 29. The effect of acute blood loss anemia on immune cell infiltration in cardiac tissue. Flow cytometric analysis of immune cell infiltration in cardiac tissue (10 mg) isolated from acute anemic (red bar) and sham mice (white bar). Data are presented as mean ± SEM. Two groups were compared using an unpaired Student ‘s t-test. *p ≤ 0.05; n.s., not significant

Table 19: Overview of immune cell populations in the acute anemia model without IR

N	Acute	Sham	P-Value
CD45	1926 ± 349	1259 ± 115	0.1121
Lymphocyte	589 ± 145	534 ± 70	.07511
Monocyte, Macrophage	640 ± 138	356 ± 57	0.0892
Natural killer cells (NK)	254 ± 53	141 ± 38	0.1269
B-cells	132 ± 23	211 ± 46	0.1754
T-cells	11 ± 6	8 ± 4	0.7007
Neutrophil	153 ± 39	57 ± 10	0.0433

6.2.2 The effect of the chronic blood loss anemia on immune cell infiltration in cardiac tissue

To investigate the effects of chronic blood loss anemia on immune cell infiltration in cardiac tissue, main immune cell types were analyzed in both chronic anemic and sham mice using flow cytometry. The analysis was focused on immune cell types, such as CD45 cells, lymphocytes, monocytes/macrophages, NK cell, B-cell, T-cell, and neutrophils. Total CD45 cell infiltration was not different between the chronic (1582 ± 350) and the sham (1789 ± 421) group of mice (Figure 30A, Table 20). Lymphocyte infiltration was comparable between the chronic anemic (352 ± 142) and the sham (435 ± 130) group of mice (Figure 30B, Table 20). Monocyte/macrophage infiltration remained similar between the anemic (515 ± 110) and the sham (353 ± 68) group of mice (Figure 30C, Table 20). Similarly, NK cell infiltration was not differed between the chronic mice (171 ± 41) and the control (338 ± 79) group (Figure 30D, Table 20). B cell infiltration was similar between the anemic (150 ± 52) and the sham (270 ± 102) group of mice (Figure 30E, Table 20). Similarly. T cell infiltration remained unaffected between the chronic (25 ± 11) and the control (27 ± 10) group of mice (Figure 30F, Table 20). Neutrophils infiltration was similar between the chronic mice (53 ± 12) and the sham (72 ± 27) group (Figure 30G, Table 20). These results conclude that immune infiltration was not increased in chronic anemia.

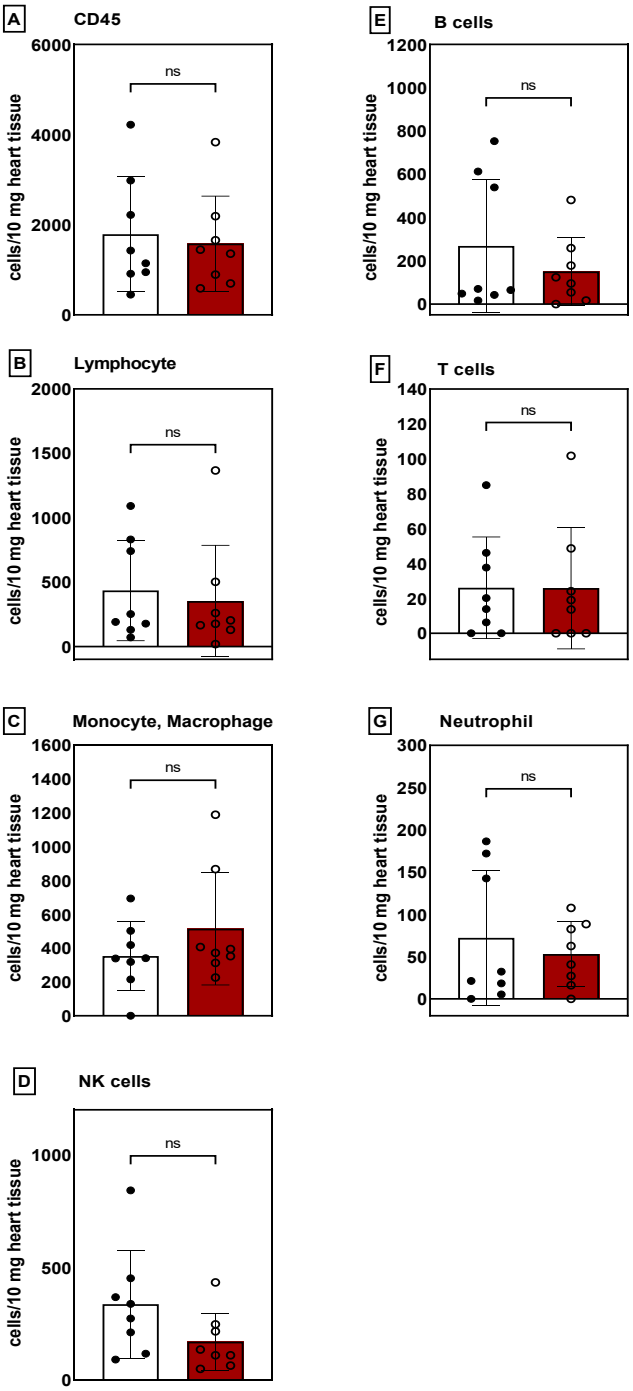

Figure 30. The effect of chronic blood loss anemia on immune cell infiltration in cardiac tissue. Flow cytometric analysis of immune cell infiltration in cardiac tissue (10 mg) isolated from chronic anemic (dark red bar) and sham anemic (white bar). Data are presented as mean ± SEM. Two groups were compared using an unpaired Student's t-test. n.s., not significant.

.

Table 20: Overview of immune cell populations in the chronic anmeia model without IR

N	Chronic	Sham	P-Value
CD45	1582 ± 350	1789 ± 421	0,7298
Lymphocyte	352 ± 142	435 ± 130	0,6942
Monocyte, Macrophage	515 ± 110	353 ± 68	0,2610
NK cells	171 ± 41	338 ± 79	0,1038
B-cells	150 ± 52	270 ± 102	0,3550
T-cells	25 ± 11	27 ± 10	0,9887
Neutrophil	53 ± 12	72 ± 27	0,5513

6.2.3 The effect of the acute blood loss anemia on immune cell infiltration in cardiac tissue 24 hours post-IR

To investigate the effects of acute blood loss anemia on immune cell infiltration in cardiac tissue 24 hours post-IR, main immune cell types were analyzed in both acute anemic and sham mice using flow cytometry. The analysis was focused on immune cell types, such as CD45 cells, lymphocytes, monocytes/macrophages, NK cells, B-cells, T-cells, and neutrophils. Total CD45 cell infiltration remains unchanged between the acute (11166 ± 4489) and the sham (7109 ± 1925) group of mice (Figure 31A, Table 21). The lymphocyte infiltration was comparable between the acute mice (826 ± 323) and the sham (668 ± 266) group (Figure 31B, Table 21). Monocyte/macrophage infiltration was similar between the acute (5245 ± 2041) and the control (3315 ± 1006) group of mice (Figure 31C, Table 21). NK cell infiltration was not different between the anemic mice (643 ± 259) and the sham (356 ± 84) group (Figure 31D, Table 21). Similarly, B cell infiltration was not different between the acute (285 ± 119) and the sham (196 ± 76) group of mice (Figure 31E, Table 21). T cell infiltration was similar between the acute mice (228 ± 118) and the sham (151 ± 75) group (Figure 31F, Table 21). Neutrophil infiltration was comparable between the anemic (3001 ± 1003) and the sham (1668 ± 418) group of mice (Figure 31G, Table 21). These results conclude that immune infiltration was not increased in acute anemia.

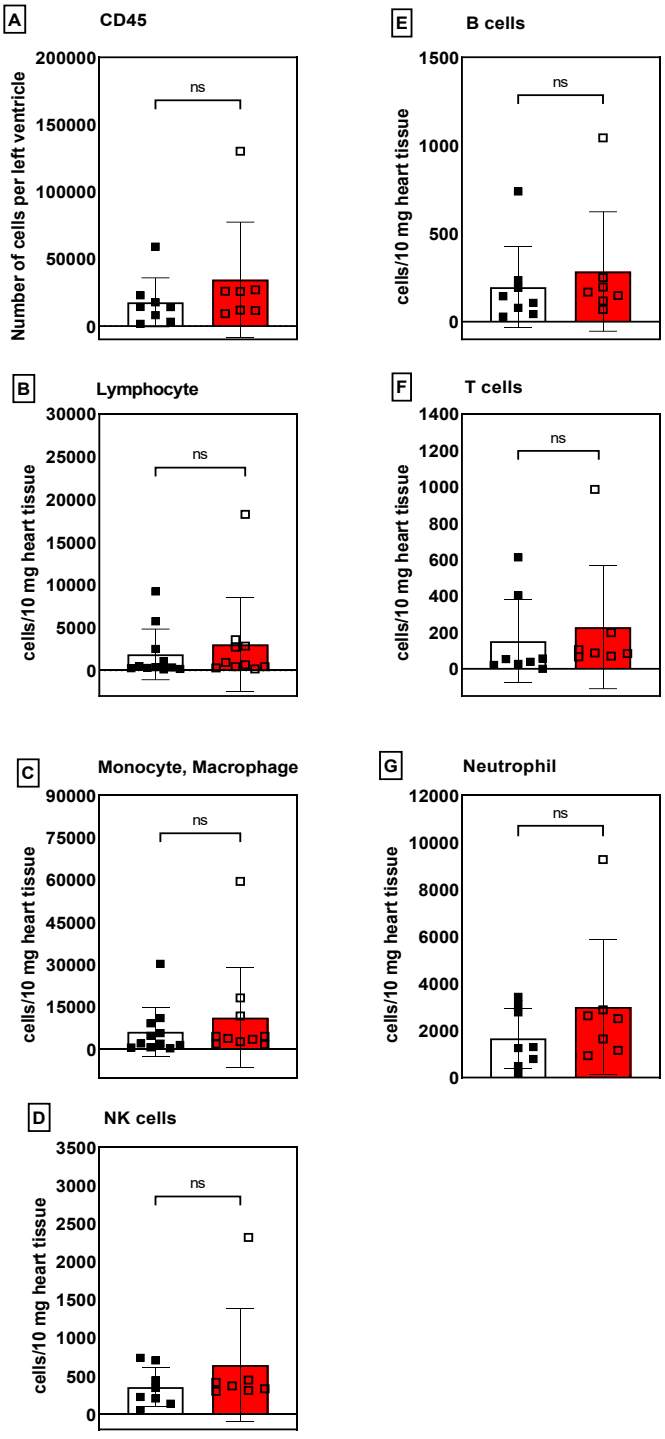

Figure 31. The effect of acute blood loss anemia on immune cell infiltration in cardiac tissue 24 hours post-IR. Flow cytometric analysis of immune cell infiltration in cardiac tissue (10 mg) isolated from acute anemic mice (red bar) and sham mice (white bar) 24 hours post-IR. Data are presented as mean ± SEM. Two groups were compared using an unpaired Student's t-test. n.s., not significant.

Table 21: Overview of immune cell populations in the acute anemia model with IR

n	Acute	Sham	P-Value
CD45	11166 ± 4489	7109 ± 1925	0.4339
Lymphocyte	826 ± 323	668 ± 266	0.5494
Monocyte, Macrophage	5245 ± 2041	3315 ± 1006	0.4122
NK cells	643 ± 259	356 ± 84	0.3209
B-cells	285 ± 119	196 ± 76	0.5596
T-cells	228 ± 118	151 ± 75	0.6099
Neutrophil	3001 ± 1003	1668 ± 418	0.2532

6.2.4 The effect of the chronic blood loss anemia on immune cell infiltration in cardiac tissue 24 hours post-IR

To investigate the effects of chronic blood loss anemia on immune cell infiltration in cardiac tissue 24 hours post-IR, main immune cell types were analyzed in both chronic anemic and sham mice using flow cytometry. The analysis was focused on immune cell types, such as CD45 cells, lymphocytes, monocytes/macrophages, NK cell, B-cell, T-cell, and neutrophils. Total CD45 cell infiltration remains unchanged between the chronic (7483 ± 1049) and the sham (6781 ± 1959) group of mice (Figure 32A, Table 22). Lymphocyte infiltration was comparable between the chronic mice (519 ± 119) and the sham (548 ± 231) group (Figure 32B, Table 22). Monocyte/macrophage infiltration was similar between the chronic (2991 ± 471) and the control (2980 ± 971) group of mice (Figure 32C, Table 22). NK cell infiltration was not different between the anemic mice (517 ± 60) and the sham (539 ± 150) group (Figure 32D, Table 22). Similarly, B cell infiltration was similar between the chronic (294 ± 96) and the sham (348 ± 151) group of mice (Figure 32E, Table 22). T cell infiltration was not different between the chronic mice (106 ± 27) and the sham (101 ± 65) group (Figure 32F, Table 22). Neutrophil infiltration was comparable between the anemic (2043 ± 379) and the sham (2253 ± 844) group of mice (Figure 32G, Table 22). These results conclude that immune infiltration was not increased in chronic anemia.

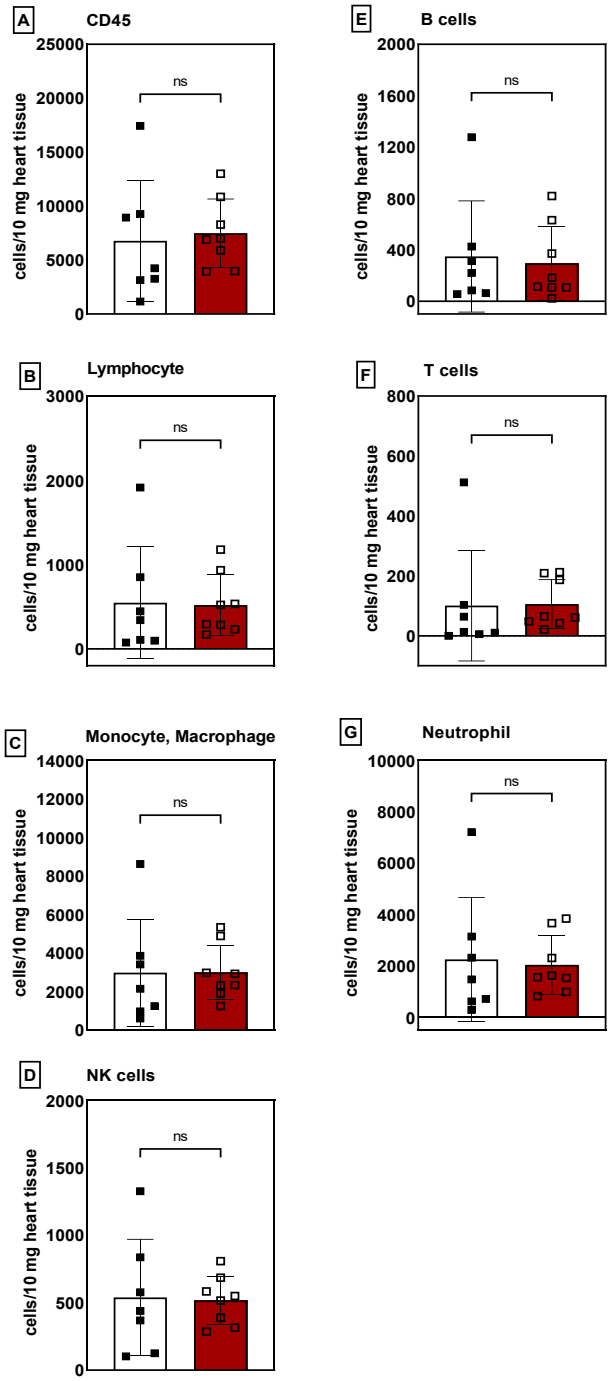

Figure 32. The effect of chronic blood loss anemia on immune cell infiltration in cardiac tissue 24 hours post-IR. Flow cytometric analysis of immune cell infiltration in cardiac tissue (10 mg) isolated from chronic anemic (dark red bar) and sham mice (white bar) 24 hours post-IR. Data are

presented as mean ± SEM. Two groups were compared using an unpaired Student's t-test. n.s., not significant.

Table 22: Overview of immune cell populations in the chronic anemia model with IR

n	Chronic	Sham	P-Value
CD45	7483 ± 1049	6781 ± 1959	0.7658
Lymphocyte	519 ± 119	548 ± 231	0.9172
Monocyte, Macrophage	2991 ± 471	2980 ± 971	0.9922
NK cells	517 ± 60	539 ± 150	0.8930
B-cells	294 ± 96	348 ± 151	0.7779
T-cells	106 ± 27	101 ± 65	0.9506
Neutrophil	2043 ± 379	2253 ± 844	0.8293

6.3 Immunohistochemistry (IHC)

6.3.1 Neutrophil infiltration in acute anemic mice 24 hours post-AMI

Immunohistochemical analysis was performed to assess neutrophil abundance in acute anemic mice 24 hours post-AMI. Neutrophils were identified using Ly6G, a specific marker for neutrophils, and cell nuclei were stained with DAPI. $Ly6G^+$ neutrophils were detected within the myocardial tissue, confirming neutrophil infiltration 24 hours post-AMI. The merged image (Ly6G and DAPI) illustrates the abundance of neutrophils in the myocardial tissue.

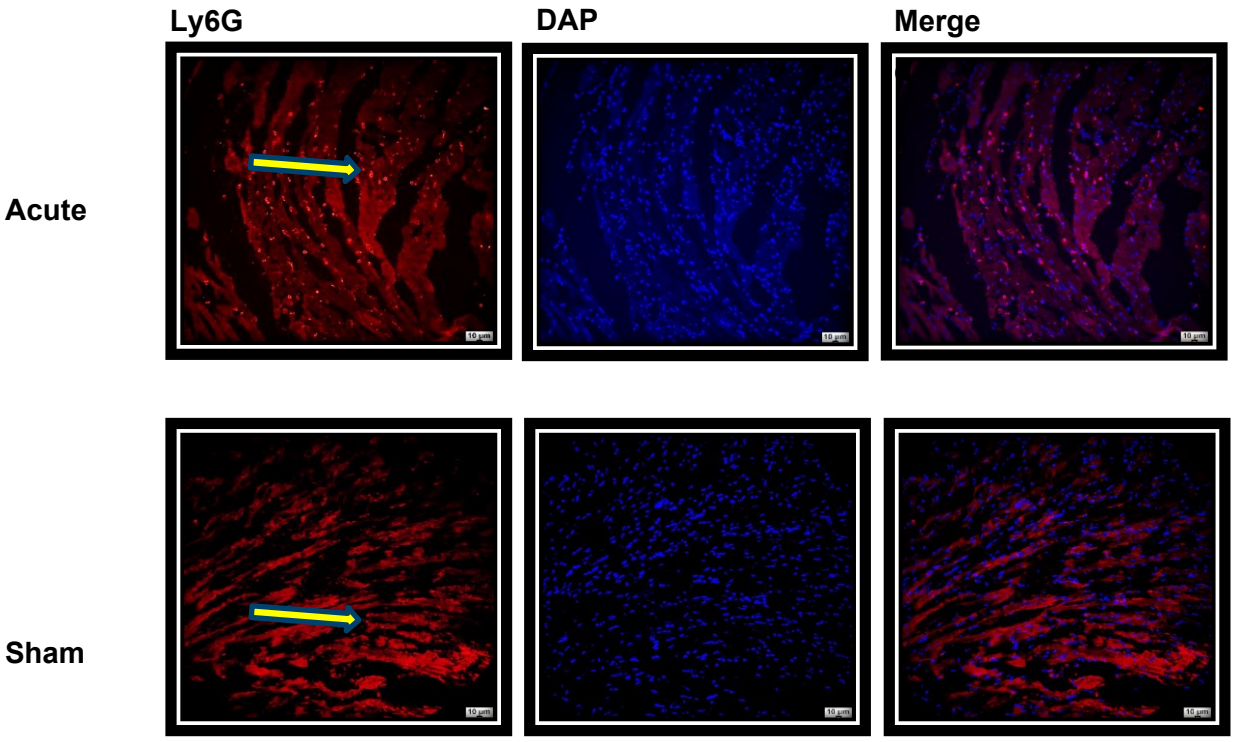

Figure 33. Immunofluorescence assessment of neutrophil infiltration in the heart of acute anemic mice 24 hours post-AMI. A: Neutrophils were stained with Ly6G staining (red). **B:** DAPI staining indicates the nuclei of all cells. **C:** The merged image illustrates the localization of neutrophils in the heart tissue. The yellow arrows point at neutrophils location in the left ventricle.

6.3.2 Quantification of Ly6G$^+$ neutrophils abundance in hearts of acute anemic mice 24 hours post-AMI

We further quantified Ly6G$^+$ neutrophils abundance in anemic and sham mice 24 hours post-AMI. The neutrophil abundance was higher in acute anemic mice (68 ± 9 %) compared to the sham group (57 ± 4%) of mice (Figure 34, Table 23), but the difference was not significant. These results conclude that acute anemia does not significantly affect Ly6G$^+$ neutrophil infiltration in the heart 24 hours post-AMI.

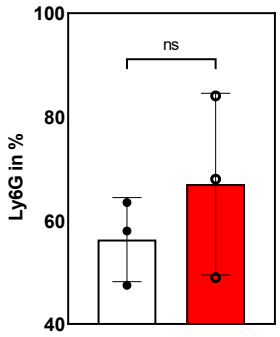

Figure 34. The effect of acute anemia on neutrophil infiltration in cardiac tissue 24 hours post-AMI. Immunohistochemistry analysis of Ly6G$^+$ neutrophil infiltration in the heart tissue isolated from acute anemic (red bar) and sham (white bar) mice 24 hours post-AMI. Data are presented as mean ± SEM. Two groups were compared using unpaired Student's t-test. n.s., not significant.

Table 23: Overview of Ly6G$^+$ neutrophil populations in the acute anemia model post-AMI

N	Acute	Sham	P-Value
Ly6G (Neutrophils)	68 ± 9	57 ± 4	0.3924

7 Discussion

In this research project, we evaluated the effects of acute and chronic anemia on heart function and immune infiltration, as well as the role of an antioxidant treatment strategy in improving heart function. Our major findings are the following: Acute anemia is associated with a reduced HR and CO 24 hours post-AMI, whereas these changes were abolished 7 days post-AMI with an increase in SV. Chronic anemia is associated with a compensatory increase in end-diastolic volume, which was abolished 7 days post-AMI. NAC supplementation did not improve or alter heart function in both acute and chronic anemic mice 24 hours post-AMI and 7 days post-AMI. Immune infiltration analysis (leukocytes, monocytes, NK cell, B cell, T cell, and neutrophils) revealed that neutrophil content was significantly enhanced in the myocardium of acute anemic mice in the basal state; however, 24 hours after AMI, infiltration was similar in acute anemic mice and non-anemic group. In chronic anemic mice, infiltration of (leukocytes, monocytes, NK cells, B cells, T cells, and neutrophils) remained unchanged.

7.1 Mouse models of anemia

Anemia, among several comorbidities, significantly contributes to adverse outcomes following AMI, particularly in elderly patients during admission, hospitalization, or the post-AMI period (Colombo et al., 2023; Salisbury et al., 2011). Blood loss anemia is a key factor leading to reduced Hb levels during hospitalization of patients, primarily due to frequent blood sampling for laboratory tests and necessary clinical interventions, such as the insertion of catheters, endotracheal tubes, and other similar procedures (Czempik, Wilczek, Herzyk, & Krzych, 2022; Solga et al., 2024). These interventions are unavoidable in hospital settings for better diagnosis and care. In this research project, we used well established acute and chronic blood loss anemic mouse models to simulate the blood loss anemia observed in hospitalized patients. Importantly, our previous research demonstrated that these mouse models exhibit mild anemia without severe complications such as oedema due to blood loss (Wischmann et al., 2020). To further understand the association between anemia and adverse outcomes on heart function and immune infiltration, AMI was induced in both mouse models to explore potential mechanisms underlying the poor prognosis in anemic patients following AMI. We studied the heart function at two different time points after AMI i.e. 24 hr and 7 days.

7.2 Heart function in acute and chronic anemia

This study aims to address gaps in our understanding of functional cardiac parameters under conditions such as anemia and AMI. Prior studies have shown that acute anemia triggers compensatory mechanisms to maintain cardiac function, evidenced by increases in LV functional parameters such as EDV, SV, ESV, and CO in acute mouse models (Wischmann et al., 2020). These compensatory increases in heart function can be explained by two mechanisms: increased flow-mediated dilation in the peripheral vascular system with reduced vascular resistance, and reduced oxygen-carrying RBCs in the circulation, leading to changes in blood viscosity (Wischmann et al., 2020). However, we recently demonstrated that chronic anemia, or a combination of both acute and chronic anemia with AMI, results in a loss of compensatory vascular function due to severe endothelial dysfunction. In line with these findings, this study shows that acute anemia is associated with reduced cardiac output 24 hours after AMI. Interestingly, at 7 days post-AMI, the acute anemic mice exhibited improved heart function despite the presence of anemia. These findings demonstrate that the effects of anemia are more prominent during the acute phase of AMI. In contrast, chronic anemic mice showed an enhanced compensatory increase in EDV 24 hours after AMI. These findings suggest that chronic anemic mice exhibit adaptive increases in heart function. Of note, our unpublished data showed that chronic anemia drastically affects both smooth muscle and endothelial function after AMI. We speculate that, to compensate for severe vascular dysfunction, chronic

anemic mice show enhanced EDV. However, other cardiac functional parameters remain unaltered, indicating that the adaptive cardiac changes are minimal.

7.3 The Effect of anemia on Immune Cell Infiltration

Following AMI, immune cell infiltration is a critical determinant of the inflammatory response and subsequent cardiac repair. Neutrophils are the first responders, rapidly migrating to the ischemic myocardium within hours (Epelman et al., 2015; Puhl & Steffens, 2019). These cells initiate the inflammatory cascade by releasing ROS, proteolytic enzymes, and pro-inflammatory mediators (Carbone et al., 2013; Ma et al., 2013). While neutrophils are crucial for clearing necrotic debris, excessive ROS production and respiratory bursts can exacerbate myocardial injury (Amulic et al., 2012; Kolaczkowska & Kubes, 2013; Ma et al., 2013).

In this study, we observed significant neutrophil infiltration into the myocardium of acute anemic mice even in the absence of AMI. This is a novel finding not previously described. We have previously shown that anemia is associated with increased oxidative stress in the vasculature (Chennupati et al., 2023), which was partly mediated by MPO. Unpublished data from our group also demonstrated increased MPO activity in the myocardium of acute anemic mice. Consistent with this, the hearts of acute anemic mice showed increased oxidative stress, which may promote neutrophil infiltration.

Following AMI, neutrophil infiltration was drastically enhanced in both anemic and non-anemic groups compared to the basal state (without AMI). However, although neutrophil infiltration was slightly increased in acute anemic mice after AMI, the difference was not statistically significant compared to non-anemic mice. This lack of significance may be attributed to high individual variation within the experimental groups. Immunohistochemistry analysis confirmed these findings, showing similar $Ly6G^{+}$ positive neutrophil abundance in acute and chronic anemic mice after AMI. Interestingly, in chronic anemia, we did not observe any significant changes in neutrophil infiltration either before or after AMI. These unexpected results could potentially be explained by adaptive changes in the vascular system during chronic anemic state.

Monocytes, another cell type well known to infiltrate the infarcted myocardium, differentiate into macrophages with distinct roles depending on the phase of the immune response (Wiktor-Jedrzejczak & Gordon, 1996). During the early inflammatory phase, macrophages exacerbate tissue damage by secreting pro-inflammatory cytokines (Kubota & Frangogiannis, 2022). However, as the immune response progresses, macrophages adopt a reparative phenotype, contributing to tissue repair via efferocytosis (Frangogiannis et al., 2003; Hilgendorf et al., 2014; Mouton et al., 2018), fibrosis induction, and angiogenesis (Kubota & Frangogiannis, 2022; Sager et al., 2016). In our

study, macrophage infiltration was drastically enhanced in both anemic groups and their respective controls following AMI. However, neither acute nor chronic anemia altered macrophage infiltration.

Next, we evaluated adaptive immune cells, including T and B lymphocytes, which are activated following AMI. Effector T cells infiltrate the myocardium and release cytokines that initiate inflammation and tissue regeneration (Hofmann & Frantz, 2015). B cells, in turn, secrete cytokines with both pro-inflammatory and anti-inflammatory effects, including IL-10, which reduces myocardial damage and supports cardiac function (L. Wu et al., 2019). Following AMI, T and B lymphocyte infiltration was drastically enhanced in both anemic groups and their respective controls. Interestingly, neither acute nor chronic anemia altered the infiltration of T and B lymphocytes, suggesting that anemia does not additionally evoke adaptive immune cell responses under basal conditions or following AMI. Previous studies demonstrated that in a model of anemia caused by iron deficiency, T cell activation and proliferation are significantly reduced. This impairment arises due to limited iron availability, which disrupts key cellular functions essential for effective T-cell responses (Brock & Mulero, 2000; Musallam & Taher, 2018; Savy et al., 2009; Stoffel & Drakesmith, 2024). Similarly, in a model of anemia involving mutations in the transferring receptor (TFRC), a critical protein for iron uptake, patients displayed decreased levels of circulating IgG and memory B- cells. These deficiencies attributed to impaired immune cell iron acquisition, which comprises their proliferation and function (Frost et al., 2021; Stoffel & Drakesmith, 2024).

We further evaluated the effect of acute and chronic anemia on natural killer (NK) cell infiltration into the myocardium. NK cells, primarily known for their cytotoxic activity, also contribute to post-AMI inflammation by releasing pro-inflammatory cytokines (Bjorkstrom et al., 2010; Morice, 2007; Trinchieri, 1989). Studies have shown that NK cell numbers may decrease under certain cardiovascular conditions due to apoptosis, potentially impairing their regulatory functions (Backteman et al., 2014; Biron et al., 1999; Ortega-Rodriguez et al., 2020). In our study, NK cell infiltration was drastically enhanced in both anemic groups and their respective controls following AMI. However, neither acute nor chronic anemia altered NK cell infiltration.

8 Conclusion

We evaluated the effects of acute and chronic anemia on heart function after AMI. We demonstrated that acute anemia is associated with worsening heart function 24 hours post-AMI, whereas chronic anemia is associated with a compensatory increase in heart function, as demonstrated by increased end-diastolic volume 24 hours post-AMI. Both chronic and acute anemic mice, despite anemia, showed improved heart function 7 days post-AMI. Additionally, NAC supplementation in acute anemic mice did not result in improved heart function, indicating that antioxidant therapy does not improve heart function. Immune infiltration analysis revealed that AMI is associated with enhanced immune infiltration (leukocytes, monocytes, NK cells, B cells, T cells, and neutrophils), independent of anemia. Neutrophil infiltration is specifically enhanced in acute anemic mice without AMI. However, after AMI, neutrophil infiltration increased, but it was not significantly different in acute anemic mice compared to the control group. Further studies are needed to investigate the specific role of neutrophils in acute anemia-associated altered heart function.

9 References

1. Amulic, B., Cazalet, C., Hayes, G. L., Metzler, K. D., & Zychlinsky, A. (2012). Neutrophil function: from mechanisms to disease. *Annu Rev Immunol, 30*, 459-489. doi:10.1146/annurev-immunol-020711-074942
2. Anderson, J. L., & Morrow, D. A. (2017). Acute Myocardial Infarction. *N Engl J Med, 376*(21), 2053-2064. doi:10.1056/NEJMra1606915
3. Anker, S. D., Voors, A., Okonko, D., Clark, A. L., James, M. K., von Haehling, S., … Investigators, O. (2009). Prevalence, incidence, and prognostic value of anaemia in patients after an acute myocardial infarction: data from the OPTIMAAL trial. *Eur Heart J, 30*(11), 1331-1339. doi:10.1093/eurheartj/ehp116
4. Aoyama, T., Chen, M., Fujiwara, H., Masaki, T., & Sawamura, T. (2000). LOX-1 mediates lysophosphatidylcholine-induced oxidized LDL uptake in smooth muscle cells. *FEBS Lett, 467*(2-3), 217-220. doi:10.1016/s0014-5793(00)01154-6
5. Aronson, D., Dann, E. J., Bonstein, L., Blich, M., Kapeliovich, M., Beyar, R., … Hammerman, H. (2008). Impact of red blood cell transfusion on clinical outcomes in patients with acute myocardial infarction. *Am J Cardiol, 102*(2), 115-119. doi:10.1016/j.amjcard.2008.03.027
6. Auffray, C., Sieweke, M. H., & Geissmann, F. (2009). Blood monocytes: development, heterogeneity, and relationship with dendritic cells. *Annu Rev Immunol, 27*, 669-692. doi:10.1146/annurev.immunol.021908.132557
7. Awad Hegazy, A. (2022). Myocardial Infarction: Risk Factors, Pathophysiology, Classification, Assessment and Management. *Cardiology Research and Reports*.
8. Backteman, K., Ernerudh, J., & Jonasson, L. (2014). Natural killer (NK) cell deficit in coronary artery disease: no aberrations in phenotype but sustained reduction of NK cells is associated with low-grade inflammation. *Clin Exp Immunol, 175*(1), 104-112. doi:10.1111/cei.12210
9. Badireddy, M., Baradhi, K. M., & Wilhite, A. (2024). Chronic Anemia (Nursing). In *StatPearls*. Treasure Island (FL).
10. Barbalato, L., & Pillarisetty, L. S. (2024). Histology, Red Blood Cell. In *StatPearls*. Treasure Island (FL).
11. Bentzon, J. F., Otsuka, F., Virmani, R., & Falk, E. (2014). Mechanisms of plaque formation and rupture. *Circ Res, 114*(12), 1852-1866. doi:10.1161/CIRCRESAHA.114.302721
12. Beutler, E. (1994). G6PD deficiency. *Blood, 84*(11), 3613-3636. Retrieved from https://www.ncbi.nlm.nih.gov/pubmed/7949118
13. Biron, C. A., Nguyen, K. B., Pien, G. C., Cousens, L. P., & Salazar-Mather, T. P. (1999). Natural killer cells in antiviral defense: function and regulation by innate cytokines. *Annu Rev Immunol, 17*, 189-220. doi:10.1146/annurev.immunol.17.1.189
14. Bjorkstrom, N. K., Riese, P., Heuts, F., Andersson, S., Fauriat, C., Ivarsson, M. A., … Malmberg, K. J. (2010). Expression patterns of NKG2A, KIR, and CD57 define a process of CD56dim NK-cell differentiation uncoupled from NK-cell education. *Blood, 116*(19), 3853-3864. doi:10.1182/blood-2010-04-281675
15. Blanton, R. M., Carrillo-Salinas, F. J., & Alcaide, P. (2019). T-cell recruitment to the heart: friendly guests or unwelcome visitors? *Am J Physiol Heart Circ Physiol, 317*(1), H124-H140. doi:10.1152/ajpheart.00028.2019
16. Brakenhielm, E., & Alitalo, K. (2019). Cardiac lymphatics in health and disease. *Nat Rev Cardiol, 16*(1), 56-68. doi:10.1038/s41569-018-0087-8
17. Brock, J. H., & Mulero, V. (2000). Cellular and molecular aspects of iron and immune function. *Proc Nutr Soc, 59*(4), 537-540. doi:10.1017/s002966510000077x
18. Burgener, S. S., & Schroder, K. (2020). Neutrophil Extracellular Traps in Host Defense. *Cold Spring Harb Perspect Biol, 12*(7)doi:10.1101/cshperspect.a037028
19. Burn, G. L., Foti, A., Marsman, G., Patel, D. F., & Zychlinsky, A. (2021). The Neutrophil. *Immunity, 54*(7), 1377-1391. doi:10.1016/j.immuni.2021.06.006

20. Carai, P., Gonzalez, L. F., Van Bruggen, S., Spalart, V., De Giorgio, D., Geuens, N., … Heymans, S. (2023). Neutrophil inhibition improves acute inflammation in a murine model of viral myocarditis. *Cardiovasc Res, 118*(17), 3331-3345. doi:10.1093/cvr/cvac052
21. Carbone, F., Nencioni, A., Mach, F., Vuilleumier, N., & Montecucco, F. (2013). Pathophysiological role of neutrophils in acute myocardial infarction. *Thromb Haemost, 110*(3), 501-514. doi:10.1160/TH13-03-0211
22. Casanova-Acebes, M., Nicolas-Avila, J. A., Li, J. L., Garcia-Silva, S., Balachander, A., Rubio-Ponce, A., … Hidalgo, A. (2018). Neutrophils instruct homeostatic and pathological states in naive tissues. *J Exp Med, 215*(11), 2778-2795. doi:10.1084/jem.20181468
23. Chen, L. Y., & Mehta, J. L. (1998). Evidence for the presence of L-arginine-nitric oxide pathway in human red blood cells: relevance in the effects of red blood cells on platelet function. *J Cardiovasc Pharmacol, 32*(1), 57-61. doi:10.1097/00005344-199807000-00009
24. Chennupati, R., Solga, I., Wischmann, P., Dahlmann, P., Celik, F. G., Pacht, D., … Jung, C. (2023). Chronic anemia is associated with systemic endothelial dysfunction. *Front Cardiovasc Med, 10*, 1099069. doi:10.3389/fcvm.2023.1099069
25. Colombo, C., Rebora, P., Montalto, C., Cantoni, S., Sacco, A., Mauri, M., … Morici, N. (2023). Hospital-Acquired Anemia in Patients with Acute Coronary Syndrome: Epidemiology and Potential Impact on Long-Term Outcome. *Am J Med, 136*(12), 1203-1210 e1204. doi:10.1016/j.amjmed.2023.08.012
26. Colotta, F., Re, F., Polentarutti, N., Sozzani, S., & Mantovani, A. (1992). Modulation of granulocyte survival and programmed cell death by cytokines and bacterial products. *Blood, 80*(8), 2012-2020. Retrieved from https://www.ncbi.nlm.nih.gov/pubmed/1382715
27. Czempik, P. F., Wilczek, D., Herzyk, J., & Krzych, L. J. (2022). Hospital-Acquired Anemia in Patients Hospitalized in the Intensive Care Unit: A Retrospective Cohort Study. *J Clin Med, 11*(14)doi:10.3390/jcm11143939
28. Danesh, J., Collins, R., Peto, R., & Lowe, G. D. (2000). Haematocrit, viscosity, erythrocyte sedimentation rate: meta-analyses of prospective studies of coronary heart disease. *Eur Heart J, 21*(7), 515-520. doi:10.1053/euhj.1999.1699
29. Denning, N. L., Aziz, M., Gurien, S. D., & Wang, P. (2019). DAMPs and NETs in Sepsis. *Front Immunol, 10*, 2536. doi:10.3389/fimmu.2019.02536
30. Ducrocq, G., Puymirat, E., Steg, P. G., Henry, P., Martelet, M., Karam, C., … Danchin, N. (2015). Blood transfusion, bleeding, anemia, and survival in patients with acute myocardial infarction: FAST-MI registry. *Am Heart J, 170*(4), 726-734 e722. doi:10.1016/j.ahj.2015.07.004
31. Epelman, S., Liu, P. P., & Mann, D. L. (2015). Role of innate and adaptive immune mechanisms in cardiac injury and repair. *Nat Rev Immunol, 15*(2), 117-129. doi:10.1038/nri3800
32. Fahy, R. J., Doseff, A. I., & Wewers, M. D. (1999). Spontaneous human monocyte apoptosis utilizes a caspase-3-dependent pathway that is blocked by endotoxin and is independent of caspase-1. *J Immunol, 163*(4), 1755-1762. Retrieved from https://www.ncbi.nlm.nih.gov/pubmed/10438906
33. Fang, P., Li, X., Dai, J., Cole, L., Camacho, J. A., Zhang, Y., … Wang, H. (2018). Immune cell subset differentiation and tissue inflammation. *J Hematol Oncol, 11*(1), 97. doi:10.1186/s13045-018-0637-x
34. Farah, C., Michel, L. Y. M., & Balligand, J. L. (2018). Nitric oxide signalling in cardiovascular health and disease. *Nat Rev Cardiol, 15*(5), 292-316. doi:10.1038/nrcardio.2017.224
35. Frangogiannis, N. G. (2015). Pathophysiology of Myocardial Infarction. *Compr Physiol, 5*(4), 1841-1875. doi:10.1002/cphy.c150006
36. Frangogiannis, N. G., Mendoza, L. H., Ren, G., Akrivakis, S., Jackson, P. L., Michael, L. H., … Entman, M. L. (2003). MCSF expression is induced in healing myocardial infarcts and may regulate monocyte and endothelial cell phenotype. *Am J Physiol Heart Circ Physiol, 285*(2), H483-492. doi:10.1152/ajpheart.01016.2002
37. Frantz, S., Falcao-Pires, I., Balligand, J. L., Bauersachs, J., Brutsaert, D., Ciccarelli, M., … Heymans, S. (2018). The innate immune system in chronic cardiomyopathy: a European Society of Cardiology (ESC) scientific statement from the Working Group on Myocardial Function of the ESC. *Eur J Heart Fail, 20*(3), 445-459. doi:10.1002/ejhf.1138

38. Frost, J. N., Tan, T. K., Abbas, M., Wideman, S. K., Bonadonna, M., Stoffel, N. U., … Drakesmith, H. (2021). Hepcidin-Mediated Hypoferremia Disrupts Immune Responses to Vaccination and Infection. *Med, 2*(2), 164-179 e112. doi:10.1016/j.medj.2020.10.004
39. Futosi, K., Fodor, S., & Mocsai, A. (2013). Reprint of Neutrophil cell surface receptors and their intracellular signal transduction pathways. *Int Immunopharmacol, 17*(4), 1185-1197. doi:10.1016/j.intimp.2013.11.010
40. G.A. Fishbein, M.C. Fishbein, L.M. Buja, Chapter 7 - Myocardial Ischemia and Its Complications, Editor(s): L. Maximilian Buja, Jagdish Butany, Cardiovascular Pathology (Fourth Edition), Academic Press, 2016, Pages 239-270, ISBN 9780124202191, https://doi.org/10.1016/B978-0-12-420219-1.00007-0.
41. Goyal, A., Wang, Y., Graham, M. M., Doseff, A. I., Bhatt, N. Y., & Marsh, C. B. (2002). Monocyte survival factors induce Akt activation and suppress caspase-3. *Am J Respir Cell Mol Biol, 26*(2), 224-230. doi:10.1165/ajrcmb.26.2.4640
42. Hilgendorf, I., Gerhardt, L. M., Tan, T. C., Winter, C., Holderried, T. A., Chousterman, B. G., … Swirski, F. K. (2014). Ly-6Chigh monocytes depend on Nr4a1 to balance both inflammatory and reparative phases in the infarcted myocardium. *Circ Res, 114*(10), 1611-1622. doi:10.1161/CIRCRESAHA.114.303204
43. Hofmann, U., & Frantz, S. (2015). Role of lymphocytes in myocardial injury, healing, and remodeling after myocardial infarction. *Circ Res, 116*(2), 354-367. doi:10.1161/CIRCRESAHA.116.304072
44. Johnson, R. M., Goyette, G., Jr., Ravindranath, Y., & Ho, Y. S. (2005). Hemoglobin autoxidation and regulation of endogenous H2O2 levels in erythrocytes. *Free Radic Biol Med, 39*(11), 1407-1417. doi:10.1016/j.freeradbiomed.2005.07.002
45. Jolicoeur, E. M., O'Neill, W. W., Hellkamp, A., Hamm, C. W., Holmes, D. R., Jr., Al-Khalidi, H. R., … Investigators, A.-A. (2009). Transfusion and mortality in patients with ST-segment elevation myocardial infarction treated with primary percutaneous coronary intervention. *Eur Heart J, 30*(21), 2575-2583. doi:10.1093/eurheartj/ehp279
46. Kanic, V., Kompara, G., Vollrath, M., Suran, D., & Kanic, Z. (2019). Age-Specific Sex-Based Differences in Anemia in Patients with Myocardial Infarction. *J Womens Health (Larchmt), 28*(7), 1004-1010. doi:10.1089/jwh.2018.7211
47. Kaplan, R. C., Psaty, B. M., Heckbert, S. R., Smith, N. L., & Lemaitre, R. N. (1999). Blood pressure level and incidence of myocardial infarction among patients treated for hypertension. *Am J Public Health, 89*(9), 1414-1417. doi:10.2105/ajph.89.9.1414
48. Kaushansky, K. (2006). Lineage-specific hematopoietic growth factors. *N Engl J Med, 354*(19), 2034-2045. doi:10.1056/NEJMra052706
49. Kaveri, S. V., Silverman, G. J., & Bayry, J. (2012). Natural IgM in immune equilibrium and harnessing their therapeutic potential. *J Immunol, 188*(3), 939-945. doi:10.4049/jimmunol.1102107
50. Kim, C. H. (2010). Homeostatic and pathogenic extramedullary hematopoiesis. *J Blood Med, 1*, 13-19. doi:10.2147/JBM.S7224
51. Klebanoff, S. J., Kettle, A. J., Rosen, H., Winterbourn, C. C., & Nauseef, W. M. (2013). Myeloperoxidase: a front-line defender against phagocytosed microorganisms. *J Leukoc Biol, 93*(2), 185-198. doi:10.1189/jlb.0712349
52. Kleinbongard, P., Schulz, R., Rassaf, T., Lauer, T., Dejam, A., Jax, T., … Kelm, M. (2006). Red blood cells express a functional endothelial nitric oxide synthase. *Blood, 107*(7), 2943-2951. doi:10.1182/blood-2005-10-3992
53. Kolaczkowska, E., & Kubes, P. (2013). Neutrophil recruitment and function in health and inflammation. *Nat Rev Immunol, 13*(3), 159-175. doi:10.1038/nri3399
54. Kubota, A., & Frangogiannis, N. G. (2022). Macrophages in myocardial infarction. *Am J Physiol Cell Physiol, 323*(4), C1304-C1324. doi:10.1152/ajpcell.00230.2022
55. Kuhn, V., Diederich, L., Keller, T. C. S. t., Kramer, C. M., Luckstadt, W., Panknin, C., … Cortese-Krott, M. M. (2017). Red Blood Cell Function and Dysfunction: Redox Regulation, Nitric Oxide Metabolism, Anemia. *Antioxid Redox Signal, 26*(13), 718-742. doi:10.1089/ars.2016.6954
56. Libby, P., Ridker, P. M., & Hansson, G. K. (2011). Progress and challenges in translating the biology of atherosclerosis. *Nature, 473*(7347), 317-325. doi:10.1038/nature10146

57. Lichtman, M. A., Chamberlain, J. K., Weed, R. I., Pincus, A., & Santillo, P. A. (1977). The regulation of the release of granulocytes from normal marrow. *Prog Clin Biol Res, 13*, 53-75. Retrieved from https://www.ncbi.nlm.nih.gov/pubmed/400761
58. Linton, M. F., Yancey, P. G., Davies, S. S., Jerome, W. G., Linton, E. F., Song, W. L., … Vickers, K. C. (2000). The Role of Lipids and Lipoproteins in Atherosclerosis. In K. R. Feingold, B. Anawalt, M. R. Blackman, A. Boyce, G. Chrousos, E. Corpas, W. W. de Herder, K. Dhatariya, K. Dungan, J. Hofland, S. Kalra, G. Kaltsas, N. Kapoor, C. Koch, P. Kopp, M. Korbonits, C. S. Kovacs, W. Kuohung, B. Laferrere, M. Levy, E. A. McGee, R. McLachlan, M. New, J. Purnell, R. Sahay, A. S. Shah, F. Singer, M. A. Sperling, C. A. Stratakis, D. L. Trence, & D. P. Wilson (Eds.), *Endotext*. South Dartmouth (MA).
59. Loyola-Leyva, A., Loyola-Rodriguez, J. P., Atzori, M., & Gonzalez, F. J. (2018). Morphological changes in erythrocytes of people with type 2 diabetes mellitus evaluated with atomic force microscopy: A brief review. *Micron, 105*, 11-17. doi:10.1016/j.micron.2017.11.001
60. Luscher, T. F., Pieper, M., Tendera, M., Vrolix, M., Rutsch, W., van den Branden, F., … Munzel, T. (2009). A randomized placebo-controlled study on the effect of nifedipine on coronary endothelial function and plaque formation in patients with coronary artery disease: the ENCORE II study. *Eur Heart J, 30*(13), 1590-1597. doi:10.1093/eurheartj/ehp151
61. Luzzatto, L., Ally, M., & Notaro, R. (2020). Glucose-6-phosphate dehydrogenase deficiency. *Blood, 136*(11), 1225-1240. doi:10.1182/blood.2019000944
62. Ma, Y., Yabluchanskiy, A., & Lindsey, M. L. (2013). Neutrophil roles in left ventricular remodeling following myocardial infarction. *Fibrogenesis Tissue Repair, 6*(1), 11. doi:10.1186/1755-1536-6-11
63. Madjid, M., & Fatemi, O. (2013). Components of the complete blood count as risk predictors for coronary heart disease: in-depth review and update. *Tex Heart Inst J, 40*(1), 17-29. Retrieved from https://www.ncbi.nlm.nih.gov/pubmed/23467296
64. Magaki, S., Hojat, S. A., Wei, B., So, A., & Yong, W. H. (2019). An Introduction to the Performance of Immunohistochemistry. *Methods Mol Biol, 1897*, 289-298. doi:10.1007/978-1-4939-8935-5_25
65. Maldonado Rolon, E. (1975). [Psychological comfort]. *Bol Col Prof Enferm P R, 1*(4), 26. Retrieved from https://www.ncbi.nlm.nih.gov/pubmed/1059430
66. Mantovani, A., Cassatella, M. A., Costantini, C., & Jaillon, S. (2011). Neutrophils in the activation and regulation of innate and adaptive immunity. *Nat Rev Immunol, 11*(8), 519-531. doi:10.1038/nri3024
67. Martin, C., Yu, A. Y., Jiang, B. H., Davis, L., Kimberly, D., Hohimer, A. R., & Semenza, G. L. (1998). Cardiac hypertrophy in chronically anemic fetal sheep: Increased vascularization is associated with increased myocardial expression of vascular endothelial growth factor and hypoxia-inducible factor 1. *Am J Obstet Gynecol, 178*(3), 527-534. doi:10.1016/s0002-9378(98)70433-8
68. McKinnon, K. M. (2018). Flow Cytometry: An Overview. *Curr Protoc Immunol, 120*, 5.1.1-5.1.11. doi:10.1002/cpim.40
69. Metivier, F., Marchais, S. J., Guerin, A. P., Pannier, B., & London, G. M. (2000). Pathophysiology of anaemia: focus on the heart and blood vessels. *Nephrol Dial Transplant, 15 Suppl 3*, 14-18. doi:10.1093/oxfordjournals.ndt.a027970
70. Mitsis, A., & Gragnano, F. (2021). Myocardial Infarction with and without ST-segment Elevation: a Contemporary Reappraisal of Similarities and Differences. *Curr Cardiol Rev, 17*(4), e230421189013. doi:10.2174/1573403X16999201210195702
71. Moghaddam, N., Wong, G. C., Cairns, J. A., Goodman, S. G., Perry-Arnesen, M., Tocher, W., … Fordyce, C. B. (2018). Association of Anemia With Outcomes Among ST-Segment-Elevation Myocardial Infarction Patients Receiving Primary Percutaneous Coronary Intervention. *Circ Cardiovasc Interv, 11*(12), e007175. doi:10.1161/CIRCINTERVENTIONS.118.007175
72. Mohandas, N., & Gallagher, P. G. (2008). Red cell membrane: past, present, and future. *Blood, 112*(10), 3939-3948. doi:10.1182/blood-2008-07-161166
73. Mohanty, J. G., Nagababu, E., & Rifkind, J. M. (2014). Red blood cell oxidative stress impairs oxygen delivery and induces red blood cell aging. *Front Physiol, 5*, 84. doi:10.3389/fphys.2014.00084

74. Moliterno, D. J., Willard, J. E., Lange, R. A., Negus, B. H., Boehrer, J. D., Glamann, D. B., … Hillis, L. D. (1994). Coronary-artery vasoconstriction induced by cocaine, cigarette smoking, or both. *N Engl J Med, 330*(7), 454-459. doi:10.1056/NEJM199402173300702
75. Morice, W. G. (2007). The immunophenotypic attributes of NK cells and NK-cell lineage lymphoproliferative disorders. *Am J Clin Pathol, 127*(6), 881-886. doi:10.1309/Q49CRJ030L22MHLF
76. Mouton, A. J., DeLeon-Pennell, K. Y., Rivera Gonzalez, O. J., Flynn, E. R., Freeman, T. C., Saucerman, J. J., … Lindsey, M. L. (2018). Mapping macrophage polarization over the myocardial infarction time continuum. *Basic Res Cardiol, 113*(4), 26. doi:10.1007/s00395-018-0686-x
77. Mozos, I. (2015). Mechanisms linking red blood cell disorders and cardiovascular diseases. *Biomed Res Int, 2015*, 682054. doi:10.1155/2015/682054
78. Musallam, K. M., & Taher, A. T. (2018). Iron deficiency beyond erythropoiesis: should we be concerned? *Curr Med Res Opin, 34*(1), 81-93. doi:10.1080/03007995.2017.1394833
79. Nian, M., Lee, P., Khaper, N., & Liu, P. (2004). Inflammatory cytokines and postmyocardial infarction remodeling. *Circ Res, 94*(12), 1543-1553. doi:10.1161/01.RES.0000130526.20854.fa
80. Nordenfelt, P., & Tapper, H. (2011). Phagosome dynamics during phagocytosis by neutrophils. *J Leukoc Biol, 90*(2), 271-284. doi:10.1189/jlb.0810457
81. Ojha, N., & Dhamoon, A. S. (2024). Myocardial Infarction. In *StatPearls*. Treasure Island (FL).
82. Orrico, F., Laurance, S., Lopez, A. C., Lefevre, S. D., Thomson, L., Moller, M. N., & Ostuni, M. A. (2023). Oxidative Stress in Healthy and Pathological Red Blood Cells. *Biomolecules, 13*(8)doi:10.3390/biom13081262
83. Ortega-Rodriguez, A. C., Marin-Jauregui, L. S., Martinez-Shio, E., Hernandez Castro, B., Gonzalez-Amaro, R., Escobedo-Uribe, C. D., & Monsivais-Urenda, A. E. (2020). Altered NK cell receptor repertoire and function of natural killer cells in patients with acute myocardial infarction: A three-month follow-up study. *Immunobiology, 225*(3), 151909. doi:10.1016/j.imbio.2020.151909
84. Padda, J., Khalid, K., Hitawala, G., Batra, N., Pokhriyal, S., Mohan, A., … Jean-Charles, G. (2021). Acute Anemia and Myocardial Infarction. *Cureus, 13*(8), e17096. doi:10.7759/cureus.17096
85. Papayannopoulos, V. (2018). Neutrophil extracellular traps in immunity and disease. *Nat Rev Immunol, 18*(2), 134-147. doi:10.1038/nri.2017.105
86. Parihar, A., Eubank, T. D., & Doseff, A. I. (2010). Monocytes and macrophages regulate immunity through dynamic networks of survival and cell death. *J Innate Immun, 2*(3), 204-215. doi:10.1159/000296507
87. Peiseler, M., & Kubes, P. (2019). More friend than foe: the emerging role of neutrophils in tissue repair. *J Clin Invest, 129*(7), 2629-2639. doi:10.1172/JCI124616
88. Peña, F. J., Ball, B. A., & Squires, E. L. (2018). A New Method for Evaluating Stallion Sperm Viability and Mitochondrial Membrane Potential in Fixed Semen Samples. *Cytometry B Clin Cytom, 94*(2), 302-311. doi:10.1002/cyto.b.21506
89. Pernow, J., Mahdi, A., Yang, J., & Zhou, Z. (2019). Red blood cell dysfunction: a new player in cardiovascular disease. *Cardiovasc Res, 115*(11), 1596-1605. doi:10.1093/cvr/cvz156
90. Piegas, L. S., Avezum, A., Pereira, J. C., Neto, J. M., Hoepfner, C., Farran, J. A., … Investigators, A. S. (2003). Risk factors for myocardial infarction in Brazil. *Am Heart J, 146*(2), 331-338. doi:10.1016/S0002-8703(03)00181-9
91. Prescott, E., Hippe, M., Schnohr, P., Hein, H. O., & Vestbo, J. (1998). Smoking and risk of myocardial infarction in women and men: longitudinal population study. *BMJ, 316*(7137), 1043-1047. doi:10.1136/bmj.316.7137.1043
92. Puhl, S. L., & Steffens, S. (2019). Neutrophils in Post-myocardial Infarction Inflammation: Damage vs. Resolution? *Front Cardiovasc Med, 6*, 25. doi:10.3389/fcvm.2019.00025
93. Rassaf, T., Preik, M., Kleinbongard, P., Lauer, T., Heiss, C., Strauer, B. E., … Kelm, M. (2002). Evidence for in vivo transport of bioactive nitric oxide in human plasma. *J Clin Invest, 109*(9), 1241-1248. doi:10.1172/JCI14995
94. Rehman, I., & Rehman, A. (2024). Anatomy, Thorax, Heart. In *StatPearls*. Treasure Island (FL).

95. Reimer, K. A., Jennings, R. B., & Tatum, A. H. (1983). Pathobiology of acute myocardial ischemia: metabolic, functional and ultrastructural studies. *Am J Cardiol, 52*(2), 72A-81A. doi:10.1016/0002-9149(83)90180-7
96. Riley, R. F., Newby, L. K., Don, C. W., Alexander, K. P., Peterson, E. D., Peng, S. A., … Herrington, D. M. (2013). Guidelines-based treatment of anaemic STEMI patients: practice patterns and effects on in-hospital mortality: a retrospective analysis from the NCDR. *Eur Heart J Acute Cardiovasc Care, 2*(1), 35-43. doi:10.1177/2048872612471216
97. Robertson, M. J., & Ritz, J. (1990). Biology and clinical relevance of human natural killer cells. *Blood, 76*(12), 2421-2438. Retrieved from https://www.ncbi.nlm.nih.gov/pubmed/2265240
98. Rousseau, M., Yan, R. T., Tan, M., Lefkowitz, C. J., Casanova, A., Fitchett, D., … Enoxaparin Randomized Assessment of Acute Coronary Syndrome Treatment Trial, I. (2010). Relation between hemoglobin level and recurrent myocardial ischemia in acute coronary syndromes detected by continuous electrocardiographic monitoring. *Am J Cardiol, 106*(10), 1417-1422. doi:10.1016/j.amjcard.2010.07.009
99. Sager, H. B., Hulsmans, M., Lavine, K. J., Moreira, M. B., Heidt, T., Courties, G., … Nahrendorf, M. (2016). Proliferation and Recruitment Contribute to Myocardial Macrophage Expansion in Chronic Heart Failure. *Circ Res, 119*(7), 853-864. doi:10.1161/CIRCRESAHA.116.309001
100. Saleh, M., & Ambrose, J. A. (2018). Understanding myocardial infarction. *F1000Res, 7*doi:10.12688/f1000research.15096.1
101. Salgado, M. T., Cao, Z., Nagababu, E., Mohanty, J. G., & Rifkind, J. M. (2015). Red blood cell membrane-facilitated release of nitrite-derived nitric oxide bioactivity. *Biochemistry, 54*(44), 6712-6723. doi:10.1021/acs.biochem.5b00643
102. Salisbury, A. C., Amin, A. P., Reid, K. J., Wang, T. Y., Masoudi, F. A., Chan, P. S., … Kosiborod, M. (2011). Hospital-acquired anemia and in-hospital mortality in patients with acute myocardial infarction. *Am Heart J, 162*(2), 300-309 e303. doi:10.1016/j.ahj.2011.05.021
103. Savill, J., & Fadok, V. (2000). Corpse clearance defines the meaning of cell death. *Nature, 407*(6805), 784-788. doi:10.1038/35037722
104. Savy, M., Edmond, K., Fine, P. E., Hall, A., Hennig, B. J., Moore, S. E., … Prentice, A. M. (2009). Landscape analysis of interactions between nutrition and vaccine responses in children. *J Nutr, 139*(11), 2154S-2218S. doi:10.3945/jn.109.105312
105. Saxton, A., Tariq, M. A., & Bordoni, B. (2024). Anatomy, Thorax, Cardiac Muscle. In *StatPearls*. Treasure Island (FL).
106. Schade, D., Kotthaus, J., & Clement, B. (2010). Modulating the NO generating system from a medicinal chemistry perspective: current trends and therapeutic options in cardiovascular disease. *Pharmacol Ther, 126*(3), 279-300. doi:10.1016/j.pharmthera.2010.02.005
107. Segal, A. W. (2005). How neutrophils kill microbes. *Annu Rev Immunol, 23*, 197-223. doi:10.1146/annurev.immunol.23.021704.115653
108. Severino, P., D'Amato, A., Netti, L., Pucci, M., Infusino, F., Maestrini, V., … Fedele, F. (2019). Myocardial Ischemia and Diabetes Mellitus: Role of Oxidative Stress in the Connection between Cardiac Metabolism and Coronary Blood Flow. *J Diabetes Res, 2019*, 9489826. doi:10.1155/2019/9489826
109. Shacham, Y., Leshem-Rubinow, E., Ben-Assa, E., Roth, A., & Steinvil, A. (2014). Lower admission hemoglobin levels are associated with longer symptom duration in acute ST-elevation myocardial infarction. *Clin Cardiol, 37*(2), 73-77. doi:10.1002/clc.22215
110. Shu, D. H., Ransom, T. P., O'Connell, C. M., Cox, J. L., Kaiser, S. M., Gee, S. A., … Imran, S. A. (2006). Anemia is an independent risk for mortality after acute myocardial infarction in patients with and without diabetes. *Cardiovasc Diabetol, 5*, 8. doi:10.1186/1475-2840-5-8
111. Singh, D. K., Winocour, P., & Farrington, K. (2009). Erythropoietic stress and anemia in diabetes mellitus. *Nat Rev Endocrinol, 5*(4), 204-210. doi:10.1038/nrendo.2009.17
112. Smith, J. E. (1987). Erythrocyte membrane: structure, function, and pathophysiology. *Vet Pathol, 24*(6), 471-476. doi:10.1177/030098588702400601
113. Solga, I., Sahin, A., Yogathasan, V., Hofer, L., Celik, F. G., Rai, A. E., … Chennupati, R. (2024). Distinct effects of acute and chronic blood loss anemia on vascular function after acute myocardial infarction. *bioRxiv*.

114. Steinvil, A., Banai, S., Leshem-Rubinow, E., Rogowski, O., Halkin, A., Keren, G., … Arbel, Y. (2012). The development of anemia of inflammation during acute myocardial infarction. *Int J Cardiol, 156*(2), 160-164. doi:10.1016/j.ijcard.2010.10.031
115. Stevens, R. J., Coleman, R. L., Adler, A. I., Stratton, I. M., Matthews, D. R., & Holman, R. R. (2004). Risk factors for myocardial infarction case fatality and stroke case fatality in type 2 diabetes: UKPDS 66. *Diabetes Care, 27*(1), 201-207. doi:10.2337/diacare.27.1.201
116. Stoffel, N. U., & Drakesmith, H. (2024). Effects of Iron Status on Adaptive Immunity and Vaccine Efficacy: A Review. *Adv Nutr, 15*(6), 100238. doi:10.1016/j.advnut.2024.100238
117. Sun, K., Li, Y. Y., & Jin, J. (2021). A double-edged sword of immuno-microenvironment in cardiac homeostasis and injury repair. *Signal Transduct Target Ther, 6*(1), 79. doi:10.1038/s41392-020-00455-6
118. Surendran, A., Atefi, N., Zhang, H., Aliani, M., & Ravandi, A. (2021). Defining Acute Coronary Syndrome through Metabolomics. *Metabolites, 11*(10)doi:10.3390/metabo11100685
119. Szaloki, G., & Goda, K. (2015). Compensation in multicolor flow cytometry. *Cytometry A, 87*(11), 982-985. doi:10.1002/cyto.a.22736
120. Tahir, N., & Zahra, F. (2024). Neutrophilia. In *StatPearls*. Treasure Island (FL).
121. Tak, T., Tesselaar, K., Pillay, J., Borghans, J. A., & Koenderman, L. (2013). What's your age again? Determination of human neutrophil half-lives revisited. *J Leukoc Biol, 94*(4), 595-601. doi:10.1189/jlb.1112571
122. Tenen, D. G., Hromas, R., Licht, J. D., & Zhang, D. E. (1997). Transcription factors, normal myeloid development, and leukemia. *Blood, 90*(2), 489-519. Retrieved from https://www.ncbi.nlm.nih.gov/pubmed/9226149
123. Thapa, P., & Farber, D. L. (2019). The Role of the Thymus in the Immune Response. *Thorac Surg Clin, 29*(2), 123-131. doi:10.1016/j.thorsurg.2018.12.001
124. Thygesen, K., Alpert, J. S., White, H. D., & Joint, E. S. C. A. A. H. A. W. H. F. T. F. f. t. R. o. M. I. (2007). Universal definition of myocardial infarction. *J Am Coll Cardiol, 50*(22), 2173-2195. doi:10.1016/j.jacc.2007.09.011
125. Tran, D. B., Weber, C., & Lopez, R. A. (2024). Anatomy, Thorax, Heart Muscles. In *StatPearls*. Treasure Island (FL).
126. Trinchieri, G. (1989). Biology of natural killer cells. *Adv Immunol, 47*, 187-376. doi:10.1016/s0065-2776(08)60664-1
127. Tschope, C., Ammirati, E., Bozkurt, B., Caforio, A. L. P., Cooper, L. T., Felix, S. B., … Van Linthout, S. (2021). Myocarditis and inflammatory cardiomyopathy: current evidence and future directions. *Nat Rev Cardiol, 18*(3), 169-193. doi:10.1038/s41569-020-00435-x
128. Turner, J., Parsi, M., & Badireddy, M. (2024). Anemia. In *StatPearls*. Treasure Island (FL).
129. Ulfig, A., & Leichert, L. I. (2021). The effects of neutrophil-generated hypochlorous acid and other hypohalous acids on host and pathogens. *Cell Mol Life Sci, 78*(2), 385-414. doi:10.1007/s00018-020-03591-y
130. Valenta, H., Erard, M., Dupre-Crochet, S., & Nubetae, O. (2020). The NADPH Oxidase and the Phagosome. *Adv Exp Med Biol, 1246*, 153-177. doi:10.1007/978-3-030-40406-2_9
131. Vanhoutte, P. M., Shimokawa, H., Tang, E. H., & Feletou, M. (2009). Endothelial dysfunction and vascular disease. *Acta Physiol (Oxf), 196*(2), 193-222. doi:10.1111/j.1748-1716.2009.01964.x
132. Voss, O. H., Batra, S., Kolattukudy, S. J., Gonzalez-Mejia, M. E., Smith, J. B., & Doseff, A. I. (2007). Binding of caspase-3 prodomain to heat shock protein 27 regulates monocyte apoptosis by inhibiting caspase-3 proteolytic activation. *J Biol Chem, 282*(34), 25088-25099. doi:10.1074/jbc.M701740200
133. Wan, E., Yeap, X. Y., Dehn, S., Terry, R., Novak, M., Zhang, S., … Thorp, E. B. (2013). Enhanced efferocytosis of apoptotic cardiomyocytes through myeloid-epithelial-reproductive tyrosine kinase links acute inflammation resolution to cardiac repair after infarction. *Circ Res, 113*(8), 1004-1012. doi:10.1161/CIRCRESAHA.113.301198
134. White, P. D., Mallory, G. K., & Salcedo-Salgar, J. (1936). The Speed of Healing of Myocardial Infarcts. *Trans Am Clin Climatol Assoc, 52*, 97-104 101. doi:10.1016/s0002-8703(39)90845-8

135. Wiktor-Jedrzejczak, W., & Gordon, S. (1996). Cytokine regulation of the macrophage (M phi) system studied using the colony stimulating factor-1-deficient op/op mouse. *Physiol Rev, 76*(4), 927-947. doi:10.1152/physrev.1996.76.4.927
136. Williams, A., Bissinger, R., Shamaa, H., Patel, S., Bourne, L., Artunc, F., & Qadri, S. M. (2023). Pathophysiology of Red Blood Cell Dysfunction in Diabetes and Its Complications. *Pathophysiology, 30*(3), 327-345. doi:10.3390/pathophysiology30030026
137. Winterbourn, C. C., Kettle, A. J., & Hampton, M. B. (2016). Reactive Oxygen Species and Neutrophil Function. *Annu Rev Biochem, 85*, 765-792. doi:10.1146/annurev-biochem-060815-014442
138. Wischmann, P., Kuhn, V., Suvorava, T., Muessig, J. M., Fischer, J. W., Isakson, B. E., … Kelm, M. (2020). Anaemia is associated with severe RBC dysfunction and a reduced circulating NO pool: vascular and cardiac eNOS are crucial for the adaptation to anaemia. *Basic Res Cardiol, 115*(4), 43. doi:10.1007/s00395-020-0799-x
139. Wood, K. C., Cortese-Krott, M. M., Kovacic, J. C., Noguchi, A., Liu, V. B., Wang, X., … Gladwin, M. T. (2013). Circulating blood endothelial nitric oxide synthase contributes to the regulation of systemic blood pressure and nitrite homeostasis. *Arterioscler Thromb Vasc Biol, 33*(8), 1861-1871. doi:10.1161/ATVBAHA.112.301068
140. Wu, L., Dalal, R., Cao, C. D., Postoak, J. L., Yang, G., Zhang, Q., … Van Kaer, L. (2019). IL-10-producing B cells are enriched in murine pericardial adipose tissues and ameliorate the outcome of acute myocardial infarction. *Proc Natl Acad Sci U S A, 116*(43), 21673-21684. doi:10.1073/pnas.1911464116
141. Wu, Y., Pan, N., An, Y., Xu, M., Tan, L., & Zhang, L. (2020). Diagnostic and Prognostic Biomarkers for Myocardial Infarction. *Front Cardiovasc Med, 7*, 617277. doi:10.3389/fcvm.2020.617277
142. Yoshida, H., Kondratenko, N., Green, S., Steinberg, D., & Quehenberger, O. (1998). Identification of the lectin-like receptor for oxidized low-density lipoprotein in human macrophages and its potential role as a scavenger receptor. *Biochem J, 334 (Pt 1)*(Pt 1), 9-13. doi:10.1042/bj3340009
143. Yusuf, S., Hawken, S., Ounpuu, S., Dans, T., Avezum, A., Lanas, F., … Investigators, I. S. (2004). Effect of potentially modifiable risk factors associated with myocardial infarction in 52 countries (the INTERHEART study): case-control study. *Lancet, 364*(9438), 937-952. doi:10.1016/S0140-6736(04)17018-9

10 Acknowledgement

I would like to take this opportunity to express my deepest thanks to all those who have supported me throughout the preparation of this thesis.

First, I am immensely grateful to Prof. Dr. Gerdes (head of the department) for giving me the opportunity to conduct my master´s thesis in the Cardiovascular Research Laboratory (CVRL).

I would like to extend my heartfelt appreciation to Dr. Ramesh Chennupati for his exceptional supervision, unwavering support, and insightful advice during my master´s thesis.

I am also deeply thankful to my working group and all my colleagues at CVRL for creating a great working atmosphere and supporting with any questions.

Finally, and most importantly, i am profoundly grateful to my husband and my family for their unconditional love, constant encouragement, and steadfast belief in me. Your unwavering support has been my greatest source of strength throughout this journey.